

AWARD NUMBER: W81XWH-15-1-0049

TITLE: A Knock-in Reporter for a Novel AR-Targeted Therapy

PRINCIPAL INVESTIGATOR: Chunhong Yan, Ph.D.

CONTRACTING ORGANIZATION: Georgia Regents Research Institute, Inc.
Augusta, GA 30912

REPORT DATE: May 2016

TYPE OF REPORT: Final report

PREPARED FOR: U.S. Army Medical Research and Materiel Command
Fort Detrick, Maryland 21702-5012

DISTRIBUTION STATEMENT: Approved for Public Release;
Distribution Unlimited

The views, opinions and/or findings contained in this report are those of the author(s) and should not be construed as an official Department of the Army position, policy or decision unless so designated by other documentation.

REPORT DOCUMENTATION PAGE

Form Approved
OMB No. 0704-0188

Public reporting burden for this collection of information is estimated to average 1 hour per response, including the time for reviewing instructions, searching existing data sources, gathering and maintaining the data needed, and completing and reviewing this collection of information. Send comments regarding this burden estimate or any other aspect of this collection of information, including suggestions for reducing this burden to Department of Defense, Washington Headquarters Services, Directorate for Information Operations and Reports (0704-0188), 1215 Jefferson Davis Highway, Suite 1204, Arlington, VA 22202-4302. Respondents should be aware that notwithstanding any other provision of law, no person shall be subject to any penalty for failing to comply with a collection of information if it does not display a currently valid OMB control number. **PLEASE DO NOT RETURN YOUR FORM TO THE ABOVE ADDRESS.**

1. REPORT DATE May 2016		2. REPORT TYPE Final		3. DATES COVERED 1 Mar 2015 - 29 Feb 2016	
4. TITLE AND SUBTITLE A Knock-in Reporter for a Novel AR-Targeted Therapy				5a. CONTRACT NUMBER	
				5b. GRANT NUMBER W81XWH-15-1-0049	
				5c. PROGRAM ELEMENT NUMBER	
6. AUTHOR(S) Chunhong Yan, Ph.D. E-Mail: cyan@augusta.edu				5d. PROJECT NUMBER	
				5e. TASK NUMBER	
				5f. WORK UNIT NUMBER	
7. PERFORMING ORGANIZATION NAME(S) AND ADDRESS(ES) Georgia Regents Research Institute, Inc., 1120 15 th Street, St# CJ3301, Augusta, GA 30912				8. PERFORMING ORGANIZATION REPORT NUMBER	
9. SPONSORING / MONITORING AGENCY NAME(S) AND ADDRESS(ES) U.S. Army Medical Research and Materiel Command Fort Detrick, Maryland 21702-5012				10. SPONSOR/MONITOR'S ACRONYM(S)	
				11. SPONSOR/MONITOR'S REPORT NUMBER(S)	
12. DISTRIBUTION / AVAILABILITY STATEMENT Approved for Public Release; Distribution Unlimited					
13. SUPPLEMENTARY NOTES					
14. ABSTRACT Since castration resistance of prostate cancer is often caused by AR overexpression, down-regulation of AR expression using small molecules is a promising yet untested strategy to combat castration-resistant prostate cancer (CRPC). The main objective of this research is to explore a possibility whether the CRISPR-Cas9 technology, an emerging genome-editing approach, could be applied to develop a reliable high-throughput drug screening platform for the identification of small-molecule AR transcriptional inhibitors to treat CRPC. We demonstrated in this report that the CRISPR-Cas9 system could indeed mediate high-efficient insertion of a selection gene into a site immediately downstream of the AR stop codon in castration-resistant C4-2 and 22Rv1 cells. Replacing the selection gene with a firefly luciferase (FLuc) gene led by an internal ribosomal entry site (IRES) through recombinase-mediated cassette exchange, we have successfully developed a C4-2-based recombinant cell line carrying FLuc in the AR gene locus and thereby bicistronically co-expressing the reporter gene with AR under the control of the endogenous AR promoter and enhancer. While the knock-in reporter is expected to faithfully reproduce chemical responses of the endogenous AR gene, we carried out a pilot screen using the NCI Diversity-set library and demonstrated that the genome-edited prostate cancer cells were useful in identifying small molecules inhibitory for AR expression.					
15. SUBJECT TERMS Androgen receptor, high-throughput drug screening assay, reporter gene assay, CRISPR-Cas9, genome editing, therapy, castration-resistant prostate cancer					
16. SECURITY CLASSIFICATION OF:			17. LIMITATION OF ABSTRACT	18. NUMBER OF PAGES	19a. NAME OF RESPONSIBLE PERSON
a. REPORT	b. ABSTRACT	c. THIS PAGE			19b. TELEPHONE NUMBER (include area code)
Unclassified	Unclassified	Unclassified	Unclassified	52	USAMRMC

Table of Contents

Page 3

Introduction.....	4
Keywords.....	4
Accomplishments	4
Impact.....	7
Changes/Problems.....	7
Products.....	8
Participants & Other Collaborating Organizations.....	9
Special Reporting Requirements.....	9
Appendices.....	10

1. INTRODUCTION

Small molecules inhibitory for *AR* expression are in urgent need due to their potential application in treating advanced, castration-resistant prostate cancer. The overall objective of this Exploration-Hypothesis Development project is to develop a reliable, knock-in *AR* reporter for high-throughput screening of small-molecule *AR* inhibitors. We proposed to employ the emerging genome-editing tool, the CRISPR-Cas9 system, to insert a bioluminescent reporter (firefly luciferase, FLuc) to the 3'-end of the *AR* gene, allowing the reporter gene bicistronically co-expressed with the endogenous *AR* gene under the control of the endogenous *AR* promoter and enhancer. Such a knock-in reporter can faithfully reproduce chemical responses of the endogenous *AR* gene, and thus is expected to be useful in search of small-molecule *AR* inhibitors with high confidence.

2. KEYWORDS

AR

Castration resistance

Reporter

Genome editing

CRISPR-Cas9

Luciferase

Internal ribosomal entry site (IRES)

Bicistronic co-expression

Drug screening

Drug discovery

3. ACCOMPLISHMENTS

What were the major goals and objective of the project?

The main goal of this project is to develop recombinant cells carrying a luciferase reporter gene in the native *AR* gene locus (knock-in reporter) for high-throughput screening to identify small molecules inhibitory for *AR* expression. Toward this goal, a major task and 2 minor tasks were proposed. The major task, which was in line with the main goal of this project and proposed to be completed in the first 7 months, was to develop recombinant cells carrying the knock-in reporter. We have successfully, fully accomplished this major task, and achieved the milestone, i.e., obtained recombinant cells carrying the knock-in reporter. Due to unexpected low genome-editing efficiency of prostate cancer cells, this major task was accomplished by the end of November, 2015 (9 months), about 2 months later than planned. The two minor tasks include a pilot screening using the recombinant cells and preliminary tests of anti-cancer effects of selected screening hits. We have completed the pilot screening (~ 1,600 compounds) by the end of January, 2016, and attempted to validate the screening hits in February. The anti-cancer effects of validated hits have not been tested due to the lack of sufficient amounts of these compounds. These compounds will need to be requested from NCI or purchased from commercial sources.

What was accomplished under these goals?

Given that a knock-in reporter would faithfully reproduce chemical responses of an endogenous gene, we proposed to employ the emerging CRISPR-Cas9 technology to insert a firefly luciferase gene (FLuc) to a site immediate downstream of the *AR* stop codon. We proposed a direct strategy (Strategy A) and an alternative 2-step strategy (Strategy B) to achieve this genome-editing goal. Strategy A, which attempts to directly knock the IRES-FLuc DNA into the *AR* locus in prostate cancer cells, was unsuccessful due to low transfection efficiency and the lack of a resistant gene for selection of targeted editing events. We therefore turned to the

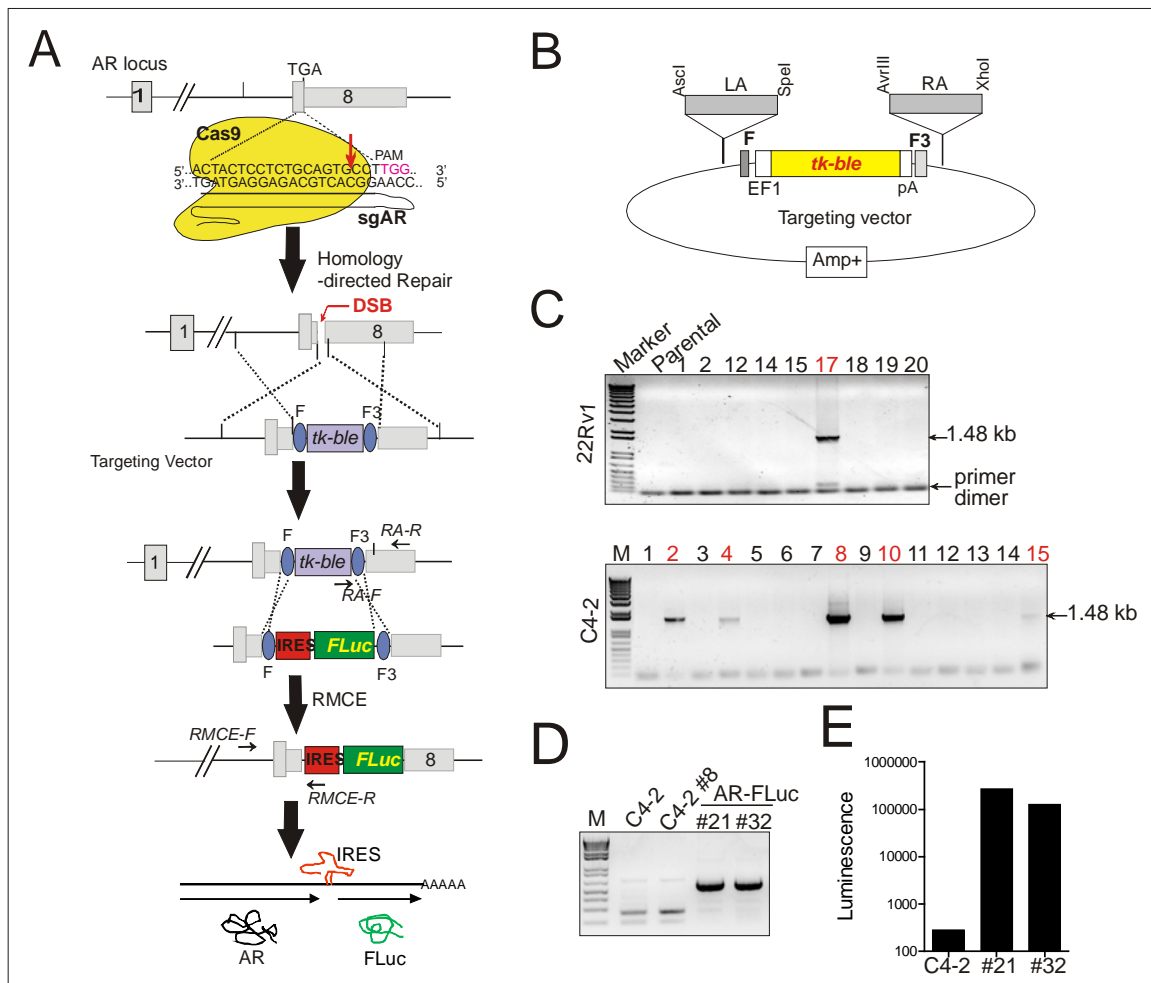


Fig 1. Development of a knock-in AR reporter. (A) Schematic presentation of the indirect strategy used for developing cells carrying a firefly luciferase in the native *AR* gene locus. sgAR, single-guided RNA targeting *AR*; DSB, double-strand break; F, wildtype FRT site; F3, mutant FRT site; RMCE, recombinase-mediated cassette exchange; IRES, internal ribosomal entry site. (B) The left (LA) and right (RA) homology arms flanked the sgAR targeting site were PCR amplified and cloned into a targeting vector carrying the *tk-ble* gene as indicated. (C) PCR identification of clones carrying the knock-in *tk-ble* gene. The PCR primers (RA-F and RA-R) are indicated in A. The targeted clone was expected to generate a 1.48 kb fragment. (D) PCR demonstration of replacement of the *tk-ble* gene with the IRES-FLuc DNA. The PCR primers (RMCE-F and RMCE-R) are indicated in A. Non-specific PCR amplification was noted in parental and the *tk-ble* knock-in clone. (E) The identified AR-FLuc clones were lysed for firefly luciferase activity assays.

alternative strategy (Fig 1A), in which a fused selection gene (*tk-ble*) was first knocked into the *AR* locus, and then replaced with the IRES-FLuc DNA by recombinase-mediated cassette exchange (RMCE). The *tk-ble* gene encodes Zeocin resistance (*ble*) for selecting knock-in events while also conferring ganciclovir (GCV) resistance (*tk*) for negatively selecting RMCE events. Accordingly, we constructed a vector expressing a single-guided RNA targeting a site ~ 90 bp downstream of the *AR* stop codon (TGA) (see sgRNA sequence in Fig 1A), and a targeting vector carrying the *tk-ble* gene flanked by ~ 1 kb of *AR* left and right homology arms (Fig 1B) amplified from genomic DNA by PCR. After transfected these two vectors to castration-resistant C4-2 and 22Rv1 cells, we selected the cells with Zeocin, obtained 20-30 resistant clones, and screened knock-in events by PCR. One (out of 20) 22Rv1 clone and 6 (out of 26) C4-2 clones were found to carry the knock-in DNA (Fig 1C). The knock-in efficiencies were not very high, which explains why the direct knock-in strategy (Strategy A) was not successful.

Next, we generated a vector carrying IRES-FLuc flanked by a wildtype FRT site (F) and a mutated FRT site (F3), and transfected it along with a Flp-expressing plasmid into C4-2 cells carrying the knock-in *tk-ble* gene (clone #8). Flp mediated cassette exchange replaced the *tk-ble* gene with IRES-FLuc, yielding GCV-resistant cells. Accordingly, we identified two clones (AR-FLuc #21 and #32) carrying the IRES-FLuc gene in the desired *AR* locus as demonstrated by PCR (Fig 1D). These two clones expressed significant high levels of firefly luciferase (Fig 1E), indicating that they are suitable for screening for small molecules inhibitory for *AR* expression.

To demonstrate these knock-in cells are useful in search of *AR* transcriptional inhibitors, we carried out a pilot screen using the NCI Diversity-set library, which contains 1,593 compounds with diverse

structures. This screen was done using 96-well plates and the cells were treated with 2.5 μ M of compounds for 16 h. While a majority of compounds did not significantly alter the luciferase expression level, we found that 68 (4.3%) compounds decreased the luciferase activity by more than 1 fold (Fig 2). This positive rate was rather high, and somehow hindered our efforts in validating and identifying hits for further investigations. It is worth to note that we and others recently published data suggesting that up to 45% of hits from a screen might be false positives (*Lang et al., Chem Biol* 22: 957-964, 2015). Therefore, in order to employ the knock-in *AR* reporter cells successfully developed in this project for high-throughput

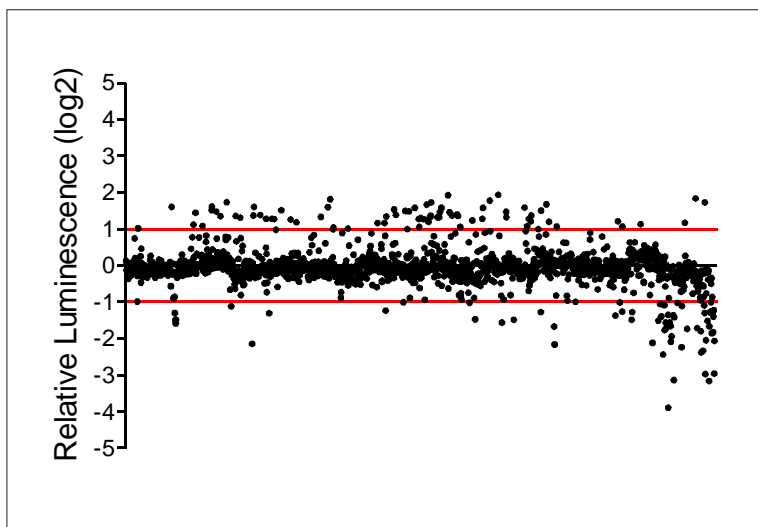


Fig 2. Pilot screening using the knock-in *AR* reporter. C4-2 cells carrying FLuc in the *AR* locus (clone #21) were plated in 96-well plates at a density of 10^5 /well, and treated with 2.5 μ M of compounds from the NCI Diversity-Set V library for 16 h. The cells were then lysed and subjected to firefly luciferase activity assays using a plate luminometer. The luciferase activity in each well relative to the DMSO group was converted to log2 and plotted.

drug screening, we will need to develop a secondary, orthogonal screening assay to exclude those false-positive compounds (*Lang et al., Chem Biol 22: 957-964, 2015*). Such a orthogonal assay can be readily developed through RMCE using the *tk-ble* knock-in cell line (*Lang et al., Chem Biol 22: 957-964, 2015*). While this goal is beyond the scope of this project, we are currently working to develop the secondary screening assay in order to apply these AR-knock-in reporters for high-throughput searches of small-molecule inhibitors.

What opportunities for training and professional development did the project provide?

Although this project is not for training purpose, the postdoctoral fellow, Ziyang Wang, had learned the CRISPR-Cas9 technology and drug screening. This would help her career development.

How were the results disseminated to communities of interest?

Nothing to Report.

What do you plan to do during the next reporting period to accomplish the goals?

Nothing to Report.

4. IMPACT

What was the impact on the development of the principal discipline(s) of the project?

In this project, we have successfully developed a knock-in AR reporter system that can faithfully reproduce chemical responses of the endogenous AR gene, and therefore can likely provide a reliable, powerful, high-throughput screening platform for identifying small-molecule AR inhibitors. The identified small molecules can serve as leads for further development of effective therapeutic agents to combat castration resistant prostate cancer.

What was the impact on other disciplines?

Nothing to Report.

What was the impact on technology transfer?

Nothing to Report.

What was the impact on society beyond science and technology?

Nothing to Report.

5. CHANGES/PROBLEMS

Changes in approach and reasons for change

The cell line used for genome editing was changed from CWR-R1 to 2 other CRPC cell lines (i.e., C4-2 and 22Rv1), because we noted that CWR-R1 cells were very heterogeneous in morphology. We were afraid that the derived knock-in clone might not represent the parental cell populations.

Actual or anticipated problems or delays and actions or plans to resolve them

The actual problem, which was anticipated in the proposal, was the low genome-editing efficiency. Accordingly, we took the alternative Strategy B, which employed a selection gene to enrich for recombinant events, to develop the knock-in cells. The latter strategy took additional time, and thus delayed the project for about two months.

Changes that had a significant impact on expenditures

Nothing to Report.

Significant changes in use or care of human subjects, vertebrate animals, biohazards, and/or select agents

Nothing to Report.

6. PRODUCTS

The following publications were partly supported by this award:

1. Wang Z, Kim J, Teng Y, Ding H-F, Zhang J, Hai T, Cowell JK, **Yan C**. (2015) Loss of ATF3 promotes hormone-induced prostate carcinogenesis and the emergence of CK5⁺CK8⁺ epithelial cells. *Oncogene* doi: 10.1038/nc.2015.417 (Epub ahead of print)
2. Cui H, Li X, Han C, Wang Q-E, Wang H, Ding H-F, Zhang J, **Yan C** *. The stress responsive gene ATF3 mediates dichotomous UV responses by regulating Tip60 and p53. *J Biol Chem* 2016 March 18. Doi: 10.1074/jbc.M115.713099 (Epub ahead of print)
3. Zhao J, Li X, Guo M, Yu J *, **Yan C** *. (2016) The common stress responsive transcription factor ATF3 binds genomic sites enriched with p300 and H3K27ac for transcriptional regulation. *BMC Genomics* 17: 335

This project also generated a knock-in AR reporter cell line. While screening and validation of AR inhibitors are ongoing, the results will be published in a scientific journal soon. The knock-in cell line will be freely distributed to other academic laboratories upon request. The project also generated several intermediate vectors that are very useful in developing knock-in reporter assays for other essential prostate-cancer-associated genes. We will also share these plasmids upon request.

7. PARTICIPANTS & COLLABORATING ORGANIZATIONS

What individuals have worked on the projects?

1) Name: Chunhong Yan, Ph.D.
Project Role: PI
Nearest person month worked: 0.6
Contribution to Project: Overall administration and direction of the project.

2) Name: Ziyan Wang, Ph.D.
Project Role: Postdoctoral fellow
Nearest person month worked: 9.6
Contribution to the Project: Carried out the experiments and organized the data

Has there been a change in the active other support of the PD/PI(s) or senior/key personnel since the last reporting period?

Nothing to report.

What other organizations were involved as partners?

Nothing to report

8. SPECIAL REPORTING REQUIREMENTS: None

9. Appendices

Copies of the 3 publications with titles listed above are attached.

ORIGINAL ARTICLE

Loss of *ATF3* promotes hormone-induced prostate carcinogenesis and the emergence of CK5⁺CK8⁺ epithelial cells

Z Wang^{1,2}, J Kim³, Y Teng¹, H-F Ding^{1,4}, J Zhang⁵, T Hai⁶, JK Cowell¹ and C Yan^{1,2,7}

Steroid sex hormones can induce prostate carcinogenesis, and are thought to contribute to the development of prostate cancer during aging. However, the mechanism for hormone-induced prostate carcinogenesis remains elusive. Here, we report that activating transcription factor 3 (*ATF3*)—a broad stress sensor—suppressed hormone-induced prostate carcinogenesis in mice. Although implantation of testosterone and estradiol (T+E₂) pellets for 2 months in wild-type mice rarely induced prostatic intraepithelial neoplasia (PIN) in dorsal prostates (one out of eight mice), the loss of *ATF3* led to the appearance of not only PIN but also invasive lesions in almost all examined animals. The enhanced carcinogenic effects of hormones on *ATF3*-deficient prostates did not appear to be caused by a change in estrogen signaling, but were more likely a consequence of elevated androgen signaling that stimulated differentiation of prostatic basal cells into transformation-preferable luminal cells. Indeed, we found that hormone-induced lesions in *ATF3*-knockout mice often contained cells with both basal and luminal characteristics, such as p63⁺ cells (a basal-cell marker) showing luminal-like morphology, or cells double-stained with basal (CK5⁺) and luminal (CK8⁺) markers. Consistent with these findings, low *ATF3* expression was found to be a poor prognostic marker for prostate cancer in a cohort of 245 patients. Our results thus support that *ATF3* is a tumor suppressor in prostate cancer.

Oncogene advance online publication, 2 November 2015; doi:10.1038/onc.2015.417

INTRODUCTION

Characterized by its strong association with aging, prostate cancer remains as one of the major health threats to men worldwide. While genetic alterations that can cause transformation of prostatic epithelia are inevitably accumulated during aging, aging men also produce fewer androgens. As a result, the ratio of plasma estrogens (for example, estradiol, E₂) to androgens (for example, testosterone) is increased with age.¹ Estrogens produced by adipose tissue, adrenal glands and testicles, or converted from testosterone in the prostate locally, can bind estrogen receptor α (ER α) or β (ER β) to regulate prostatic branching, and appears to be required for normal prostate development.² The increase in the relative level of prostatic estrogens in aging men is therefore thought to be one of the major contributors to the occurrence and development of prostate cancer.^{1,2} Indeed, not only epidemiological studies have demonstrated that an elevated plasma estrogen level correlates with a high risk of prostate cancer,³ but estradiol in combination with testosterone mimicking the hormone imbalance in aging men has been shown to induce prostate carcinogenesis in rodents.^{4,5} Although the underlying mechanism remains elusive, hormone-induced carcinogenesis in mouse prostates appears to require both estrogen and androgen signaling, as mice null for ER α are refractory to the carcinogenic effect⁵ while a treatment regimen devoid of testosterone rather induces squamous metaplasia and keratinization of prostate epithelia without neoplastic transformation.⁶ Squamous metaplasia is

thought to be caused by extensive proliferation of basal epithelial cells that is stimulated by paracrine signaling mediated by ER α predominantly expressed in adult prostatic stroma.⁷ On the other hand, androgen signaling triggered by binding of testosterone to the androgen receptor (AR) in the prostatic luminal epithelium or stroma is indispensable for sustaining the prostate epithelium in a differentiated and relatively growth-quiescent state.⁸ Elevated androgen signaling, however, can also drive prostatic proliferation and is responsible for the outgrowth and survival of prostate cancer cells.^{9,10} Indeed, targeting androgen signaling or AR is one of the major strategies for treating prostate cancer. Not surprisingly, the AR activity, presented as transactivation of androgen-responsive genes, is regulated by a complex network comprised of transcription co-factors that are often aberrantly expressed in prostate cancer.^{11,12}

Previously, we identified *ATF3* (activating transcription factor 3), a member of the ATF/CREB family member, as a major AR repressor in the prostatic epithelium and prostate cancer cells.¹³ *ATF3* binds AR at its DNA-binding domain, thereby preventing AR from binding to androgen-responsive genes.¹³ *ATF3* can also bind the AR C-terminal ligand-binding domain, disrupting the AR intramolecular interaction required for its transcriptional activity.¹³ Best known for its rapid induction by broad cellular stresses including DNA damage, oxidative stress and oncogenic stimuli,¹⁴ *ATF3* engages in a number of cellular signal pathways, such as those mediated by p53, TGF- β and Toll-like receptor 4, through

¹GRU Cancer Center, Georgia Regents University, Augusta, GA, USA; ²Center for Cell Biology and Cancer Research, Albany Medical College, Albany, NY, USA; ³Department of Statistics, Sungkyunkwan University, Seoul, South Korea; ⁴Department of Pathology, Medical College of Georgia, Georgia Regents University, Augusta, GA, USA; ⁵Department of Radiation Oncology, School of Medicine, Case Western Reserve University, Cleveland, OH, USA; ⁶Department of Biological Chemistry and Pharmacology, Ohio State University, Columbus, OH, USA and ⁷Department of Biochemistry and Molecular Biology, Medical College of Georgia, Georgia Regents University, Augusta, GA, USA. Correspondence: Dr C Yan, GRU Cancer Center, Georgia Regents University, 1410 Laney Walker Boulevard, CN2134, Augusta, GA 30912, USA.

E-mail: cyan@gru.edu

Received 27 May 2015; revised 28 September 2015; accepted 5 October 2015

interacting with other proteins or binding to the consensus ATF/CREB *cis*-regulatory element.^{15–17} While it is generally believed that ATF3 is important for triggering appropriate cellular responses to immune and oncogenic stimulation,^{18,19} aberrant ATF3 expression is frequently associated with human diseases such as prostate cancer.²⁰ Indeed, unbiased cancer profiling analyses have revealed that ATF3 expression is often downregulated in prostate cancer, particularly in advanced diseases.²¹ Using a genetically engineered mouse model, we recently demonstrated that ATF3 suppresses the development of prostate cancer caused by *Pten* loss²¹—one of the most frequent genetic

alterations occurring in human prostate cancer. We also showed that *ATF3* deficiency leads to increased Akt signaling in both transformed mouse prostatic epithelia and human prostate cancer cells.²¹ These results in combination with the earlier findings that ATF3 is an AR repressor and can activate the tumor suppressor p53^{13,15} strongly argue for a notion that ATF3 has an important role in the suppression of prostate cancer.²² However, ATF3 has also been shown to be oncogenic in other cellular contexts, such as in breast cancer.²³

Given that hormone signaling may function as an oncogenic stimulus to promote prostate cancer development, we sought to test whether *ATF3* deficiency in mice also contributes to prostate carcinogenesis induced by steroid sex hormones. Our results indicate that loss of *ATF3* in mice accelerated hormone-induced prostate carcinogenesis, an effect which was likely achieved through promoting differentiation of basal epithelial cells into luminal cells. The latter cell type appears to be favored as the cell of origin for prostate cancer.²⁴ We therefore provide an additional line of genetic evidence supporting that ATF3 is a tumor suppressor for prostate cancer.

RESULTS

Low ATF3 expression is a poor prognosis marker for prostate cancer. Previous studies found that *ATF3* expression is frequently downregulated in prostate cancer.^{21,25,26} To further explore the role of ATF3 in prostate cancer, we examined *ATF3* expression in 419 prostate cancer samples and 52 normal tissues using the RNA-seq data deposited in the Cancer Genome Atlas (TCGA) database. Consistent with previous reports, we found that the *ATF3* expression level was significantly lower in prostate tumors than that in normal tissues ($P = 0.0004$) (Figure 1a). Further comparison of *ATF3* expression between prostate tumors and their corresponding adjacent normal tissues also showed decreased *ATF3* expression in tumors ($P = 0.005$, $n = 52$) (Figure 1b). We also carried out immunohistochemical staining on 14 prostate cancer samples and their corresponding normal prostate tissues. We found that the ATF3 staining intensity was significantly lower in 9 out of 14 prostate tumor samples (64.2%) as compared with their normal prostatic epithelia (Figure 1c). In contrast, elevated ATF3 staining was found in only one of these tumors. Intriguingly, when the survival data for prostate cancer patients registered in the TCGA database were analyzed, we found that low *ATF3* expression was significantly associated with a poor relapse-free survival in patients ($P = 0.006$) (Figure 1d). Our results thus support the role of ATF3 that has in the suppression of prostate cancer.

ATF3 is hormone-inducible and expressed in both basal and luminal cells

As hormone signaling can promote prostate carcinogenesis,^{1,2} we asked whether ATF3 also suppresses prostate carcinogenesis

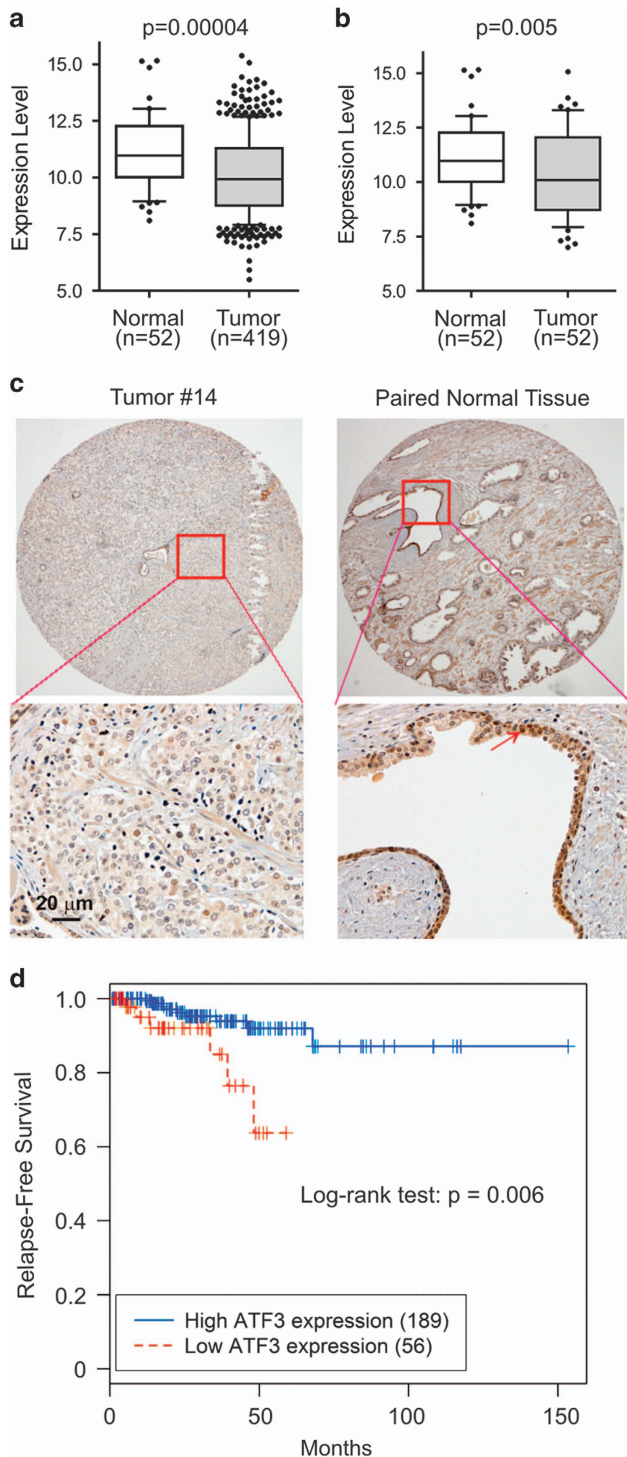


Figure 1. ATF3 expression is downregulated in human prostate cancer. **(a)** ATF3 expression data measured by RNA-seq were retrieved from TCGA, and used for comparison between prostate cancer samples and normal tissues. The data are presented as box and whiskers (10–90 percentile). The P -value was calculated by Student's t -test. **(b)** ATF3 expression was compared between prostate cancer samples and their paired normal tissues. The P -value was calculated by paired Student's t -test. **(c)** Representative immunohistochemistry (IHC) results of ATF3 expression in human prostate tumors and their paired normal tissue. Tissue array slides from Super Bio Chips and US Biomax were stained for ATF3 expression by IHC. The arrow indicates normal prostate epithelial cells with higher nuclear staining. **(d)** The Kaplan–Meier survival curves for patients with high or low ATF3 expression shows low ATF3 expression is a poor prognosis marker for prostate cancer.

induced by steroid sex hormones. To explore this possibility, we first tested whether *ATF3* expression is induced by hormone stimulation. We, respectively, treated PC3 cells that carry functional ER α and LNCaP cells known to express AR²⁷ with estradiol (E₂) and a synthetic androgen R1881 for western blotting. While these hormones induced expression of ER/AR target genes progesterone receptor (PR) and NKX3.1 as expected, we found that E₂ and R1881 rapidly induced an increase in the ATF3 protein level (Figures 2a and b). The hormones also rapidly increased the *ATF3* mRNA levels (Figure 2c), suggesting that they likely induced *ATF3* expression at the transcription level. As ER and AR regulate prostatic basal and luminal epithelial cells, respectively, we examined *ATF3* expression in these two distinct cell types by immunohistochemistry. In support of the possibility that *ATF3* may regulate hormone-induced events, *ATF3* was expressed in both basal (red arrows) and luminal cells (black arrows) of human (Figure 2d) and mouse prostates (Figure 2e). Of note, p63 staining was used to label basal cells in the mouse tissue (Figure 2e).

ATF3 deficiency does not affect hormone-induced squamous metaplasia in APs

We next determined the contribution of *ATF3* to hormone-induced prostate carcinogenesis by subcutaneously implanting pellets embedded with 25 mg of testosterone (T) and 2.5 mg of E₂,

or placebo, into *ATF3* wild-type (WT) or knockout (KO) mice (C57BL/6). These pellets allow for continuous release of the hormones for 2 months until we subjected mouse prostates to histopathological examinations. Treating mice with T+E₂ at these doses were expected to reproduce circulating plasma hormone levels similar to those found in aging men.⁵ While we did not notice apparent alteration in the growth and behavior of mice, the hormone treatments induced squamous metaplasia in mouse anterior prostates (APs) evidenced by epithelial keratinization and dramatic expansion of enlarged, flat epithelial cells in these glands (Figure 3a). These highly proliferative (PCNA-positive) cells were often positive for p63 staining (p63⁺) (Figure 3a), indicating their basal-cell origin. These results were different from those in an early report that T+E₂ embedded in Silastic tubing induced prostatic intraepithelial neoplasia in mouse APs.⁵ This discrepancy might be due to different hormone release kinetics. The pellets used in our study might release E₂ more efficiently and thus predominantly stimulate estrogen signaling in APs—the glands most sensitive to estrogens. Indeed, squamous metaplasia, known as a major estrogenic effect in rodents,⁶ was only seen in APs in our experiments. Moreover, expression of PR, a well-characterized ER target gene, was strongly induced by the hormone treatments (Figure 3a). Importantly, loss of *ATF3* did not appear to alter the estrogenic effects, as the hormones induced squamous metaplasia

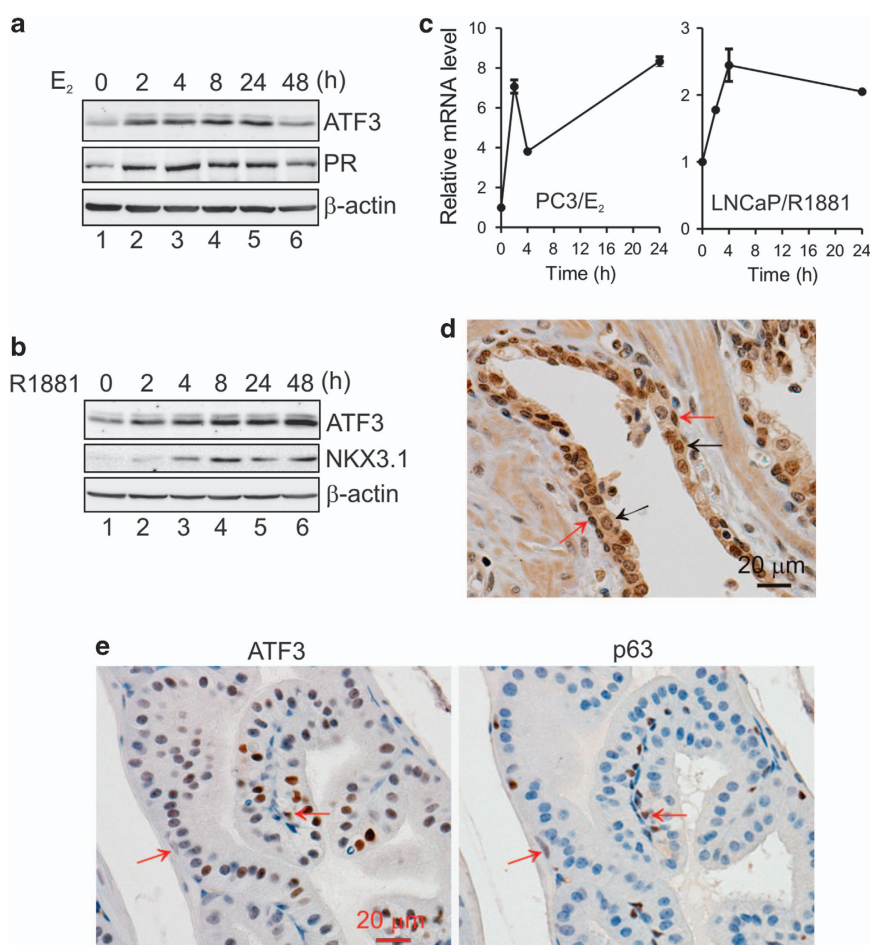


Figure 2. ATF3 is hormone-inducible and expressed in both prostate basal and luminal cells. (a) PC3 cells were treated with 10 nM of E₂ for western blotting assays. (b) LNCaP cells were treated with 1 nM of R1881 for western blotting analysis. (c) PC3 and LNCaP cells were treated with E₂ and R1881, respectively, and then subjected to qRT-PCR to measure the *ATF3* mRNA level. (d) Normal human prostate samples were stained for *ATF3* expression by immunohistochemistry (IHC). Red and black arrows indicate basal and luminal cells, respectively. (e) Adjacent serial sections of mouse APs were stained for *ATF3* and p63 expression by IHC. Red arrows indicate two representative basal cells positive for both *ATF3* and p63 staining.

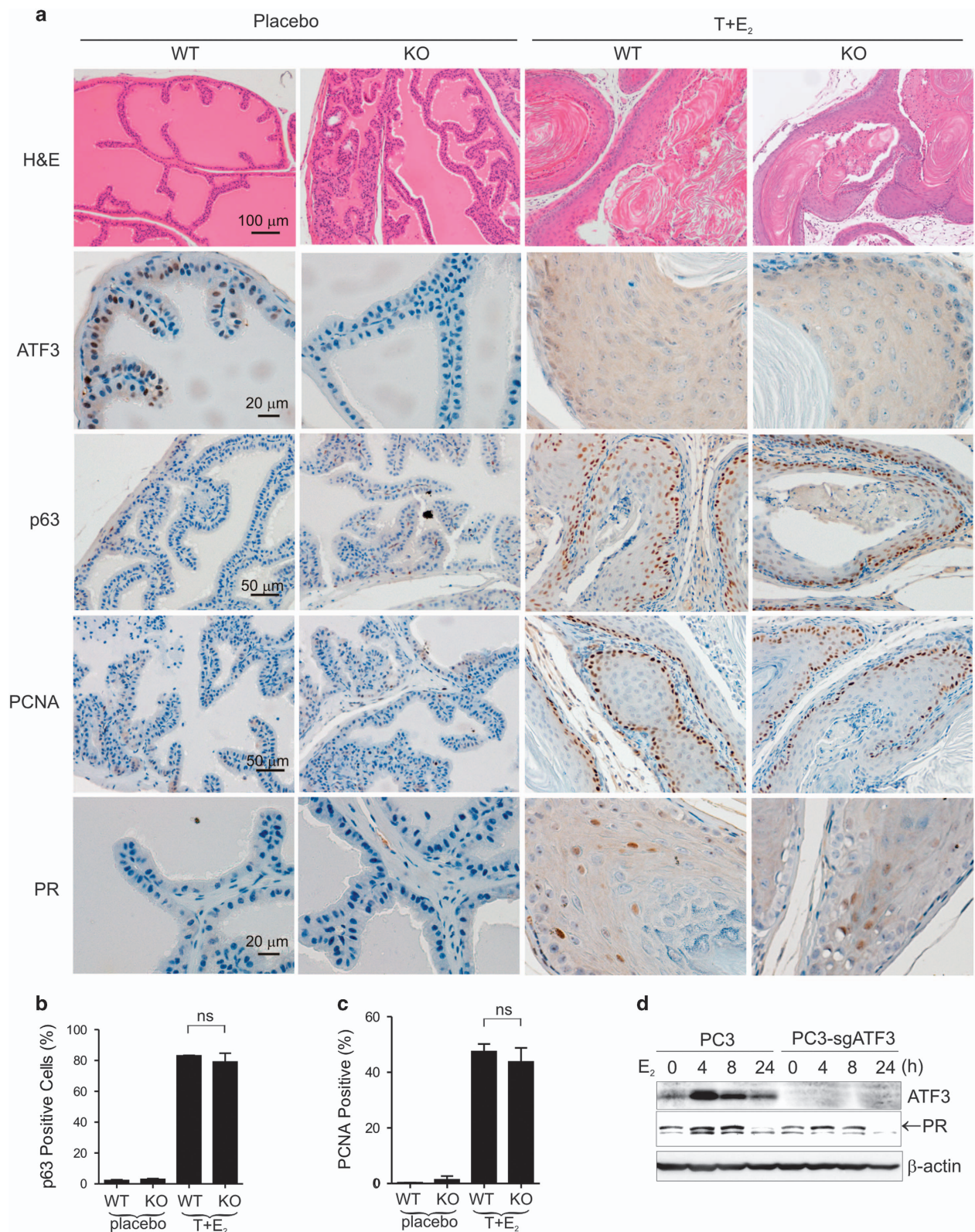


Figure 3. *ATF3* deficiency does not affect hormone-induced squamous metaplasia in APs. **(a)** Sections of APs from placebo and hormone-treated mice (T+E₂) were stained with hematoxylin and eosin, or subjected to immunohistochemical staining, as indicated. **(b, c)** p63-positive **(b)** or PCNA-positive **(c)** cells were counted from random microscopic fields. Percentages of positive cells were depicted as mean ± s.d. and showed in the graphs. ns, no significant difference, Student's *t*-test. **(d)** PC3 cells and a clone lacking *ATF3* expression (generated by a single-guided RNA, i.e., sgATF3) were treated with 10 nM of E₂ for different time, and subjected to western blotting for PR expression.

in *ATF3*-deficient APs to the same extent as the WT glands (Figure 3a). Consistent with these results, *ATF3* deficiency did not change the number of p63-positive or PCNA-positive cells (Figures 3b and c). These results indicate that *ATF3* had a negligible effect on estrogen signaling. Indeed, knockout of *ATF3* expression by a single-guided RNA in PC3 cells²¹ only marginally altered PR expression induced by E_2 (Figure 3d).

Loss of *ATF3* promotes hormone-induced carcinogenesis in dorsal prostates (DPs)

As *ATF3* can repress androgen signaling in the prostatic epithelium,¹³ we next asked a question as to whether the loss of *ATF3* leads to different hormone responses in less-estrogenic glands like DPs. Although we did not find obvious abnormality in ventral and lateral prostates (Table 1), the hormone treatments appeared to induce prostatic intraepithelial neoplasia lesions in DPs of one WT mice, but hyperplasia, in other WT mice (Figures 4a and b), suggesting a minor carcinogenic effect of the hormones on DPs. Intriguingly, *ATF3* deficiency appeared to promote this carcinogenic effect, as 11 out of 12 KO mice developed prostatic intraepithelial neoplasia lesions in their DPs (Figures 4a and b). Moreover, staining for α -smooth muscle actin expression in these *ATF3*-deficient DPs revealed that a number of lesions (6–30%) were surrounded by disintegrated smooth muscle layers that were invaded by transformed epithelial cells (Figures 4a and c), indicating their invasiveness. In contrast, only one of the WT mice appeared to have invasive lesions (Figure 4b). These results thus demonstrate that *ATF3* deficiency promoted prostate carcinogenesis induced by T+E₂. Of note, DPs of placebo-treated KO mice were hyperplastic (Figures 4a and b), a finding reminiscent of our previous results.¹³

ATF3 deficiency promotes epithelial cell proliferation in DPs

To explore the underlying mechanism for carcinogenesis promoted by loss of *ATF3*, we determined the proliferation rate of prostatic epithelial cells by PCNA staining. Without the hormone treatments, *ATF3*-deficient DPs had a higher proliferation rate than WT glands (Figures 5a and b), consistent with the results that the KO glands were hyperplastic (Figure 4b). As expected, while the hormone treatments significantly increased the proliferation rate, loss of *ATF3* further enhanced prostatic epithelial proliferation induced by the hormones (Figures 5a and b). As hormone-induced PR expression (as a marker for ER signaling) was not significantly different between WT and KO glands (Figures 5a and c), the increased proliferation in KO cells was more likely caused by the increased sensitivity to androgen stimulation. Indeed, we have previously demonstrated that the loss of *ATF3* can promote androgen signaling in the prostatic epithelium.¹³

Hormone-induced KO tumors contain cells with a basal-cell origin
Prostate cancer can be originated from either basal cells or luminal cells.²⁸ Whereas luminal cells are more susceptible to transformation, prostate tumorigenesis originated from basal cells has a long latency and appears to require basal-to-luminal differentiation.^{29,30} To better understand the mechanism underlying the promotion of

hormonal carcinogenesis by *ATF3*, we stained DPs with antibodies to AR and p63 to label luminal and basal cells, respectively. Whereas AR positivity was mainly found in columnar luminal cells in the placebo group as expected, most cells in the hormone-induced prostate lesions were also AR-positive but negative for p63 staining (Figure 6a). On the contrary, p63 staining was mainly found in basal cells (Figure 6a). As a consequence of growth stimulation by E_2 , the number of p63-positive (p63⁺) basal cells in both WT and KO glands was increased by the hormone treatments (Figure 6b). Although there was no difference in the total number of p63⁺ cells, we found, to our surprise, that the prostate lesions in KO mice were comprised of many p63⁺ cells with a luminal-like morphology, that is, large oval-shaped nuclei aligned vertically to the basement membrane (Figure 6a, red arrows). These luminal-like p63⁺ cells were often dislodged and moved away from the basement membrane (Figure 6a). Given that basal cells can be differentiated into luminal cells under certain conditions such as AR expression,^{31,32} these luminal-like p63⁺ cells were likely derived from basal-to-luminal differentiation. Although we occasionally found these intermediate cells in the hormone-treated WT glands, the number of glands containing such cells was significantly smaller than that of the KO glands (Figure 6c). As luminal cells appear to be the favorable cell of origin for prostate cancer,²⁴ these results suggest that basal-to-luminal differentiation promoted by *ATF3* deficiency would generate luminal cells that are more transformation-competent,²⁹ thereby facilitating prostate carcinogenesis induced by hormones.

Loss of *ATF3* promotes the emergence of CK5⁺CK8⁺ epithelial cells

To confirm the existence of intermediate cells in the lesions of KO mice, we double-stained DPs with antibodies to cytokeratin 5 (CK5) and cytokeratin 8 (CK8) to visualize basal and luminal cells simultaneously. As expected, CK8-positive (CK8⁺) luminal cells rested on a layer of CK5-positive (CK5⁺) basal cells and extruded towards lumens in DPs of the placebo-treated mice (Figure 7a). Whereas the hormones increased the numbers of CK5⁺ and CK8⁺ cells as expected, we saw a few CK5 and CK8 double positive (CK5⁺CK8⁺) cells scattered in WT DPs. In striking contrast, we found a significantly larger number of CK5⁺CK8⁺ cells in DPs of hormone-treated KO mice (Figure 7a). Localized on the top of a layer of CK5⁺ basal cells, these CK5⁺CK8⁺ cells had cuboidal shapes, aligned vertically to the basement membrane, and often mingled with CK8⁺ luminal cells (Figure 7a). Overall, more than 20% of epithelial cells in the *ATF3*-deficient DPs were CK5⁺CK8⁺, comparing with 2% of CK5⁺CK8⁺ cells in the WT glands (Figure 7b). Moreover, a significantly higher number of *ATF3*-deficient glands contained CK5⁺CK8⁺ cells as compared with their WT counterparts (Figure 7c). When CK5 staining was examined alone, CK5⁺ cells appeared to frequently form two or more layers in the KO glands (Figure 7a). Indeed, we found that the number of glands with multiple layers of CK5⁺ cells was significantly increased in the *ATF3*-deficient DPs (Figure 7d). These results thus suggest that the loss of *ATF3* could promote basal-to-luminal transformation in mouse prostates. As a simple test of the possible effect of *ATF3* on prostate epithelial differentiation, we knocked down *ATF3* expression in RWPE-1 cells using an *ATF3*-specific siRNA (siATF3, Figure 7f)¹³ and stained the cells for differentiation markers. As RWPE-1 is a normal human prostate epithelial cell line mainly harboring a basal-cell phenotype, fewer than 1% of cells were positive for CK8 staining (Figures 7e and f). In line with the notion that *ATF3* deficiency could promote basal-to-luminal differentiation, knockdown of *ATF3* expression significantly increased the number of CK8⁺ cells by fivefold (Figures 7e and f). Of note, most of these CK8⁺ cells remained positive for CK5 staining. Therefore, *ATF3* appears to induce human prostate basal cells to differentiate into luminal cells.

Table 1. Mouse phenotypes induced by the hormones

	<i>ATF3</i> WT	<i>ATF3</i> KO
AP	Squamous metaplasia	Squamous metaplasia
DP	1/8 PIN/invasive carcinoma 7/8 hyperplasia	11/12 PIN/invasive carcinoma 1/12 hyperplasia
VP/LP	Normal	Normal

Abbreviations: AP, anterior prostate; DP, dorsal prostate; KO, knockout; PIN, prostatic intraepithelial neoplasia; WT, wild type.

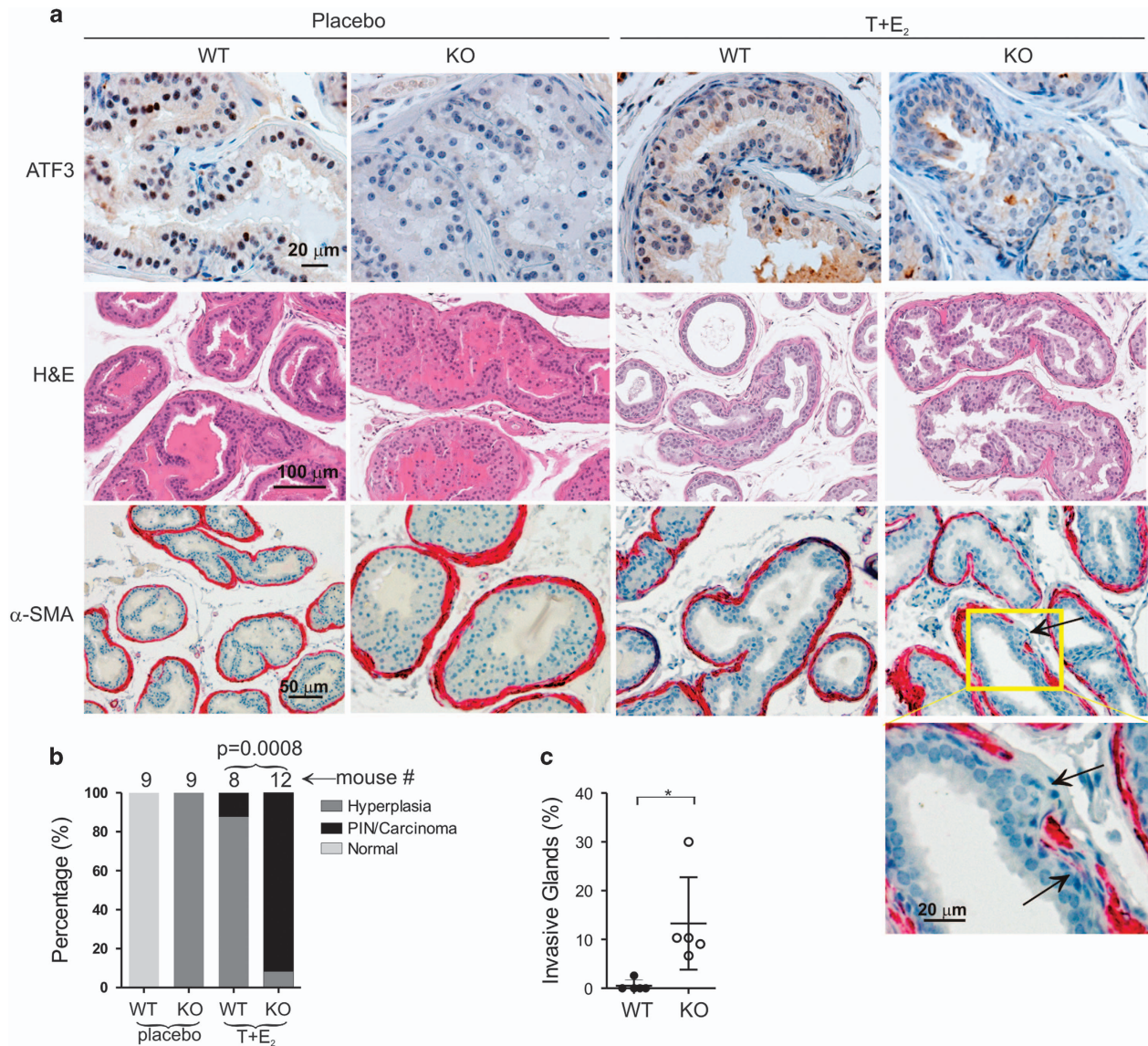


Figure 4. Loss of ATF3 promotes hormone-induced prostate carcinogenesis in DPs. **(a)** DP sections were subjected to hematoxylin and eosin staining, or immunohistochemical staining for ATF3 and α -smooth muscle actin (α -SMA) expression as indicated. Arrows indicate invasion sites. **(b)** Percentages of mice with hyperplasia or prostatic intraepithelial neoplasia/carcinoma in their DPs. Fisher's Exact test. **(c)** Percentages of invasive glands in WT and KO mice (five mice for each genotype) as determined by α -SMA staining. * $P < 0.05$, Mann-Whitney test.

DISCUSSION

Decrease in androgen production and accumulation of genetic alterations during aging are two major risk factors for prostate cancer. Although it has been established that ATF3 has important roles in provoking cellular responses to oxidative stresses that can accumulate naturally and cause genetic alterations during aging,^{33,34} we demonstrated in this report that loss of ATF3 promoted prostate carcinogenesis in mice under a condition mimicking the estrogen/androgen imbalance in aging men.⁵ Our results thus argue for a notion that ATF3 dysfunction contributes to the genesis and the development of prostate cancer. Indeed, while it was frequently found that ATF3 expression is downregulated in human prostate cancer,²¹ decreased ATF3 expression appeared to be associated with poor survival of prostate cancer patients (Figure 1d). This notion is in line with previous findings that ATF3 is proapoptotic^{35,36} and can repress androgen signaling required for the outgrowth and survival of prostate cancer cells.¹³ Moreover, we recently demonstrated that ATF3 deficiency promotes prostate tumorigenesis induced by

genetic ablation of *Pten* in mice.²¹ Together, our studies provide direct genetic evidence supporting the role of ATF3 in the suppression of prostate cancer.

Hormone-induced prostate carcinogenesis in mice requires both estrogen and androgen signaling.⁵ While estrogens stimulate proliferation of basal cells and are likely the driving force for cellular transformation, the role of androgen signaling in prostate carcinogenesis is unclear and thought to outcompete with estrogens to preserve a glandular phenotype and prevent prostatic atrophy.⁵ Different from the previous report,⁵ however, the T+E₂ combination only induced squamous metaplasia in the most estrogen-sensitive APs in our animal model (Figure 3). These results indicate that the estrogenic effects appear to be dominant in APs in our model. Although ATF3 expression could be transiently induced by E₂ in prostatic epithelial cells (Figure 2a), ATF3 did not appear to affect estrogen signaling, as loss of ATF3 neither caused phenotypic changes in APs nor altered PR expression induced by the hormones (Figure 3). Accordingly, it was more likely that the loss of ATF3 promoted hormonal

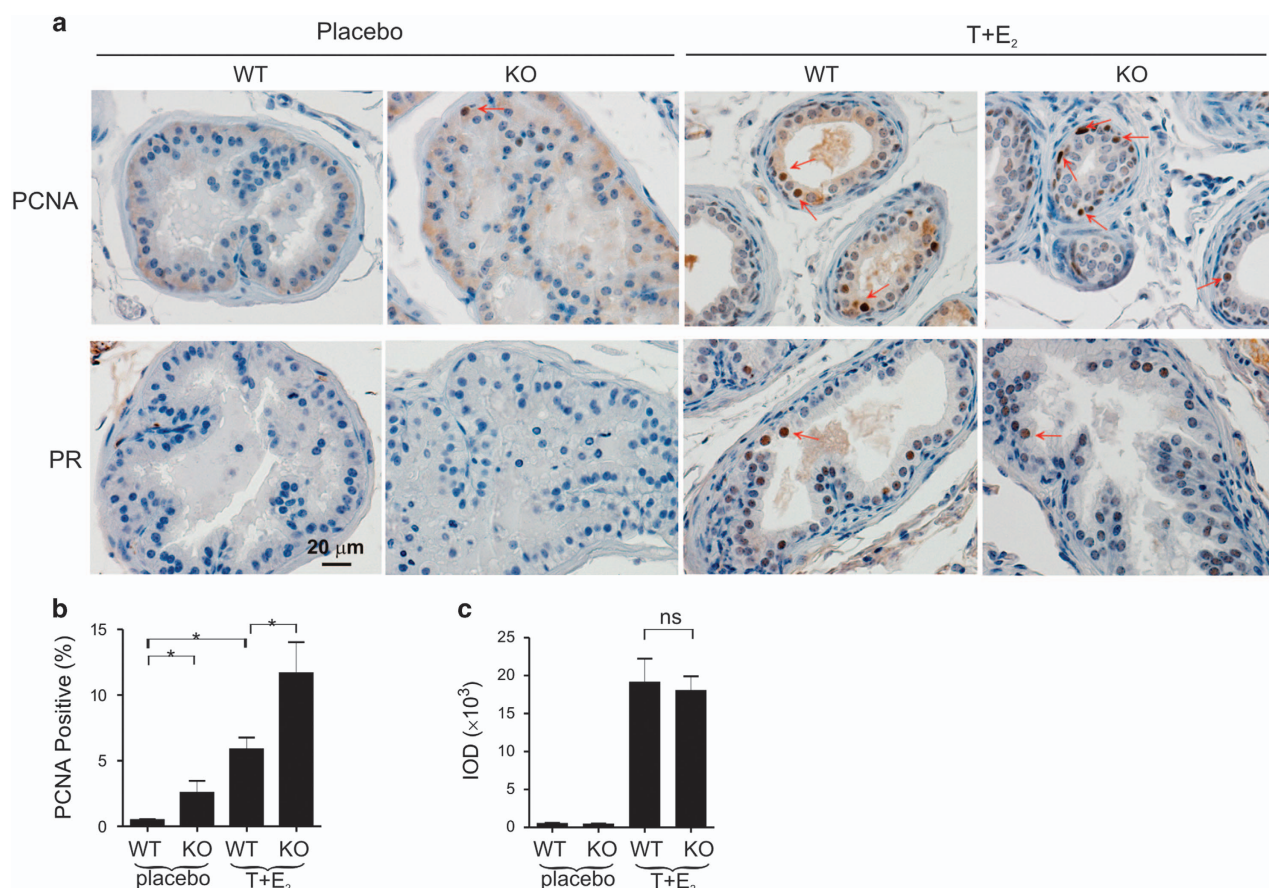


Figure 5. *ATF3* deficiency increases proliferation of prostatic epithelial cells in DP. **(a)** DP sections were stained for PCNA and PR expression. Arrows indicate positive cells. **(b)** PCNA-positive cells were counted from random microscopic fields. The data were presented as mean \pm s.d. $*P < 0.05$, Student *t*-test. **(c)** PR staining was quantitated using the Image-Pro Plus software and presented as integrated optical density (IOD). ns, not significant, Student's *t*-test.

carcinogenesis through increasing androgen signaling. Although our efforts in determining effects of *ATF3* on androgen signaling in our mouse model were hindered by the lack of commercial antibodies suitable for detecting androgen-responsive genes by immunohistochemistry, we have previously demonstrated that the loss of *ATF3* is sufficient to enhance androgen signaling in mouse prostatic epithelia.¹³ Interestingly, *ATF3* expression could be induced by both androgen stimulation (Figure 2b) and androgen deprivation.¹³ Although these observations are consistent with the notion that *ATF3* is a broad stress sensor, it would be interesting to further elucidate the mechanism(s) underlying *ATF3* induction by androgen alterations for a better understanding of the regulation of androgen signaling by *ATF3*.

An important finding from this study is that loss of *ATF3* induced the emergence of prostate epithelial cells expressing both basal-cell and luminal-cell markers, suggesting that *ATF3* deficiency might promote prostatic basal epithelial cells to differentiate into luminal cells. Not only luminal-like p63⁺ cells were wide-spread in *ATF3*-KO prostate lesions, but we found a significant increase in the number of CK5⁺CK8⁺ cells that were likely intermediate between basal and luminal cells. Although both basal cells and luminal cells can be self-sustained and serve as the cell of origin for prostate cancer,²⁹ basal cells are often considered stem-like cells³¹ and can be converted into luminal cells likely through asymmetrical division.³⁷ Indeed, the intermediate cells found in the *ATF3*-deficient lesions were often localized vertically to the basement membrane (Figures 6a and 7a), suggesting that they might be generated from asymmetrical division of stem-like basal cells. Although the

definite origin of these intermediate cells would need to be determined through cell lineage tracing using fluorescent reporters, our results suggest that hormone-induced prostate lesions had a basal-cell origin. This notion appears to contradict a recent report, which concluded that luminal cells are favored as the cell of origin for hormone-induced prostate cancer.²⁴ However, the lineage-tracing approach used in this recent study has a limitation in that only a portion of basal cells are fluorescently labeled.²⁹ Thus, the possibility that hormone-induced prostate lesions were partially derived from a small portion of unlabeled basal cells cannot be excluded. It is important to note that prostate tumors derived from basal cells often have a long latency,²⁹ but appear to be more invasive likely owing to alterations in the *Spp1* and *Smad4*-mediated pathways that have been shown to promote invasion and metastasis of prostate cancer in a genetically engineered mouse model.^{38,39} It is thus likely that differentiation of basal cells into luminal cells (which are more competent to transformation) is a contributing factor for prostate tumorigenesis with a basal-cell origin.^{29,30} Interestingly, whereas T+E₂ can induce prostatic intraepithelial neoplasia in the WT prostate glands (albeit at a low frequency in our experiments, also see reference Ricke *et al.*⁵), we found that prostate lesions generated in the *ATF3*-deficient mice were invasive in almost all animals examined (Figures 4a and b). This observation provides an additional support to the notion that the loss of *ATF3* promoted basal-to-luminal differentiation leading to prostate lesions that were originated, at least in part, from basal cells. As AR has been shown to promote basal-to-luminal differentiation,³² it is highly likely that the enhanced androgen signaling led to the

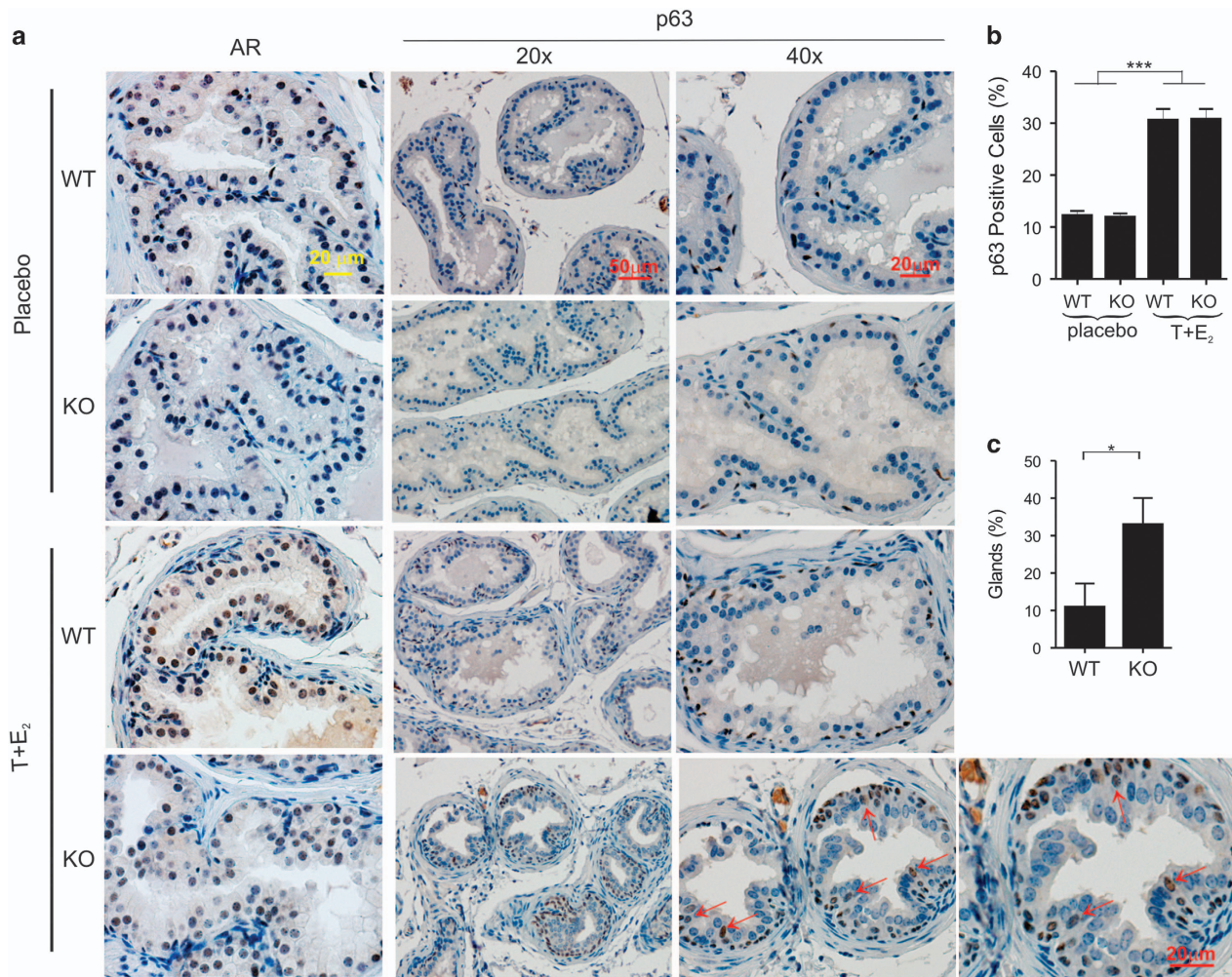


Figure 6. *ATF3*-deficient prostate lesions contain luminal-like, p63⁺ cells. **(a)** DP sections were subjected to immunohistochemical staining for AR and p63 expression. Arrows indicate luminal-like, p63⁺ cells. **(b)** Percentages of p63⁺ cells. Cells in random fields (×20) (sections from three mice for each group) were counted. **(c)** DP glands containing luminal-like, p63⁺ cells were counted as **(b)** and presented as percentages in the graph. **P* < 0.05; ****P* < 0.001; Student's *t*-test.

differentiation in the *ATF3*-deficient prostates. Interestingly, when CK5⁺CK8⁺ cells were examined in the prostate lesions generated by genetic ablation of the tumor suppressor *Pten*, we only saw very few double-stained cells, and *ATF3* deficiency did not appear to increase the number of intermediate cells in this mouse model (data not shown). These observations were not unexpected, given that it is known that AR signaling is impaired in *Pten*-deficient prostates.^{40,41} These results thus provide an additional support to the notion that enhanced androgen signaling due to loss of *ATF3* likely lead to the basal-to-luminal differentiation found in the hormone-induced prostate lesions. Accordingly, given that the role of androgen signaling in hormone-induced prostate carcinogenesis is unclear, it would be interesting to test whether testosterone serves to induce basal-to-luminal differentiation thereby facilitating cellular transformation stimulated by estradiol.

MATERIALS AND METHODS

Animals and hormone treatments

Animal experiments were carried out according to protocols approved by the Institutional Committee of Animal Care and Use (ICACU) of the Albany Medical College and the ICACU of Georgia Regents University. *ATF3*-KO (*ATF3*^{-/-}) mice were described previously.^{13,42} For prostate carcinogenesis, 8 to 12 mice (C57BL/6) were subcutaneously implanted with pellets embedded with 25 mg of testosterone propionate (SA-211) and 2.5 mg of β-estradiol 17-

acetate (SE-271) (Innovative Research of America, Sarasota, FL, USA), or placebo (SC-111), at the age of 8 weeks. Mice were killed 2 months later, and subjected to histopathological examinations as described previously.¹³

Immunohistochemistry and immunofluorescence staining

These were carried out essentially as described previously.¹³ In brief, prostate sections were treated with a hot citrate buffer, and subjected to immunohistochemical staining using the ABC Elite Kit and the DAB Kit (Vector laboratories, Burlingame, CA, USA) according to the manufacturers' protocols. PCNA (sc-56, 1:1000), *ATF3* (sc-188, 1:200), AR (sc-816, 1:200) and p63 (sc-8430, 1:200) antibodies were purchased from Santa Cruz (Dallas, TX, USA). α-smooth muscle actin staining was performed using an alkaline phosphatase-conjugated anti-α-smooth muscle actin antibody (Sigma, St Louis, MO, USA; 1:600) and SIGMAFAST Fast Red TR/Naphthol AS-MX tablets (F4523, Sigma-Aldrich, St Louis, MO, USA) according to the supplier's protocol. For CK5/CK8 double staining, prostate sections were incubated with CK5 (PRB-160P, 1:500) and CK8 (MMS-162P, 1:500) antibodies (Biolegend, San Diego, CA, USA), followed by incubation with Alexa Fluor 594-conjugated anti-rabbit IgG (A-24923) and Alexa Fluor 488-conjugated anti-mouse IgG (A-21131, ThermoFisher Scientific, Waltham, MA, USA).

Cell culture and generation of *ATF3*-KO PC3 cells

LNCAp and PC3 cells, originally from ATCC, were cultured in RPMI1640 medium supplemented with 10% fetal bovine serum. For hormone treatments, cells were first cultured in charcoal-stripped medium, followed by supplementing

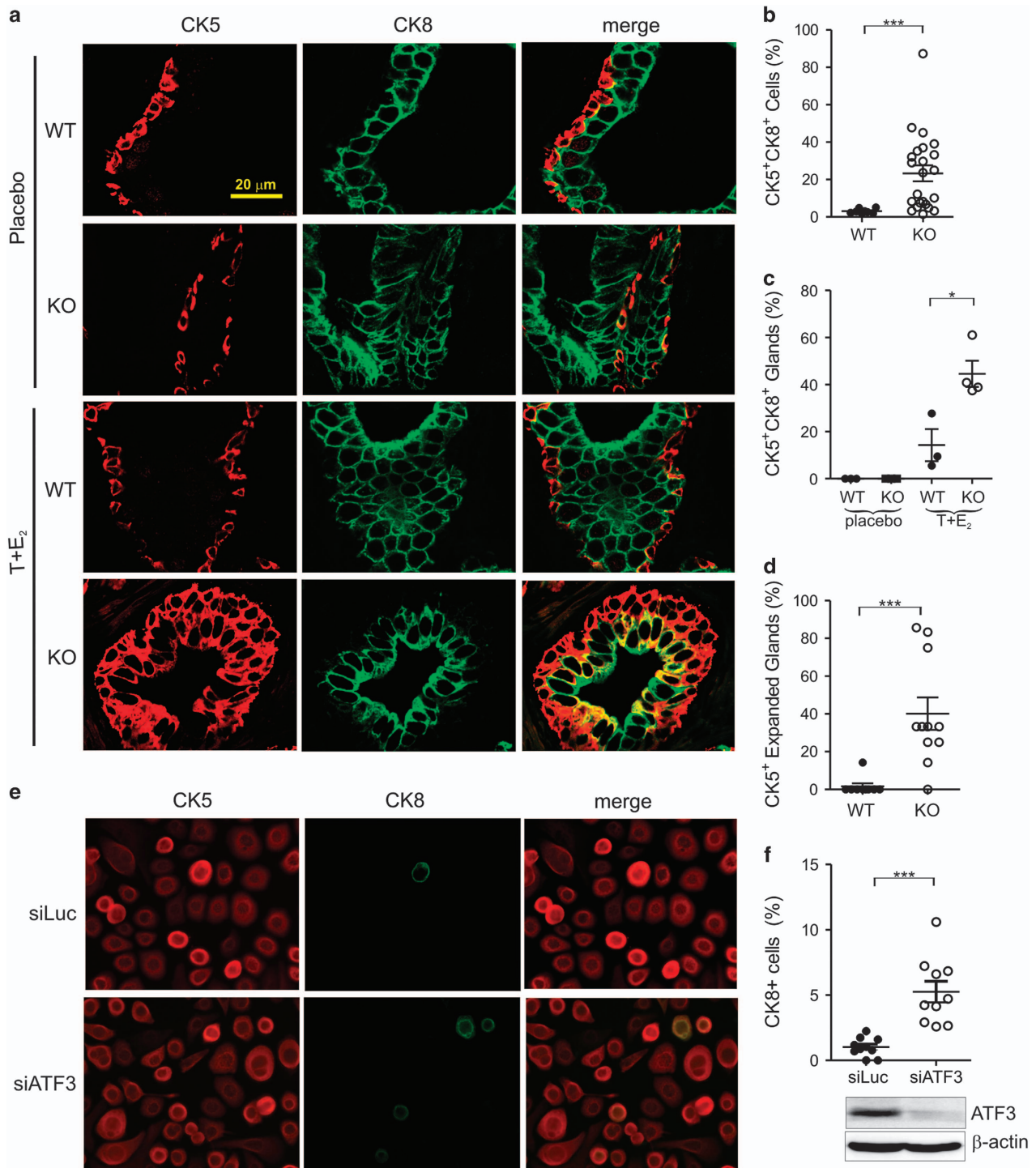


Figure 7. Loss of ATF3 increased the CK5⁺CK8⁺ cell number in T+E₂-treated DPs. **(a)** DP sections were double-stained with CK5 (red) and CK8 (green) antibodies, and observed under a confocal microscope. **(b)** CK5⁺CK8⁺ cells in each DP (from three to four mice each group) were counted and presented as percentages of total epithelial cells. **(c)** Percentage of glands containing CK5⁺CK8⁺ cells for each group (three to four mice for each group) is shown. **(d)** Glands with multiple CK5⁺ layers in random ×20 fields were counted and presented as percentages of total glands. Only hormone-treated samples were scored in panel **b** and **d**. **(e, f)** RWPE-1 cells were transfected with siATF3 or a control siRNA (siLuc) for 3 days, and then stained for CK5 and CK8 expression. CK8⁺ cells in 10 random microscopic fields (×20) were counted and the numbers were depicted in **f**. The western blots under the graph show decreased ATF3 expression in siATF3-transfected cells. **P* < 0.05; ****P* < 0.001; Student's *t*-test.

with 1 nM of R1881 (Perkin Elmer, Waltham, MA, USA) or 10 nM of E2 (Sigma). To generate ATF3-KO PC3 cells using the CRISPR-Cas9 technology, oligonucleotides containing a sequence for an ATF3-specific guided RNA (5'-AAAATGATGCTTCAACACCC-3') was inserted into pSpCas9(BB)-2A-Puro.⁴³ PC3 cells were transfected with the resulted construct for 2 days, selected with puromycin for 2 days, and then plated at a low density in 100-mm dishes.

Individual clones were then expanded, and subjected to western blotting for screening for clones lacking ATF3 expression. RWPE-1 cells were purchased from ATCC, and cultured in keratinocyte serum-free medium (Invitrogen, Carlsbad, CA, USA). Cells (the third passage) in 24-well plates were transfected with 50 pmol of siATF3 or siLuc¹³ for 3 days and then stained for CK5/CK8 expression.

Western blotting assays

Western blotting assays were performed as described previously.¹³ In brief, cells were lysed in RIPA buffer containing 50 mM Tris-HCl, pH 7.4, 1% Nonidet P-40, 0.25% sodium deoxycholate, 150 mM NaCl, 1 mM EDTA, 1 mM PMSF, and 1 mM NaF, 1 mM Na₃VO₄ and protease inhibitor cocktail (Roche, Indianapolis, IN, USA), and then resolved in sodium dodecyl sulfate-polyacrylamide electrophoresis for immunoblotting.

Data and statistical analysis

ATF3 expression data and clinical features of prostate cancer patients were retrieved from the Cancer Genome Atlas (TCGA) database. To test for the difference in ATF3 expression between normal and tumor samples, Student's *t*-test or paired *t*-test was used. In the survival analysis, all percentiles between the lower and upper quartiles of ATF3 expression were computed and the best performing threshold was used as a cutoff point for high and low ATF3 expression. The Kaplan–Meier method and the log-rank test were used to compare recurrence-free survival curves between high and low ATF3 expression groups.

CONFLICT OF INTEREST

The authors declare no conflict of interest.

ACKNOWLEDGEMENTS

This work was supported by NIH grants R01CA139107 and R01CA164006, and a Department of Defense award W81XWH-15-1-0049 to CY. We thank Dr Ahmed Chadli for providing the PR antibody.

AUTHOR CONTRIBUTIONS

ZY bred the mice and carried out the experiments with the help of YT, HD, JZ and JKC. JK performed statistical analyses of the TCGA data. TH provided the ATF3^{-/-} mice and analyzed the data. HD, JZ, TH and JKC edited the manuscript. CY conceived the study, analyzed the data and wrote the manuscript.

REFERENCES

- Ricke WA, Wang Y, Cunha GR. Steroid hormones and carcinogenesis of the prostate: The role of estrogens. *Differentiation* 2007; **75**: 871–882.
- Prins GS, Korach KS. The role of estrogens and estrogen receptors in normal prostate growth and disease. *Steroids* 2008; **73**: 233–244.
- Bosland MC. The role of estrogens in prostate carcinogenesis: A rationale for chemoprevention. *Rev Urol* 2005; **7**: S4–S10.
- Noble RL. The development of prostatic adenocarcinoma in Nb rats following prolonged sex hormone administration. *Cancer Res* 1977; **37**: 1929–1933.
- Ricke WA, McPherson SJ, Bianco JJ, Cunha GR, Wang Y, Risbridger GP. Prostatic hormonal carcinogenesis is mediated by in situ estrogen production and estrogen receptor alpha signaling. *FASEB J* 2008; **22**: 1512–1520.
- Risbridger GP, Wang H, Frydenberg M, Cunha G. The metaplastic effects of estrogen on mouse prostate epithelium: Proliferation of cells with basal cell phenotype. *Endocrinol* 2001; **142**: 2443–2450.
- Risbridger G, Wang H, Young P, Kurita T, Wong YZ, Lubahn D et al. Evidence that epithelial and mesenchymal estrogen receptor- α mediates effects of estrogen on prostatic epithelium. *Dev Biol* 2001; **229**: 432–442.
- Culing Z, Klocker H, Bartsch G, Steiner H, Hobisch A. Androgen receptors in prostate cancer. *J Urol* 2003; **170**: 1363–1369.
- Gnanapragasam VJ, Robson CN, Leung HY, Neal DE. Androgen receptor signalling in prostate. *BJU International* 2000; **86**: 1001–1013.
- Bennett NC, Gardiner RA, Hooper JD, Johnson DW, Gobe GC. Molecular cell biology of androgen receptor signaling. *Int J Biochem Cell Biol* 2010; **42**: 813–827.
- Heemers HW, Tindall DJ. Androgen receptor (AR) coregulators: A diversity of functions converging on and regulating the AR transcriptional complex. *Endocr Rev* 2005; **28**: 778–808.
- Wang L, Hsu C-L, Chang C. Androgen receptor corepressors: An overview. *Prostate* 2005; **63**: 117–130.
- Wang H, Jiang M, Cui H, Chen M, Buttyan R, Hayward SW et al. The stress response mediator ATF3 represses androgen signaling by binding the androgen receptor. *Mol Cell Biol* 2012; **32**: 3190–3202.
- Hai T, Wolfgang CD, Marsee DK, Allen AE, Sivaprasad U. ATF3 and stress responses. *Gene Expression* 1999; **7**: 321–325.
- Yan C, Lu D, Hai T, Boyd DD. Activating transcription factor 3, a stress sensor, activates p53 by blocking its ubiquitination. *EMBO J* 2005; **24**: 2425–2435.
- Kang Y, Chen C, Massague J. A self-enabling TGF β response coupled to stress signaling: Smad engages stress response factor ATF3 for *Id1* repression in epithelial cells. *Mol Cell* 2003; **11**: 915–926.
- Gilchrist M, Thorsson V, Li B, Rust AG, Korb M, Roach JC et al. Systems biology approaches identify ATF3 as a negative regulator of Toll-like receptor 4. *Nature* 2006; **441**: 173–178.
- Hai T, Wolford CC, Chang Y-S. ATF3, a hub of the cellular adaptive-response network, in the pathogenesis of diseases: Is modulation of inflammation a unifying component? *Gene Expr* 2010; **15**: 1–11.
- Thompson MR, Xu D, Williams BR. ATF3 transcription factor and its emerging role in immunity and cancer. *J Mol Med* 2009; **87**: 1053–1060.
- Yan C, Boyd DD. ATF3 regulates the stability of p53: A link to cancer. *Cell Cycle* 2006; **5**: 926–929.
- Wang Z, Xu D, Ding H-F, Kim J, Zhang J, Hai T, Yan C. Loss of ATF3 promotes Akt activation and prostate cancer development in a *Pten* knockout mouse model. *Oncogene* 2015; **34**: 4975–4981.
- Wang Z, Yan C. Emerging roles of ATF3 in the suppression of prostate cancer. *Mol Cell Oncol* (in press).
- Wolford CC, McConoughey SJ, Jalgaonkar SP, Leon M, Merchant AS, Dominick JL et al. Transcription factor ATF3 links host adaptive response to breast cancer metastasis. *J Clin Invest* 2013; **123**: 2893–2906.
- Wang ZA, Toivanen R, Bergren SK, Chambon P, Shen MM. Luminal cells are favored as the cell of origin for prostate cancer. *Cell Rep* 2014; **8**: 1339–1346.
- Lapointe J, Li C, Higgins JP, Van De Rijn M, Bair E, Montgomery K et al. Gene expression profiling identifies clinically relevant subtypes of prostate cancer. *Proc Natl Acad Sci USA* 2004; **101**: 811–816.
- Tomlinson SA, Mehra R, Rhodes DR, Cao X, Wang L, Dhanasekaran SM et al. Integrative molecular concept modeling of prostate cancer progression. *Nat Genet* 2007; **39**: 41–51.
- Lau K-M, LaSpina M, Long J, Ho S-M. Expression of estrogen receptor (ER)- α and ER- β in normal and malignant prostatic epithelial cells: Regulation by methylation and involvement in growth regulation. *Cancer Res* 2000; **60**: 3175–3182.
- Goldstein AS, Witte ON. Does the microenvironment influence the cell types of origin for prostate cancer? *Genes Dev* 2013; **27**: 1539–1544.
- Choi N, Zhang B, Zhang L, Ittmann M, Xin L. Adult murine prostate basal and luminal cells are self-sustained lineages that can both serve as targets for prostate cancer initiation. *Cancer Cell* 2012; **21**: 253–265.
- Kwon O-J, Zhang L, Ittmann MM, Xin L. Prostatic inflammation enhances basal-to-luminal differentiation and accelerates initiation of prostate cancer with a basal cell origin. *Proc Natl Acad Sci USA* 2014; **111**: E592–E600.
- Bonkhoff H, Remberger K. Differentiation pathways and histogenetic aspects of normal and abnormal prostatic growth: A stem cell model. *Prostate* 1996; **28**: 98–106.
- Berger R, Febbo PG, Majumder PK, Zhao JJ, Mukherjee S, Signoretti S et al. Androgen-induced differentiation and tumorigenicity of human prostate epithelial cells. *Cancer Res* 2004; **64**: 8867–8875.
- Okamoto A, Iwamoto Y, Maru Y. Oxidative stress-responsive transcription factor ATF3 potentially mediates diabetic angiopathy. *Mol Cell Biol* 2006; **26**: 1087–1097.
- Hoetzenecker W, Echtenacher B, Guenova E, Hoetzenecker K, Woelbling F, Bruck J et al. ROS-induced ATF3 causes susceptibility to secondary infections during sepsis-associated immunosuppression. *Nat Med* 2011; **18**: 128–134.
- Huang X, Li X, Guo B. KLF6 induced apoptosis in prostate cancer cells through upregulation of ATF3. *J Biol Chem* 2008; **283**: 29795–29801.
- Liu Y, Gao F, Jiang H, Niu L, Bi Y, Young CY et al. Induction of DNA damage and ATF3 by retigeric acid B, a novel topoisomerase II inhibitor, promotes apoptosis in prostate cancer cells. *Cancer Lett* 2013; **337**: 66–76.
- Wang J, Zhu HH, Chu M, Liu Y, Zhang C, Liu G et al. Symmetrical and asymmetrical division analysis provides evidence for a hierarchy of prostate epithelial cell lineages. *Nat Commun* 2014; **5**: 4758.
- Lu T-L, Huang Y-F, You L-R, Chao N-C, Su F-Y, Chang J-L et al. Conditionally ablated Pten in prostate basal cells promotes basal-to-luminal differentiation and causes invasive prostate cancer in mice. *Am J Pathol* 2013; **182**: 975–991.
- Ding Z, Wu CJ, Chu GC, Xiao Y, Ho D, Zhang J et al. SMAD4-dependent barrier constrains prostate cancer growth and metastatic progression. *Nature* 2011; **470**: 269–273.
- Mulholland DJ, Tran LM, Li Y, Cai H, Morim A, Wang S et al. Cell autonomous role of PTEN in regulating castration-resistant prostate cancer growth. *Cancer Cell* 2011; **19**: 792–804.
- Carverm BS, Chapinski C, Wongvipat J, Hieronymus H, Chen Y, Chandralapaty S et al. Reciprocal feedback regulation of PI3K and androgen receptor signaling in PTEN-deficient prostate cancer. *Cancer Cell* 2011; **19**: 575–586.
- Hartman MG, Lu D, Kim ML, Kociba GJ, Shukri T, Buteau J et al. Role for activating transcription factor 3 in stress-induced β -cell apoptosis. *Mol Cell Biol* 2004; **24**: 5721–5732.
- Ran FA, Hsu PD, Wright J, Agarwala V, Scott DA, Zhang F. Genome engineering using the CRISPR-Cas9 system. *Nat Protoc* 2013; **8**: 2281–2308.

The Stress Responsive Gene ATF3 Mediates Dichotomous UV Responses by Regulating Tip60 and p53

Hongmei Cui^{1,#}, Xingyao Li^{1,#}, Chunhua Han⁴, Qi-En Wang⁴, Hongbo Wang⁵, Han-Fei Ding^{1,2}, Junran Zhang⁶, Chunhong Yan^{1,3}

From ¹GRU Cancer Center, ²Department of Pathology, ³Department of Biochemistry and Molecular Biology, Medical College of Georgia, Augusta University, 1120 15th Street, Augusta, GA, 30912, USA.

⁴Department of Radiology, Ohio State University, 460 W. 12th Avenue, Columbus, OH 43210, USA.

⁵Key Laboratory of Molecular Pharmacology and Drug Evaluation, School of Pharmacy, Yantai University, Yantai 264005, P. R. China. ⁶Department of Radiation Oncology, School of Medicine, Case Western Reserve University, Cleveland, OH, 44106, USA

Running title: *ATF3 and UV response*

To whom correspondence should be addressed: Chunhong Yan, GRU Cancer Center, CN2134, 1410 Laney Walker Blvd., Augusta, GA 30912, USA. Telephone: (706)721-0099. Fax: (706)721-7376. E-mail: cyan@gru.edu. # These authors contribute equally to this work.

Key Words: stress response, p53, DNA repair, apoptosis, ATF3

ABSTRACT

The response to UV irradiation is important for a cell to maintain its genetic integrity when challenged by environmental genotoxins. An immediate early response to UV is the rapid induction of activating transcription factor 3 (ATF3) expression. Although emerging evidence has linked ATF3 to stress pathways regulated by the tumor suppressor p53 and the histone acetyltransferase Tip60, the role of ATF3 in the UV response remains largely unclear. Here, we report that ATF3 mediated dichotomous UV responses. While UV enhanced the binding of ATF3 to Tip60, knockdown of ATF3 expression decreased the Tip60 stability thereby impairing Tip60 induction by UV. In line with the role of Tip60 in mediating UV-induced apoptosis, ATF3 promoted the death of p53-defective cells in response to UV irradiation. However, ATF3 could also activate p53, and promote p53-mediated DNA repair mainly through altering histone modifications that could facilitate recruitment of DNA repair proteins (such as DDB2) to damaged DNA sites. As a result, ATF3 rather protected p53-wildtype cells from UV-induced apoptosis. Our results thus indicate that ATF3 regulates cell fates upon UV irradiation in a p53-dependent manner.

The DNA damage response is essential for the maintenance of genetic integrity in the face of

intrinsic and environmental genotoxins. In addition to γ -irradiation (IR) that often induces DNA double-strand breaks (DSB), UV irradiation represents another major genotoxic challenge that can cause bulky chemical modifications of single DNA strands such as cyclobutane pyrimidine dimers (CPDs) and (6-4)-phosphoproducts and cross-link DNA(1). Mammalian cells mobilize a mechanism referred to as nucleotide excision repair (NER) whereby a repair complex composed of up to 30 proteins is assembled at damaged sites, unwind, and excise DNA adducts from damaged strands (1). UV-induced DNA damage also provokes cellular signaling mediated by the sensor kinase ATR/ATM and notably the tumor suppressor p53, leading to rapid induction of cell cycle arrest to allow repair of damaged DNA, or apoptosis for the removal of irreparable cells (1). Intriguingly, while p53 induced by UV transactivates genes that can drive cell cycle arrest (e.g., p21) or apoptosis (e.g., Bax), it can also directly engage in NER by inducing expression of genes (i.e., DDB2 and XPC) responsible for sensing and binding DNA adducts to prime the repair of cross-linked DNA (2,3). p53 can also regulate the helicase activity of TFIIH (4), and promote UV-induced histone H3 acetylation and global chromatin relaxation required for the access of damaged sites to NER proteins (5), thereby promoting UV damage repair independent of its transcriptional activity (6). Contrary to the general view that p53 is pro-apoptotic, p53 is often pro-

survival in the UV response. Indeed, it has been shown that p53 protect cells from UV-induced apoptosis (7,8), and that p53 induced by a small molecule Nutlin-3a can effectively block apoptosis induced by UV irradiation via a mechanism involving p21-mediated repression of BRCA1 expression (9).

The MYST histone acetyltransferase (HAT) Tip60, or KAT5, is another important regulator of the cellular UV response. Although it can acetylate both histones and non-histone proteins to regulate gene expression, Tip60 is best known for its roles in regulating the cellular response to DNA double-strand breaks (10). Tip60 not only senses DSB, but promotes damage repair through altering chromatin structure, increasing deoxynucleoside triphosphate pool (11), and acetylating ATM for its activation (12). Tip60 can also selectively promote expression of pro-apoptotic genes (*e.g.*, PUMA) by acetylating p53 at lysine 120 in response to genotoxic stresses including UV (13,14). It thus comes as no surprise that Tip60 was shown to be indispensable for UV-induced apoptosis (9,15). However, recent evidence indicates that Tip60-mediated apoptosis upon UV irradiation does not require p53, but rather involves in pro-survival signaling mediated by JNK (9). Notably, although the Tip60 stability was shown to be controlled by the E3 ubiquitin ligase MDM2 (16), how Tip60 is regulated during the UV response is poorly understood.

Previously, we reported that activating transcription factor 3 (ATF3) is a major Tip60 regulator that can bind Tip60 and promote Tip60-mediated activation of ATM signaling upon IR (17). ATF3 achieves this function partly through stabilizing Tip60 as a consequence of promoting its deubiquitination mediated by the deubiquitinase USP7 (17). ATF3 is a member of the ATF/CREB transcription factor family, and can regulate gene expression through binding the consensus ATF/CREB *cis*-regulatory element via its basic-region leucine-zipper domain (bZip) (18). ATF3 can also regulate cellular functions independent of its transcriptional activity. ATF3, for instance, can directly interact with key cancer-associated proteins (*e.g.*, p53, E6, androgen receptor, and p63) and alter their interactions with DNA or other proteins (19-22). Although emerging evidence has linked ATF3 to several important human diseases including cancer

(23,24), the exact biological function of ATF3 remains largely unknown and sometimes controversial (25). As ATF3 can be rapidly induced by a wide range of cellular stresses including DNA damage (26), it is often assumed that ATF3 is required for a cell to maintain homeostasis upon cellular stresses (18). Indeed, our findings that ATF3 can activate p53 by blocking MDM2-mediated ubiquitination while regulating Tip60 and ATM activation (17,27) argue for the notion that ATF3 contributes to the maintenance of genetic stability in the face of genotoxic challenges. As ATF3 is one of the few genes immediately induced by UV in various cell types (28,29), ATF3 might also regulate the cellular response to UV-induced DNA damage. However, while ATF3 was shown to mediate UV-mediated cell death through transactivating Hif-2 α expression (30), an early study also suggests that ATF3 induces p15^{PAF} expression required for eliminating UV-induced DNA adducts and thus protect cells from UV-induced damage (31). This apparent paradox warrants further investigations into the precise role that ATF3 plays in the UV response.

Here, we provide evidence demonstrating that ATF3 mediated dichotomous cellular response to UV irradiation. While ATF3 was found to regulate Tip60 and promote UV-induced death of p53-defective cells, this stress responsive gene could rather protect p53-wildtype cells from UV-induced apoptosis by promoting p53-mediated DNA repair. ATF3 thus determined cell fates upon UV irradiation in a p53-dependent manner.

EXPERIMENTAL PROCEDURES

Cell culture - HCT116, U2OS, DU145 and PC3 cells are cultured in McCoy's 5A (HCT116), DMEM (U2OS and DU145), and RPMI 1640 medium (PC3) supplemented with 10% FBS, respectively, and routinely maintained in our laboratory. HCT116-F-Tip60 cells were genetically modified from HCT116 to express the endogenous Tip60 protein fused with a 3 \times FLAG tag (32). This modification allows to detect endogenous Tip60 using the well-characterized FLAG antibody. To generate ATF3-knockout (ATF3^{-/-}) cells, HCT116 cells were infected with adenoassociated viruses carrying a vector targeting the exon 2 of the *ATF3* gene. After the removal of the targeting vector, a 22-bp deletion was

generated within the exon (the details were described in a manuscript submitted elsewhere).

Knockdown by short-hairpin RNA (shRNA), siRNA, or single-guided RNA (sgRNA)- The pSIH-H1 shRNA Cloning and Lentivector Expression System (System Biosciences) were used to knock down ATF3 and p53 expression in HCT116 and U2OS cells as described previously (20). The targeted sequences for ATF3 and p53 were 5'-GCAAAGTGCCGAAACAAGA-3' and 5'-GACTCCAGTGGTAATCTAC-3', respectively. The Tip60 siRNA was synthesized on the basis of an earlier publication (13), and the targeted sequence was 5'-ACGGAAGGTGGAGGTGGTT-3'. To knock down ATF3 expression in PC3 and DU145 cells, a sgRNA (5'-AAAATGATGCTTCAACACCC-3') targeting a region immediate downstream of the *ATF3* start codon was co-expressed with hCas9. Clones with sgRNA-guided ATF3 knockdown were isolated as described previously (24).

Western blotting, GST-pulldown, and co-IP assays- For Western blotting, cells irradiated with UV were lysed in modified RIPA buffer containing 50 mM Tris-HCl, pH 7.4, 150 mM NaCl, 1% NP-40, 0.1% SDS, 0.5% sodium deoxycholate, 1 mM EDTA and proteinase inhibitor cocktails. Cytosolic, nucleoplasmic, and chromatin-bound proteins were separated from UV-treated cells following a protocol described recently (33). Briefly, cells were suspended in low-salt buffer (10 mM HEPES, pH7.4, 25 mM KCl, 10 mM NaCl, 1 mM MgCl₂, 0.1 mM EDTA, 0.5% NP-40 and proteinase inhibitors) at 4°C for 10 min to release cytosolic proteins. After centrifuge, pellets were suspended in high-salt buffer (50 mM Tris-HCl, pH 8.0, 1 mM EDTA, 10 mM MgCl₂, 300 mM KCl and proteinase inhibitors) and immediately centrifuged at 10,000 rpm for 5 min to extract nucleoplasmic proteins. Pellets were further suspended in MNase buffer (10 mM HEPES, pH7.9, 10 mM KCl, 1 mM CaCl₂, 1.5 mM MgCl₂, 0.35 M sucrose, 10% glycerol 0.1% Triton X-100 and 1 mM DTT) containing MNase (New England BioLabs) and incubated at 37°C for 10 min before an equal volume of solubilization buffer (MNase buffer plus 2% NP40, 2% Triton X-100 and 600 mM NaCl) was added to extract chromatin-bound proteins (33). For GST-pulldown assays (27), GST or GST fusion proteins (1 µg) immobilized

on 25 µl of glutathione-agarose (Sigma) were incubated with cell lysate containing equal amounts of Tip60 or ATF3 (adjusted on the basis of a pre-run Western blotting results) at 4°C overnight followed by extensive washes. Bound proteins were eluted and detected by Western blotting. For co-IP assay, cell lysates (1-2 mg) were incubated with 25 µl of Anti-FLAG M2 Affinity Gel (Sigma) at 4°C overnight. After extensive washes, precipitated proteins were detected by Western blotting. The antibodies were purchased from Santa Cruz (ATF3 (#sc-188), p53 DO-1 (#sc-126)), Cell Signaling (PARP (#9542) and cleaved caspase-3 (#9661)), Abcam (DDB2(#ab51017)), and Sigma (FLAG (#F3165) and β-actin (#A5441)), respectively. The Tip60 antibody was a kind gift from Dr. Bruno Amati (34).

Quantitative RT-PCR (qRT-PCR) -Total RNA was extracted from cells using Trizol (Invitrogen), reverse transcribed using the RevertAid cDNA Synthesis Kit, and subjected to real-time PCR assays using SYBR Green reagents (Qiagen) essentially as previously described (35). The sequences of the primers were: Tip60, 5'-GGGGAGATAATCGAGGGCTG-3' and 5'-TCCAGACGTTTGTGAAGTCAAT-3'; p15^{PAF}, 5'-ATGGTGC GGACTAAAGCAGAC-3' and 5'-CCTCGATGAACTGATGTCTGAAT; DDB2, 5'-CCTTCATCAAAGGGATTGGAGC-3' and 5'-TTGAGGAGGCGTAAACTGGT-3'; XPC, 5'-TTGACCCGGCTGGTATTGTC-3' and 5'-GTGCCCTTAGCAAAGGTTTCC-5'; p21, 5'-CTGGAGACTCTCAGGGTCGAAA-3' and 5'-GATTAGGGCTTCTCTTGGAGAA-3'; and GADPH, 5'-CAGCCTCAAGATCATCAGCA-3' and 5'-TGTGGTCATGAGTCCTTCCA-3'.

Colony formation assays- For colony formation assays, 200 cells plated in 6-well plates were irradiated by UV, and surviving colonies were stained with crystal violet 10 days later and counted as previously described (27).

CPD Quantitation - The cellular CPD level was measured using OxiSelect UV-induced DNA Damage ELISA Kit (Cell Biolabs, #STA-322) according to the manufacturer's protocol. Briefly, genomic DNA was prepared using Lysis buffer (10 mM Tris-HCl, pH 7.5, 10 mM EDTA, 10 mM NaCl, 0.5% SDS, 0.5 mg/ml proteinase K) at 50 °C overnight followed by phenol extraction (1:1)

and ethanol precipitation. The DNA dissolved in TE buffer was then treated with 0.2 mg/ml of RNase A at 37°C for 2 h, and purified by phenol extraction. 500 ng of DNA were then denatured and absorbed into wells of DNA High-Binding plate for ELISA using an anti-CPD antibody. To ensure that equal amounts of DNA were used for ELISA, 50 ng of DNA was also subjected to real-time PCR using primers 5'-CGCGAGGAGGAGCAACTG-3' and 5'-AGGAGCTCACATCCCCATTG-3', which amplified a 63-bp region in the human genome (chr9:80911735-80912222, hg19).

Immunofluorescence staining- This was carried out as described previously (33). Essentially, cells cultured on coverslips were washed with PBS and UV irradiated at 40 J/m² through a polycarbonate filter containing 5- μ m pores (Millipore), and then double stained with a mouse anti-DDB2 (1:50) (#ab51017, Abcam) and a rabbit anti-CPD antibody. Fluorescence images were obtained with a Nikon Fluorescence Microscope E80i, and processed with the SPOT software (Diagnostic Instruments).

Transfections and reporter assays- Transfections were carried out using Lipofectamine 2000 (Invitrogen) according to the manufacturer's protocol. pCMV-Luc was constructed by inserting a CMV promoter to pGL3 (35), and irradiated with 500 J/m² of UV before transfections. Cells in 24-well plates were co-transfected with 100 ng of UV-damaged or intact pCMV-Luc and 5 ng of pRL-CMV. 48 h later, cells were lysed for dual luciferase activity assays (Promega).

RESULTS

ATF3 stabilizes Tip60 in the UV response - We previously reported that ATF3 can stabilize Tip60 and activate ATM in response to IR (17). Given that ATF3 can be rapidly induced by UV (28,29), we sought to determine whether ATF3 also regulates Tip60 in the UV response. We thus knocked down ATF3 expression by shRNA or sgRNA in 3 genetically-diversified cancer cell lines (U2OS, PC3, and a genetically-modified HCT116 cells), treated the cells with UV (20 J/m²), and measured the Tip60 expression level by Western blotting. UV elevated the Tip60 protein level in early time points (4 and 8 h), but the Tip60 expression level was decreased to the basal level

24 h after UV (Fig 1A, 1B, and 1C). Importantly, not only the basal Tip60 level but the UV-induced increase of Tip60 expression was decreased in all 3 cell lines where ATF3 expression was knocked down (Fig 1A, 1B, and 1C). We also measured the Tip60 mRNA level by qRT-PCR. While UV rather repressed Tip60 transcription at 4 and 8 h after irradiation, ATF3 knockdown did not alter Tip60 transcription in both quiescent and UV-treated cells (Fig 1D). These results suggest that UV likely triggered an ATF3-dependent mechanism that could increase the Tip60 protein stability as an early response to UV. Indeed, we found that the Tip60 stability was decreased in UV-treated, ATF3-knockdown cells as measured by cycloheximide chase experiments (Fig 1E). These results indicate that ATF3 can stabilize Tip60 in response to UV radiation.

Interestingly, while it has been shown that ATF3 can stabilize Tip60 by binding the latter protein and promoting its deubiquitination (17), we found that UV could enhance the ATF3-Tip60 interaction. Thus, when cell lysates containing similar amounts of Tip60 were incubated with immobilized GST-ATF3, the amount of Tip60 down-pulled by GST-ATF3 from UV-treated samples was much more than that from quiescent cells (Fig 1F, lane 6 vs lane 5). This effect was also apparent 8 h after UV, but appeared to be diminished 24 h after the irradiation (Fig 1F). Co-immunoprecipitation assays confirmed that more ATF3 bound by Tip60 in UV-irradiated cells (Fig 1G, lane 2 vs lane 1). However, immobilized GST-Tip60 failed to pull down more ATF3 from lysates of UV-treated cells (data not shown), suggesting that it was UV-induced modification(s) of Tip60, but not that of ATF3, that led to the increase in the ATF3-Tip60 binding affinity.

Knockdown of ATF3 expression impairs UV-mediated apoptosis in a Tip60-dependent manner - As it has been shown that Tip60 can mediate apoptosis in the UV response (9,15), we determined whether the regulation of Tip60 by ATF3 contributes to UV-mediated cell death. Consistent with impaired Tip60 induction, UV-induced cleavage of PARP and caspase 3 - two well-established apoptosis markers - was significantly inhibited in ATF3-knockdown PC3 cells that are null for p53 (Fig 2A). Similar results were also obtained with DU145 cells harboring a p53 mutation (Fig 2B). Consistent with these

results, ATF3 down-regulated PC3 cells were resistant to UV-induced cell death as determined by colony formation assays (Fig 2C). Interestingly, while Tip60 siRNA (siTip60) impaired UV-induced apoptosis as expected, ATF3 knockdown was less effective in suppressing apoptosis in siTip60-expressing cells (Fig 2D, lane 8 vs. lane 4). These results argue for a notion that ATF3 promoted UV-mediated apoptosis by regulating Tip60.

Knockdown of ATF3 enhances UV-mediated apoptosis in HCT116 and U2OS cells - To our surprise, however, UV induced more cell death in ATF3-down-regulated U2OS and HCT116 cells, evidenced by higher levels of UV-induced cleaved PARP and caspase 3 in the shATF3-expressing cells (Fig 3A and 3B). Consistent with these observations, shATF3-expressing U2OS cells were rather sensitive to UV-induced cell death (Fig 3C). Importantly, while siTip60 remained its capability to impair UV-mediated apoptosis in HCT116 cells (Fig 3D, lane 4 vs lane 2), shATF3 expression could efficiently enhance apoptosis in Tip60-knockdown cells (Fig 3D, lane 8 vs. lane 4), suggesting that these unexpected apoptosis-promoting effects were likely independent of Tip60.

ATF3-mediated suppression of UV-induced apoptosis is dependent on p53- In addition to Tip60, ATF3 can increase the p53 stability in response to genotoxic stresses (27). Indeed, the p53 level was significantly lower in shATF3-expressing U2OS cells upon UV treatments (Fig 3B). As HCT116 and U2OS cells differ from PC3 and DU145 cells in that they carry wild-type p53, we tested a possibility that the suppression of UV-mediated death of HCT116 and U2OS cells by ATF3 was a consequence of ATF3-mediated p53 activation. Although counter-instinctual, both *in-vitro* and *in-vivo* evidence has demonstrated that p53 activation can protect cells from UV-mediated apoptosis (7-9). Employing isogenic p53-wildtype (Wt) and -null (p53^{-/-}) HCT116 cells, we confirmed that p53 deficiency promoted apoptosis induced by UV (Fig 4A, lanes 6-8 vs. lanes 2-4). Similarly, knockdown of p53 expression by shRNA in U2OS cells also increased the amounts of cleaved PARP and caspase 3 (Fig 4B, lane 4 vs. lane 2). To test our hypothesis, we generated isogenic HCT116 cells either null for ATF3 (ATF3^{-/-}) (manuscript submitted), or expressing

shATF3 in p53-null background (p53^{-/-};shATF3), and treated them along with wildtype (Wt) and p53^{-/-} HCT116 cells with UV. Knockout of ATF3 impaired UV-mediated p53 activation in HCT116 cells as expected (Fig 4C, lanes 5-6 vs lanes 2-3). Importantly, while UV-mediated apoptosis appeared to be more profound in ATF3-deficient, p53-wildtype cells (Fig 4C, lanes 5-6 vs lanes 2-3), defective ATF3 expression concurrently suppressed apoptosis induced by UV in p53-null cells (Fig 4C, lanes 11-12 vs. lanes 8-9). Colony formation assays confirmed that ATF3 defect sensitized p53-wildtype cells to, but prevented p53-deficient cells from, UV-mediated cell death (Fig 4D and 4E). Similar effects were observed when the isogenic cells were treated with higher dosages of UV radiation (Fig 4F). These results thus demonstrated that ATF3 can mediate dichotomous UV responses in a p53-dependent manner.

ATF3 promotes p53-mediated DNA repair - p53-mediated protection of UV-induced cell death is attributable to its ability to promote DNA damage repair (Fig 5A) (6). To understand the mechanism by which ATF3 protected p53-wildtype cells from UV-mediated death, we tested whether ATF3 promotes p53-mediated DNA repair. As CPDs are major DNA adducts induced by UV, we measured the CPD level in quiescent and UV-treated U2OS cells by ELISA. As expected, UV induced an increase in the CPD level, which was largely eliminated due to DNA repair 4 and 24 h after irradiation in U2OS cells (Fig 5B). Intriguingly, significantly higher levels of CPDs were detected in ATF3-knockdown cells than in shLuc cells 4 and 24 h after UV irradiation (Fig 5B). Of note, qPCR results confirmed that the samples subjected to ELISA contained an equal amount of DNA (Fig 5C). Moreover, it is unlikely that the observed difference between shATF3 and shLuc cells was due to off-target effects of shATF3, as we obtained similar results in U2OS cells engineered to knockout ATF3 expression by the CRISPR/Cas9 system (U2OS-KO) (Fig 5D). Furthermore, ATF3-knockout HCT116 cells (HCT116-KO) engineered with a different genome-editing strategy, i.e., adenoassociated virus-mediated homologous recombination (manuscript submitted), also maintained higher CPD levels after UV irradiation (Fig 5E). These

results thus indicate that ATF3 could promote DNA repair in response to UV irradiation.

To confirm that ATF3 is involved in repairing UV-damaged DNA, we transfected cells with a firefly luciferase reporter construct (pCMV-Luc) pre-irradiated with 500 J/m² of UV, and measure the luciferase activity two days after transfections. As UV irradiation generates DNA adducts that can prevent reporter expression, the relative luciferase activity measured with lysates from transfected cells represents the extent to which the DNA has been repaired. Consistent with the CPD ELISA results, the level of luciferase expressed from the UV-damaged DNA was significantly lower in ATF3-knockdown cells than in the control U2OS cells (Fig 5F). Such a decrease was not due to direct repression of reporter expression by the transcription factor ATF3, as the cells transfected with an intact, undamaged construct expressed luciferase at a same level (Fig 5F). We also carried out similar experiments using HCT116 isogenic cells (Fig 5G). While p53 deficiency resulted in impaired DNA repair as expected, the ATF3-null cells again repaired UV-damaged DNA less efficiently (Fig 5G, ATF3^{-/-} vs WT). Interestingly, ATF3 deficiency did not lead to a further decrease in the DNA repair efficiency in p53-null cells (Fig 5G, comparing ATF3^{-/-};p53^{-/-} with p53^{-/-}). These results are in line with a notion that ATF3 can promote p53-mediated DNA repair in the UV response.

ATF3 promotes p53-mediated H3 acetylation for DNA repair - It was previously reported that ATF3 can promote DNA repair by inducing p15^{PAF} expression upon UV irradiation (31). However, p15^{PAF} expression was only marginally induced by UV in both p53-wildtype and -null HCT116 cells (Fig 7A). As p53 can transactivate genes involved in NER (e.g., DDB2, XPC, and p21) (Fig 6A), we determined effects of ATF3 on p53 target gene expression for an understanding of how ATF3 promoted p53-mediated DNA repair. Although it was shown that expression of DDB2 and XPC is UV-inducible (2,3), we found that UV only slightly and transiently induced DDB2 and XPC expression in HCT116 cells (Fig 6B). However, p21 expression was strongly induced by UV (Fig 6C), indicating that UV-induced p53 was functional in these cells. Consistent with decreased p53 expression (Fig 6E, lanes 5-6 vs lanes 2-3), ATF3 deficiency caused a slight, but significant

decrease in DDB2 and XPC expression (Fig 7B), and a more profound decrease in p21 expression upon UV (Fig 7C). However, it was unlikely that these transcriptional changes were the main mechanism by which ATF3 promoted DNA repair, as knockout of ATF3 expression did not significantly alter the total DDB2 protein level (Fig 6D) while UV rather caused p21 degradation (Fig 6E). Indeed, it has been demonstrated that p21 degradation is required for efficient DNA repair in response to UV irradiation (36).

As p53 also contributes to DNA repair by inducing H3 acetylation (H3ac) that can cause an increase in the global DNA accessibility to NER proteins (Fig 6A), we tested whether ATF3 affects this transcription-independent event. As expected, UV caused a dramatic increase in the global H3ac level, which was largely impaired in p53-null cells (Fig 6F, lanes 8-9 vs. lanes 2-3). Importantly, ATF3 deficiency almost completely abolished UV-induced H3 acetylation (Fig 7E, lanes 5-6 vs. lanes 2-3). In line with the notion that these chromatin changes could lead to impaired recruitments of NER proteins to damaged DNA sites, we found that UV-induced increase of DDB2 binding to the chromatin (Fig 6G, lane 6 vs. lane 3) (33) was largely abolished in ATF3-deficient cells (Fig 6G, lane 12 vs. lane 9). Moreover, the amount of DDB2 recruited to CPD foci caused by UV microirradiation was largely decreased in a majority of ATF3-deficient U2OS cells and HCT116 cells (Fig 6G), indicating that ATF3 deficiency indeed impaired the recruitment of DDB2 to damaged DNA sites. Therefore, our results strongly suggest that ATF3 can facilitate p53-mediated DNA repair by promoting UV-induced H3 acetylation and subsequent increase of accessibility of damaged DNA to NER proteins.

DISCUSSION

The common stress-responsive transcription factor ATF3 is one of the few immediate early genes induced by UV (28,29), but its role in the UV response remains largely unknown. Two earlier studies report seemingly conflicting results, *i.e.*, ATF3 mediates UV-induced apoptosis while promoting DNA repair upon UV irradiation in the same cells (30,31). They also report that ATF3 achieves these different functions through transactivating Hif-2 α and p15^{PAF} expression, respectively (30,31). However, neither Hif-2 α

(data not shown) nor p15^{PAF} expression (Fig 6A) was noticeably induced by UV in our experimental settings. Rather, we found in this study that ATF3 mediated dichotomous UV responses in a manner independent of its transcriptional activity, but dependent on cellular contexts. In this regard, ATF3 could bind and stabilize Tip60 to promote cell death while promoting p53-mediated DNA repair to evade apoptosis upon UV. As the latter effect can outcompete Tip60-mediated apoptosis (9), ATF3 protected p53-wildtype cells from UV-induced death but promoted apoptosis in cells defective in p53 after UV irradiation (Fig 7). It is important to note that ATF3 mediated dichotomous UV responses in isogenic cell lines differing only in the p53/ATF3 status, and thus these different responses were unlikely caused by the difference in other genetic contexts. Interestingly, the early report indicating that ATF3 is pro-apoptotic in the UV response employed cells either carry a mutant p53 gene (*i.e.*, HaCaT), or express inactivated p53 protein (*i.e.*, HeLa) (30). Our results thus provide evidence arguing for a notion that p53 functionality dictates the role of ATF3 that plays in the UV response. As therapeutic agents (*e.g.*, cisplatin) often induce ATF3 expression and cause DNA damage, our findings also suggest that ATF3 might mediate different cellular responses resulting in either sensitization of, or resistance to, therapies in cancer cells with different p53 mutation status. Indeed, while ATF3 is often regarded as a pro-apoptotic molecule (22), it was also shown to suppress apoptosis induced by cisplatin in T98G glioblastoma cells (37). Although the p53 status in T98G cells remains controversial, our results support targeting ATF3 as an effective strategy for treating p53-mutated cancers (22).

Although Tip60 is required for UV-induced apoptosis (9,15), how this HAT is regulated in the UV response remains unclear. Previously, we found that ATF3 is a major Tip60 regulator and required for Tip60-mediated cellular response to DSBs (17). Here, we show that ATF3 could also bind and stabilize Tip60 in the UV response. Interestingly, while IR does not affect the ATF3-Tip60 interaction, UV enhanced the binding of Tip60 to ATF3 (Fig 1F and 1G). Such an increase in ATF3-Tip60 binding appeared to be important for cells to sustain and increase the Tip60 protein level in the early periods when UV-caused DNA

damage dramatically inhibited Tip60 transcription (Fig 1D). Indeed, we previously showed that the binding of ATF3 to Tip60 can promote the removal of ubiquitin chains by the deubiquitinase USP7 thereby preventing Tip60 from proteosomal degradation (17). As ATF3 can interact with MDM2 (38) and the latter E3 ubiquitin ligase was suggested to be involved in UV-induced Tip60 expression (16), there is also a possibility that ATF3 stabilized Tip60 by regulating MDM2 in the UV response. However, we did not find evidence that MDM2 could mediate degradation of Tip60 (data not shown). On the other hand, our results suggest that UV might cause posttranslational modifications of Tip60 thereby altering its conformation in a way in favor of its interaction with ATF3. Although it remains elusive whether UV can indeed induce Tip60 posttranslational modifications, it was recently shown that IR can induce Tip60 phosphorylation to promote its binding to methylated histones (39).

The results that ATF3 knockdown promotes UV-induced apoptosis in HCT116 and U2OS cells (Fig 4A and 4B) came initially as a surprise as Tip60 expression was significantly suppressed in these cells (Fig 1A and 1B). While our results confirmed the previous observations that ATF3 can activate p53 in response to UV (Fig 4C and 6E)(27), it is counterintuitive that p53 - the widely-regarded pro-apoptotic molecule - protects cells from UV-induced apoptosis (7-9). However, the roles of p53 in promoting NER for the repair of UV-damaged DNA have been well established (6). Although UV only slightly/modestly induced DDB2 and XPC expression in our experiments, it dramatically induced histone H3 acetylation to promote access of damaged DNA sites to NER proteins in a p53-dependent manner (5) (Fig 6F). Accordingly, ATF3 appeared to promote DNA repair mainly through regulating p53-mediated H3 acetylation. Indeed, ATF3 did not appear to promote DNA repair in p53-null HCT116 cells (Fig 5G), but could facilitate the recruitment of DDB2 to CPD foci (Fig 6H). As p53 serves as a chromatin accessibility factor by recruiting the HAT p300 to the damaged sites (5), ATF3 might regulate this p53-dependent function by promoting the interaction between p53 and p300. In support of this notion, we previously showed that p300 mediated acetylation of p53 was increased in ATF3-expressing cells (27).

Acknowledgments

This work was supported by NIH grants (R01CA139107 and R01CA164006) and a Department of Defense award (W81XWH-15-1-0049) to CY. The content is solely the responsibility of the authors and does not necessarily represent the official views of the National Institutes of Health. We thank Drs. Bert Vogelstein and Zhenghe Wang for providing HCT116 p53-null and F-Tip60 cells, and Dr. Bruno Amati for providing the Tip60 antibody.

Conflict of Interest

The authors declare that they have no conflict of interest.

Author Contributions: *HC* performed the experiments shown in Figures 1-4. *XL* performed the experiments shown in Figure 5, and the panels of Figure 6 except 6H, which was carried out by *CH* and *QW*. *HW*, *HD* and *JZ* contributed to data analysis and experimental design. *CY* designed the experiments, analyzed the data, and wrote the manuscript.

REFERENCES

1. Latonen, L. and Laiho, M. (2005) Cellular UV damage responses - Functions of tumor suppressor p53. *Biochim. Biophys. Acta* **1755**, 71-89
2. Hwang, B. J., Ford, J. M., Hanawalt, P. C., and Chu, G. (1999) Expression of the p48 xeroderma pigmentosum gene is p53-dependent and is involved in global genomic repair. *Proc. Natl. Acad. Sci. USA* **96**, 424-428
3. Adimoolam, S. and Ford, J. M. (2002) p53 and DNA damage-inducible expression of the xeroderma pigmentosum group C gene. *Proc. Natl. Acad. Sci. USA* **99**, 12985-12990
4. Wang, X. W., Yeh, H., Schaeffer, L., Roy, R., Moncollin, V., Egly, J.-M., Wang, Z., Friedberg, E. C., Evans, M. K., Taffe, B. G., Bohr, V. A., Weeda, G., Hoeijmakers, J. H. J., Forrester, K., and Harris, C. C. (1995) p53 modulation of TFIIH-associated nucleotide excision repair activity. *Nat. Genet.* **10**, 188-195
5. Rubbi, C. P. and Milner, J. (2003) p53 is a chromatin accessibility factor for nucleotide excision repair of DNA damage. *EMBO J.* **22**, 975-986
6. Sengupta, S. and Harris, C. C. (2005) p53: Traffic cop at the crossroads of DNA repair and recombination. *Nat. Rev. Mol. Cell Biol.* **6**, 44-55
7. McKay, B. C., Becerril, C., and Ljungman, M. (2001) p53 plays a protective role against UV- and cisplatin-induced apoptosis in transcription-coupled repair proficient fibroblasts. *Oncogene* **20**, 6805-6808
8. Jassim, O.W., Fink, J.L., Cagan, R.L. (2003) Dmp53 protects the *Drosophila* retina during a developmentally regulated DNA damage response. *EMBO J.* **22**, 5622-5632
9. Kranz, D., Dohmesen, C., and Dobbelstein, M. (2008) BRCA1 and Tip60 determine the cellular response to ultraviolet irradiation through distinct pathways. *J. Cell. Biol.* **182**, 197-213
10. Squatrito, M., Gorrini, C., and Amati, B. (2006) Tip60 in DNA damage response and growth control: Many tricks in one HAT. *Trends Cell. Biol.* **16**, 433-442
11. Niida, H., Katsuno, Y., Sengoku, M., Shimada, M., Yukawa, M., Ikura, M., Ikura, T., Kohno, K., Shima, H., Suzuki, H., Tashiro, S., and Nakanishi, M. (2010) Essential role of Tip60-dependent recruitment of ribonucleotide reductase at DNA damage sites in DNA repair during G1 phase. *Genes Dev.* **24**, 333-338
12. Sun, Y., Jiang, X., Chen, S., Fernandes, N., and Price, B. D. (2005) A role for the Tip60 histone acetyltransferase in the acetylation and activation of ATM. *Proc. Natl. Acad. Sci. USA* **102**, 13182-13187

13. Tang, Y., Luo, J., Zhang, W., and Gu, W. (2006) Tip60-dependent acetylation of p53 modulates the decision between cell-cycle arrest and apoptosis. *Mol. Cell* **24**, 827-839
14. Sykes, S., Hellert, H., Holbert, M., Li, K., Marmorstein, R., Lane, W., and McMahon, S. (2006) Acetylation of the p53 DNA-binding domain regulates apoptosis induction. *Mol. Cell* **24**, 841-851
15. Tyteca, S., Vandromme, M., Legube, G., Chevillard-Briet, M., and Trouche, D. (2006) Tip60 and p400 are both required for UV-induced apoptosis but play antagonistic roles in cell cycle progression. *EMBO J.* **25**, 1680-1689
16. Legube, G., Linares, L., Lemercier, C., Scheffner, M., Khochbin, S., and Trouche, D. (2002) Tip60 is targeted to proteasome-mediated degradation by Mdm2 and accumulates after UV irradiation. *EMBO J.* **21**, 1704-1712
17. Cui, H., Guo, M., Xu, D., Ding, Z.-C., Zhou, G., Ding, H.-F., Zhang, J., Tang, Y., and Yan, C. (2015) The stress-responsive gene ATF3 regulates the histone acetyltransferase Tip60. *Nat. Commun.* **6**, 6752
18. Yan, C. and Boyd, D. D. (2006) ATF3 regulates the stability of p53: A link to cancer. *Cell Cycle* **5**, 926-929
19. Stelzl, U., Worm, U., Lalowski, M., Haenig, C., Brembeck, F. H., Goehler, H., Stroedicke, M., Zenkner, M., Schoenherr, A., Koeppen, S., Timm, J., Mintzlaff, S., Abraham, C., Bock, N., Kietzmann, S., Goedde, A., Toksoz, E., Droege, A., Krobitsch, S., Korn, B., Birchmeier, W., Lehrach, H., and Wanker, E. E. (2005) A human protein-protein interaction network: A resource for annotating the proteome. *Cell* **122**, 957-968
20. Wang, H., Mo, P., Ren, S., and Yan, C. (2010) Activating transcription factor 3 activates p53 by preventing E6-associated protein from binding to E6. *J. Biol. Chem.* **285**, 13201-13210
21. Wang, H., Jiang, M., Cui, H., Chen, M., Buttyan, R., Hayward, S. W., Hai, T., Wang, Z., and Yan, C. (2012) The stress response mediator ATF3 represses androgen signaling by binding the androgen receptor. *Mol. Cell. Biol.* **32**, 3190-3202
22. Wei, S., Wang, H., Lu, C., Malmut, S., Zhang, J., Ren, S., Yu, G., Wang, W., Tang, D. D., and Yan, C. (2014) The activating transcription factor 3 protein suppresses the oncogenic function of mutant p53 proteins. *J. Biol. Chem.* **289**, 8947-8959
23. Yuan, X., Yu, L., Li, J., Xie, G., Rong, T., Zhang, L., Chen, J., Meng, Q., Irving, A. T., Wang, D., Williams, E. D., Liu, J. P., Sadler, A. J., Williams, B. R., Shen, L., and Xu, D. (2013) ATF3 suppresses metastasis of bladder cancer by regulating gelsolin-mediated remodeling of the actin cytoskeleton. *Cancer Res.* **73**, 3625-3637
24. Wang, Z., Xu, D., Ding, H.-F., Kim, J., Zhang, J., Hai, T., and Yan, C. (2015) Loss of ATF3 promotes Akt activation and prostate cancer development in a Pten knockout mouse model. *Oncogene* **34**, 4975-4984
25. Hai, T., Wolford, C. C., and Chang, Y.-S. (2010) ATF3, a hub of the cellular adaptive-response network, in the pathogenesis of diseases: Is modulation of inflammation a unifying component? *Gene Exp.* **15**, 1-11
26. Hai, T. and Hartman, M. G. (2001) The molecular biology and nomenclature of the activating transcription factor/cAMP responsive element binding family of transcription factors: activating transcription factor proteins and homeostasis. *Gene* **273**, 1-11
27. Yan, C., Lu, D., Hai, T., and Boyd, D. D. (2005) Activating transcription factor 3, a stress sensor, activates p53 by blocking its ubiquitination. *EMBO J.* **24**, 2425-2435
28. Amundson, S. A., Bittner, M., Chen, Y., Trent, J., Meltzer, P., and Fornace, A. J. (1999) Fluorescent cDNA microarray hybridization reveals complexity and heterogeneity of cellular genotoxic stresses responses. *Oncogene* **18**, 3666-3672
29. Abe, T., Oue, N., Yasui, W., and Ryoji, M. (2003) Rapid and preferential induction of ATF3 transcription in response to low doses of UVA light. *Biochem. Biophys. Res. Com.* **310**, 1168-1174
30. Turchi, L., Aberdam, E., Mazure, N., Pouyssegur, J., Deckert, M., Kitajima, S., Aberdam, D., and Virolle, T. (2008) Hif-2alpha mediates UV-induced apoptosis through a novel ATF3-dependent death pathway. *Cell Death Differ.* **15**, 1472-1480

31. Turchi, L., Fareh, M., Aberdam, E., Kitajima, S., Simpson, F., Wicking, C., Aberdam, D., and Virolle, T. (2009) ATF3 and p15^{PAF} are novel gatekeepers of genomic integrity upon UV stress. *Cell Death Differ.* **16**, 728-737
32. Du, Z., Song, J., Wang, Y., Zhao, Y., Guda, K., Yang, S., Kao, H.-Y., Xu, Y., Willis, J., Markowitz, S. D., Sedwick, D., Ewing, R. M., and Wang, Z. (2010) DNMT1 stability is regulated by proteins coordinating deubiquitination and acetylation-driven ubiquitination. *Sci. Signal.* **3**, ra80
33. Wang, Q.-E., Han, C., Zhao, R., Wani, G., Zhu, Q., Gong, L., Battu, A., Racoma, I., Sharma, N., Wani, A.A. (2013) p38 MAPK- and Akt-mediated p300 phosphorylation regulates its degradation to facilitate nucleotide excision repair. *Nucleic Acid Res* **41**, 1722-1733
34. Gorrini, C., Squatrito, M., Luise, C., Syed, N., Perna, D., Wark, L., Martinato, F., Sardella, D., Verrecchia, A., Bennett, S., Confalonieri, S., Cesaroni, M., Marchesi, F., Gasco, M., Scanziani, E., Capra, M., Mai, S., Nuciforo, P., Crook, T., Lough, J., and Amati, B. (2007) Tip60 is a haplo-insufficient tumour suppressor required for an oncogene-induced DNA damage response. *Nature* **448**, 1063-1067
35. Yan, C. and Boyd, D. D. (2006) Histone H3 acetylation and H3 K4 methylation define distinct chromatin regions permissive for transgene expression. *Mol. Cell. Biol.* **26**, 6357-6371
36. Bendjennat, M., Boulaire, J., Jascur, T., Brickner, H., Barbier, V., Sarasin, A., Fotedar, A., and Fotedar, R. (2003) UV irradiation triggers ubiquitin-dependent degradation of p21WAF1 to promote DNA repair. *Cell* **114**, 599-610
37. Hamdi, M., Popeijus, H. E., Carlotti, F., Janseen, J. M., van der Brugt, C., Cornelissen-Stijger, P., van del Water, B., Hoeben, R. C., Matsuo, K., and Van Dam, H. (2008) ATF3 and Fra1 have opposite functions in JNK- and ERK-dependent DNA damage response. *DNA Repair* **7**, 487-496
38. Mo, P., Wang, H., Lu, H., Boyd, D. D., and Yan, C. (2010) MDM2 mediates ubiquitination and degradation of activating transcription factor 3. *J. Biol. Chem.* **285**, 26908-26915
39. Kaidi, A. and Jackson, S. P. (2013) KAT5 tyrosine phosphorylation couples chromatin sensing to ATM signalling. *Nature* **498**, 70-74

FIGURE LEGENDS

Figure 1. **ATF3 stabilizes Tip60 in the UV response.** (A, B) HCT116-F-Tip60 (A) or U2OS (B) expressing shLuc or shATF3 were treated with 20 J/m² of UV, and lysed at different time for Western blotting. (C) PC3 cells and a sgATF3-targeted clone (sgATF3) were irradiated by 20 J/m² of UV for Western blotting. (D) HCT116-F-Tip60 cells expressing shLuc or shATF3 were treated with 20 J/m² of UV for qRT-PCR assays. The data are presented as mean ± SD (n=3). (E) 4 h after UV irradiation (20 J/m²), HCT116-F-Tip60 cells expressing shLuc or shATF3 were treated with 100 µg/ml of cycloheximide for indicated time, and lysed for Western blotting. The Tip60 protein was detected by the FLAG antibody. The plot shown in right presents the results from densitometric quantitation of the Tip60 protein level after normalized to the β-actin level. (F) GST or GST-ATF3 immobilized onto glutathione agarose was incubated with lysates generated from UV(20 J/m²)-treated HCT116-F-Tip60 cells and containing similar amounts of Tip60 for GST-pulldown assays. Tip60 levels were detected using the FLAG antibody. PonS, Ponceau S staining. (G) Lysates from HCT116-F-Tip60 cells treated with UV (20 J/m²) were incubated with the FLAG antibody to immunoprecipitate Tip60 and associated proteins for Western blotting. The Western blots are representative results of 3 independent experiments.

Figure 2. **ATF3 knockdown impairs UV-induced cell death by regulating Tip60.** (A, B) PC3, DU145, and corresponding sgATF3-targeted cells were treated with 20 J/m² of UV, and subjected to Western blotting assays for detection of PARP and caspase-3 cleavage. FL, full-length; CL, cleaved. (C) PC3 and PC3-sgATF3 cells were treated with 0, 5, 10, 20s and 30 J/m² of UV, and subjected to colony formation assays. The data are presented as mean ± SD (n=3). (D) PC3 and PC3-sgATF3 cells transfected with Tip60 siRNA (siTip60) or control siRNA (siLuc) were irradiated by UV (20 J/m²), and subjected to Western blotting for expression of cleaved PARP and caspase 3. The Western blots are representative results of 2-3 independent experiments.

Figure 3. **ATF3 knockdown promotes UV-mediated cell death in p53-wildtype cells.** (A, B) p53-wildtype HCT116-F-Tip60 (A) or U2OS (B) cells expressing shLuc or shATF3 were treated with UV (20 J/m²) for Western blotting. (C) U2OS cells expressing shLuc or shATF3 were treated with 0, 5, 10, 20, and 30 J/m² of UV for colony formation assays. The data are presented as mean ± SD (n=3). (D) Indicated HCT116 cells transfected with siTip60 or siLuc were subjected to UV irradiation (20 J/m²) for Western blotting. The Western blots are representative results of 2-3 independent experiments.

Figure 4. **ATF3 mediates different UV responses depending on p53 expression.** (A) HCT116 wild-type (HCT116-Wt) and p53-null (p53^{-/-}) cells were treated with UV (20 J/m²) for Western blotting. (B) U2OS cells infected with Lentiviruses expressing a p53-specific shRNA (shp53) or a control shRNA (shLuc) were treated with 20 J/m² of UV for Western blotting. (C) Indicated isogenic HCT116 cells were treated with 20 J/m² of UV for Western blotting. (D, E) Indicated isogenic HCT116 cells were treated with different doses of UV for colony formation assays. The data are presented as mean ± SD (n=3). (F) Indicated HCT116 cells were treated with different doses of UV, and lysed for Western blotting 24 h after irradiation. The Western blots are representative results of 2 independent experiments.

Figure 5. **Knockdown of ATF3 impairs DNA repair in response to UV.** (A) Schematic representation of the mechanisms by which p53 promotes nucleotide excision repair (NER) and protects cells from UV-induced apoptosis. (B, C) U2OS cells expressing shLuc or shATF3 were irradiated by 20 mJ² of UV, and harvested immediately (0 h), 4 h, or 24 h later for genomic DNA preparation. The genomic DNAs were subjected to ELISA for measuring CPD levels (B), or real-time PCR for measuring relative DNA amounts (C). (D, E) Indicated cells were treated with 20 mJ² of UV for CPD ELISA assays as in (B). (F) U2OS-knockout (U2OS-KO) and control (U2OS-Wt) cells in 24-well plates were co-transfected with 5

ng of pRL-CMV and 100 ng of UV-damaged or –undamaged (intact) pCMV-Luc plasmid for dual luciferase assays. **(G)** Indicated isogenic HCT116 cells were transfected with UV-damaged or –undamaged DNA as in (D), and subjected to dual luciferase assays. The data are presented as mean \pm SD (n=3).

Figure 6. ATF3 knockdown impairs p53-mediated mechanisms required for DNA repair. **(A)** Isogenic HCT116 cells were treated with 20 J/m² of UV for different time, and then subjected to qRT-PCR for measuring the p15^{P^{AF}} mRNA level. **(B, C)** HCT116-wildtype (ATF3-wt) and –ATF3 knockout (ATF3-KO) cells treated with 20 J/m² of UV for qRT-PCR assays to measure DDB2, XPC, and p21 mRNA levels. The data are presented as mean \pm SD (n=3). **(D, E)** The wild-type and ATF3-knockout cells were treated with 20 J/m² of UV, and subjected to Western blotting for DDB2, p53 and p21 expression as indicated. **(F)** Indicated isogenic HCT116 cells were treated with 20 J/m² of UV, and subjected to Western blotting for measuring the H3ac level. **(G)** Cytoplasmic (S), nucleoplasmic (NP), and chromatin (C) fractions were separated from indicated cells with or without UV irradiation, and subjected to Western blotting to detect DDB2 subcellular distribution. The Western blots are representative results of 3 independent experiments. **(H)** Indicated cells were subjected to UV microirradiation (40 J/m²) through polycarbonate filters, and then double stained by CPD and DDB2 antibodies. Arrows indicate representative cells where DDB2 recruitment to damaged DNA sites was reduced. This experiment was repeated once.

Figure 7. A model whereby ATF3 mediates dichotomous UV response. In response to UV, ATF3 can bind and stabilize Tip60 to promote cell death while promoting p53-mediated DNA repair to evade apoptosis upon UV. The outcome depends on whether p53 is functional in the cells. ATF3 protects p53-wildtype cells from UV-induced death but promotes apoptosis in cells defective in p53.

Figure 1

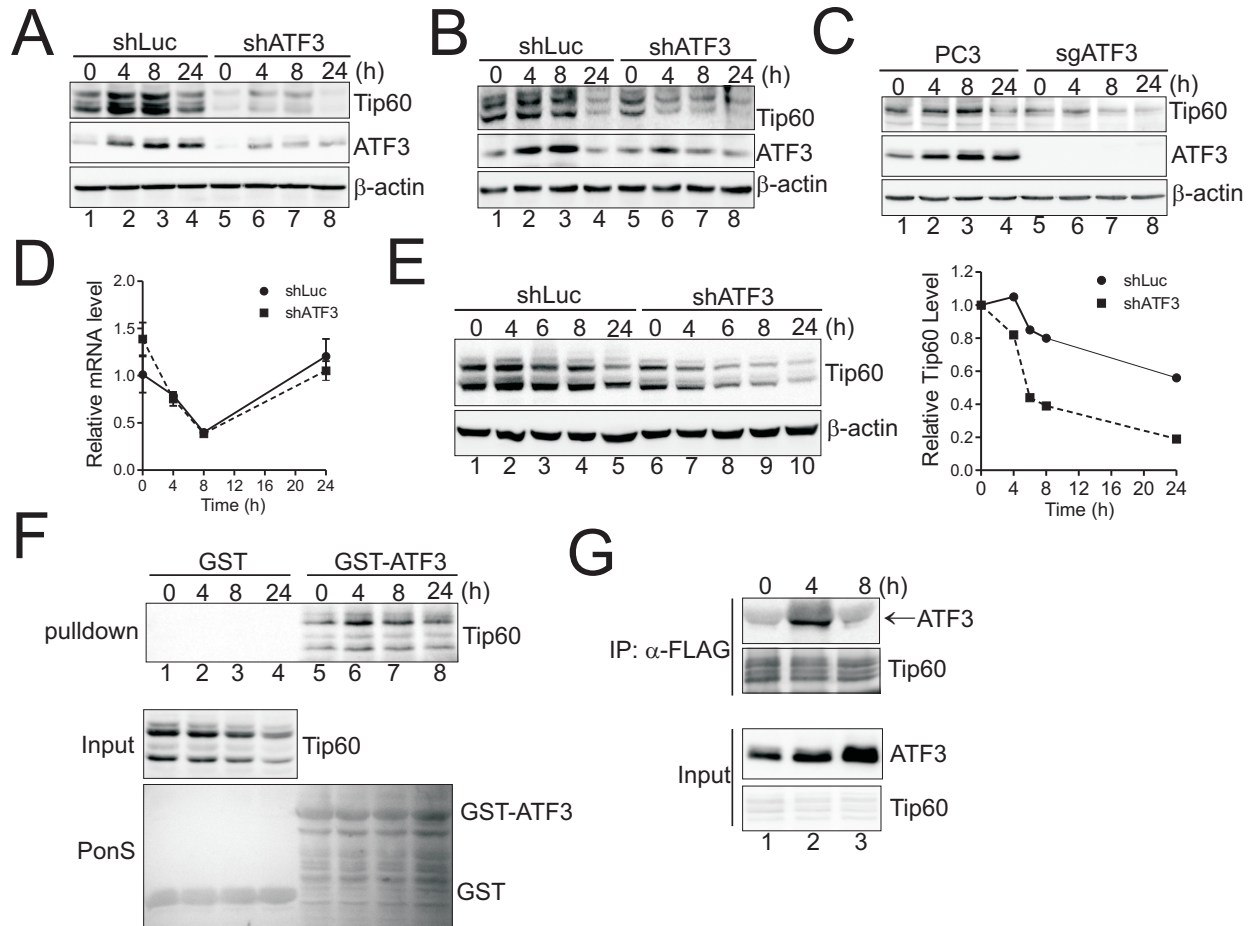


Figure 2

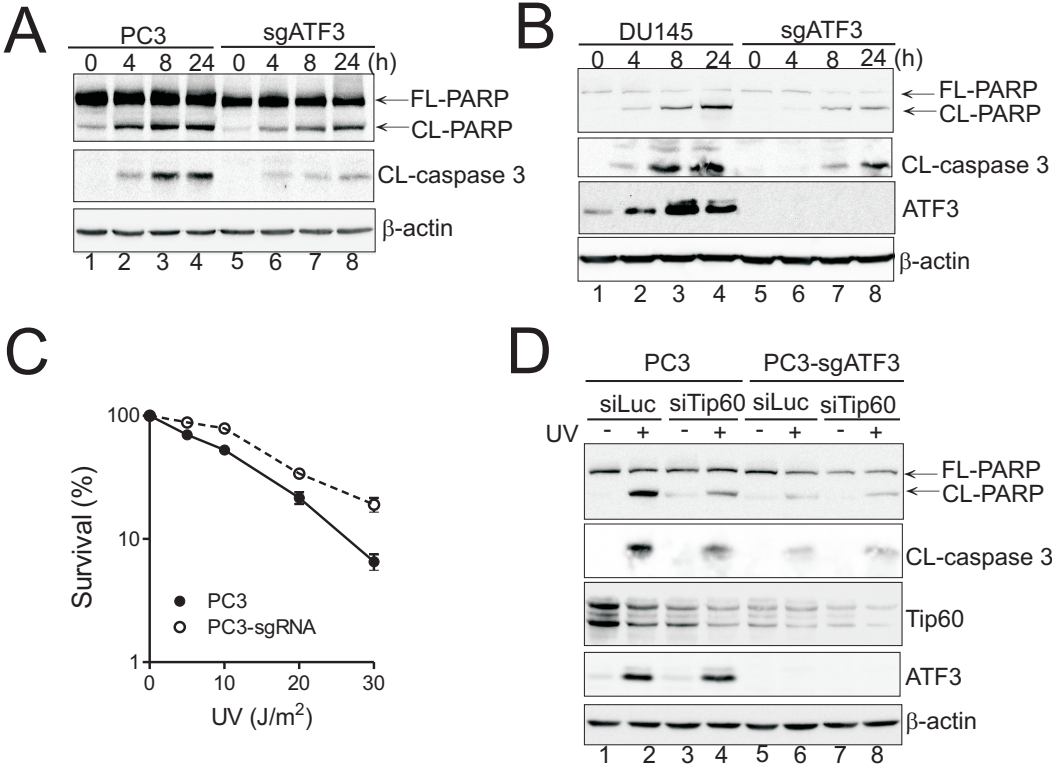


Figure 3

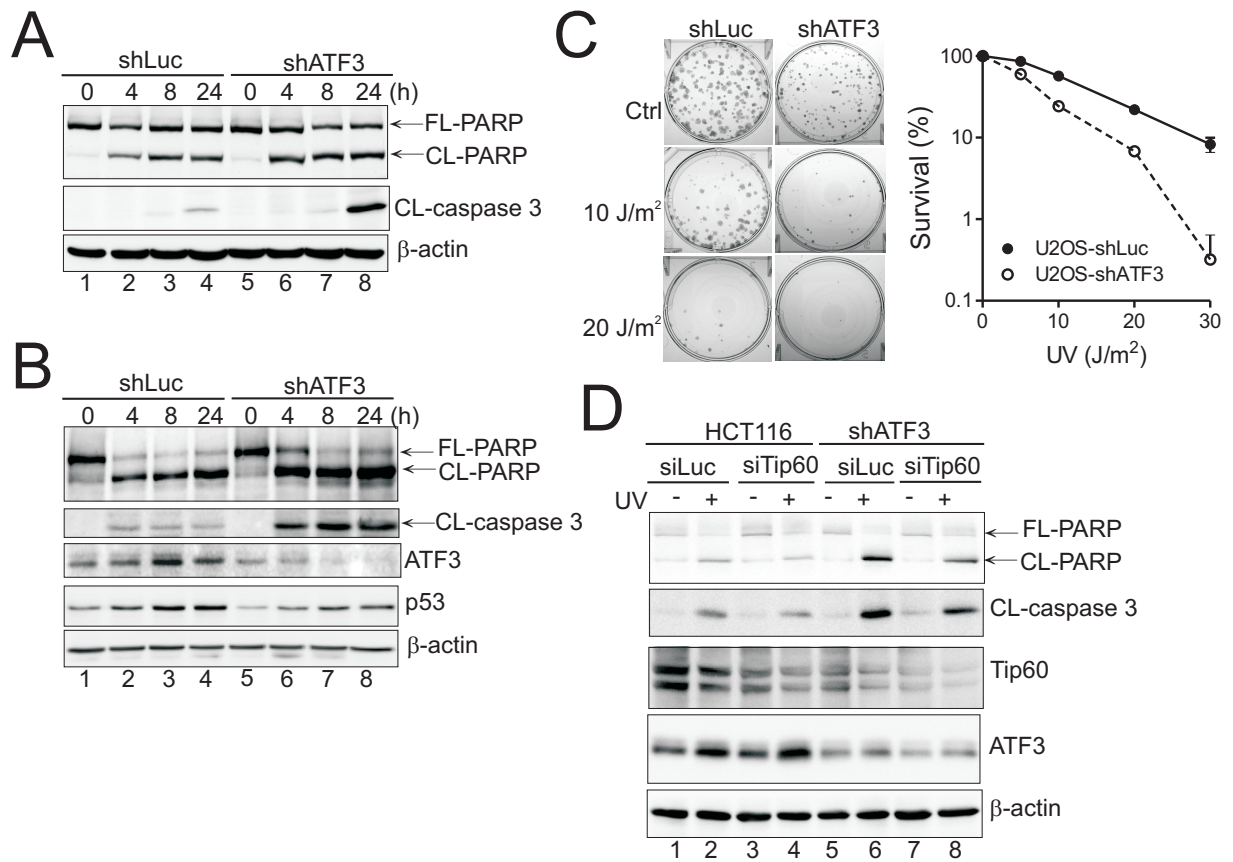


Figure 4

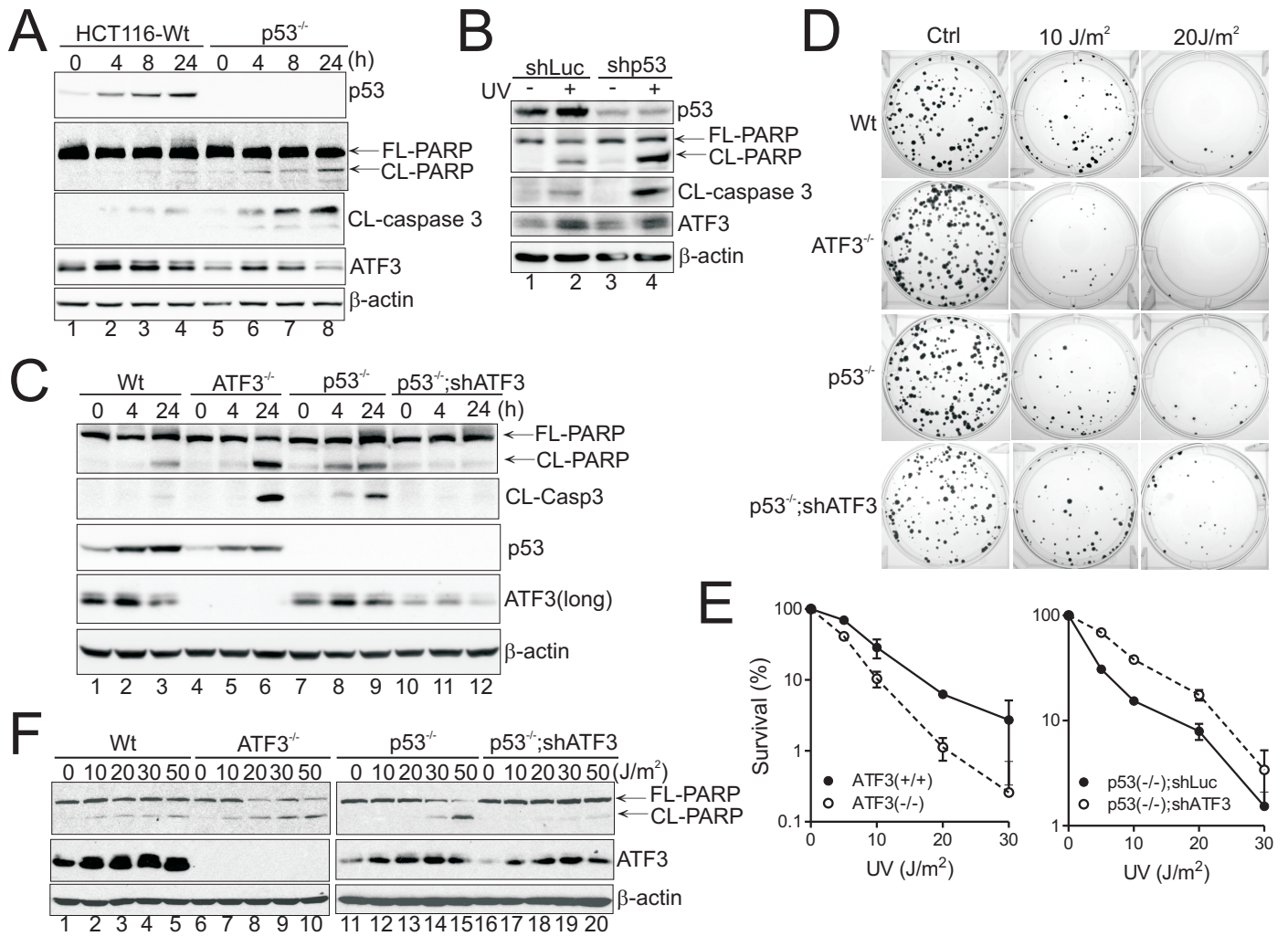


Figure 5

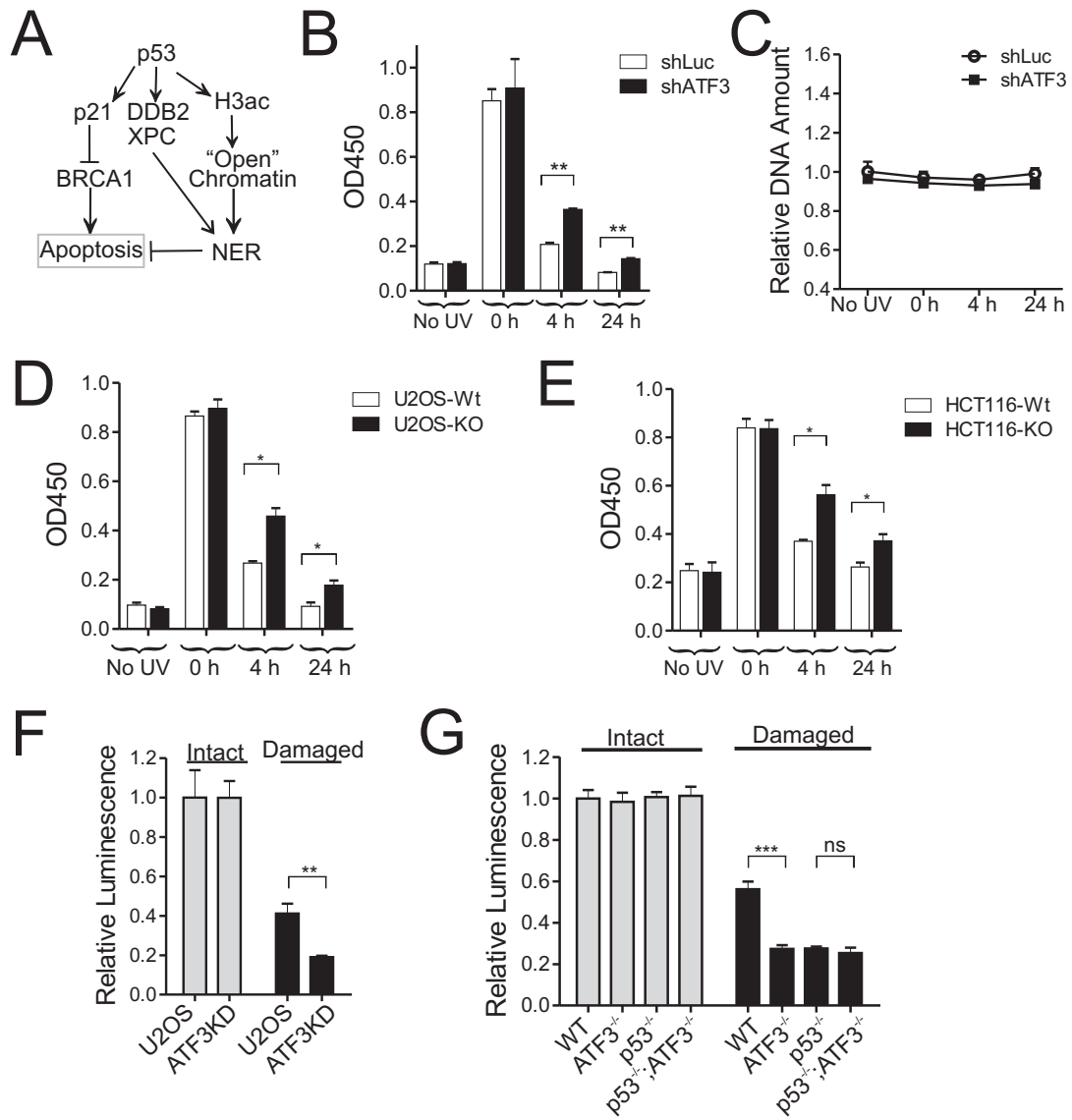


Figure 6

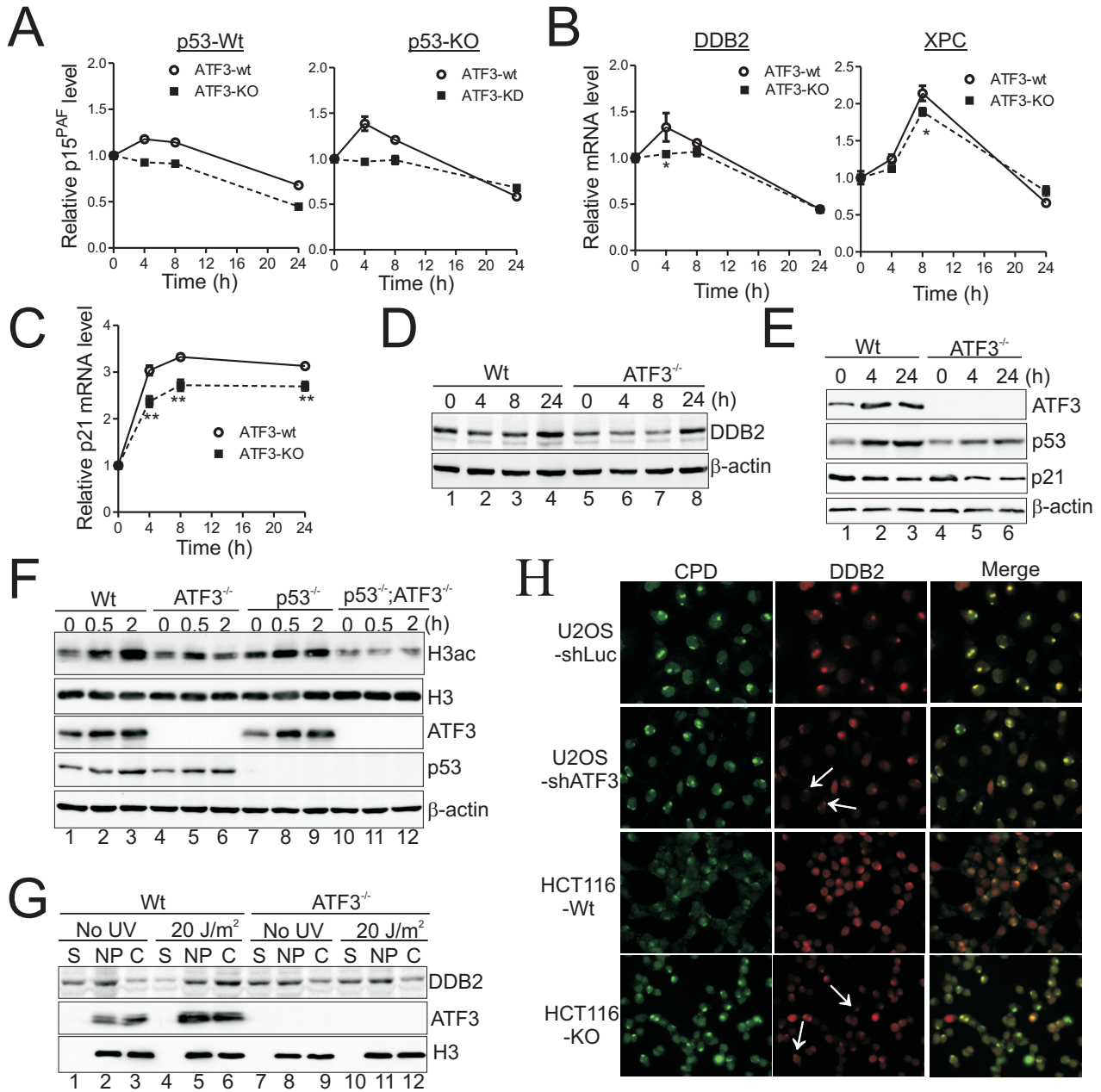
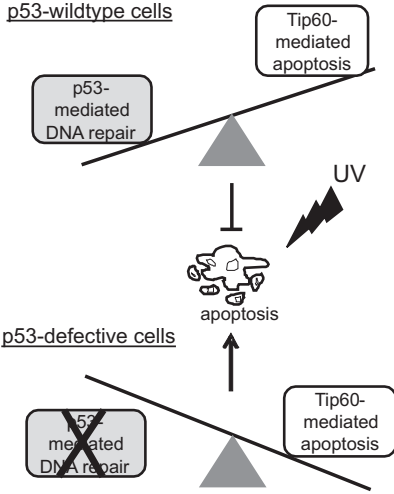


Figure 7



RESEARCH ARTICLE

Open Access



The common stress responsive transcription factor ATF3 binds genomic sites enriched with p300 and H3K27ac for transcriptional regulation

Jonathan Zhao^{1†}, Xingyao Li^{2†}, Mingxiong Guo⁴, Jindan Yu^{1*} and Chunhong Yan^{2,3,4*}

Abstract

Background: Dysregulation of the common stress responsive transcription factor ATF3 has been causally linked to many important human diseases such as cancer, atherosclerosis, infections, and hypospadias. Although it is believed that the ATF3 transcription activity is central to its cellular functions, how ATF3 regulates gene expression remains largely unknown. Here, we employed ATF3 wild-type and knockout isogenic cell lines to carry out the first comprehensive analysis of global ATF3-binding profiles in the human genome under basal and stressed (DNA damage) conditions.

Results: Although expressed at a low basal level, ATF3 was found to bind a large number of genomic sites that are often associated with genes involved in cellular stress responses. Interestingly, ATF3 appears to bind a large portion of genomic sites distal to transcription start sites and enriched with p300 and H3K27ac. Global gene expression profiling analysis indicates that genes proximal to these genomic sites were often regulated by ATF3. While DNA damage elicited by camptothecin dramatically altered the ATF3 binding profile, most of the genes regulated by ATF3 upon DNA damage were pre-bound by ATF3 before the stress. Moreover, we demonstrated that ATF3 was co-localized with the major stress responder p53 at genomic sites, thereby collaborating with p53 to regulate p53 target gene expression upon DNA damage.

Conclusions: These results suggest that ATF3 likely bookmarks genomic sites and interacts with other transcription regulators to control gene expression.

Keywords: ATF3, ChIP-seq, Enhancer, p300, H3K27ac, p53

Background

The development of human diseases is often accompanied by changes in the gene expression landscape. Regulated mainly at the transcription level, gene expression is tightly controlled by transcription factors (TF) that bind not only promoters proximal to transcription start sites (TSS), but also distal *cis*-regulatory elements (i.e., enhancers) that are far removed from TSS [1, 2]. Genome-wide profiling studies using chromatin immunoprecipitation coupled with

sequencing (ChIP-seq) have identified thousands of functional/active enhancers that are either bound by the transcriptional co-activator p300, or characterized by their association with high levels of H3 K27 acetylation (H3K27ac) [3–5]. These enhancers often carry binding sites for more than one TF, which interact with the basal transcription machinery associated with core promoters to regulate gene transcription [2]. Very often, TFs also recruit chromatin-modifying enzymes to convert the chromatin to a state permissive for transcription. Pioneer transcription factors (e.g., FoxA1, PU.1), for example, are often the first to engage in a regulatory chromatin region upon stimulation, and enhance transcription by remodeling the local chromatin to make it competent for other TFs to bind [6].

* Correspondence: jindan-yu@northwestern.edu; cyan@augusta.edu

†Equal contributors

¹Department of Medicine, Division of Hematology and Oncology, Northwestern University Feinberg School of Medicine, Chicago, IL, USA

²Georgia Cancer Center, Augusta University, Augusta, GA, USA

Full list of author information is available at the end of the article



While global profiling of genomic sites competent for TF binding is imperative for the understanding of TF functions, such work has also become increasingly important for defining disease etiologies, as mutations in *cis*-regulatory elements are frequently found to be associated with human diseases (e.g., cancer) by whole-genome sequencing studies [7].

Activating transcription factor 3 (ATF3) is a member of the ATF/CREB family of transcription factors involving in many important human diseases including cancer [8–11], atherosclerosis [12], infections [13], cardiac hypertrophy [14], and hypospadias [15]. The contributions of ATF3 to these diseases are often owing to its rapid induction by a wide-range of cellular stresses (e.g., DNA damage, oxidative stress, and endoplasmic reticulum (ER) stress), leading to activation of cellular signaling required for the maintenance of cell homeostasis. Indeed, while it binds and activates the tumor suppressor p53 in response to oncogenic challenges (e.g., DNA damage and *Pten* inactivation) [11, 16], ATF3 also engages in the immune response by interacting with NF- κ B and repressing expression of proinflammatory cytokines induced by the toll-like receptor 4 [17]. Similarly, ATF3 induced by reactive oxygen species causes high susceptibility to secondary infections by repressing interleukin 6 (IL-6) expression during sepsis-associated immunosuppression [13]. Like other ATF/CREB transcription factors, ATF3 regulates transcription by binding the canonical ATF/CRE *cis*-regulatory element (5'-TGACGTCA-3') or the similar AP-1 site (5'-TGA(C/G)TCA-3') via its basic region-leucine zipper domain (bZip) [18]. Although an over-simplified model suggests that ATF3 homodimers and heterodimers (with other bZip proteins) repress and induce gene expression, respectively [19], the mechanism by which ATF3 regulates transcription remains largely unknown. Interestingly, although the structures of the bZip domains are highly similar allowing the largely diversified ATF/CREB proteins to bind the same *cis*-regulatory elements, the genes regulated by ATF3 are distinct from those controlled by its family members. ATF3 and ATF6, for instance, regulate expression of proapoptotic genes and genes involved in protein folding and ER quality control upon ER stress, respectively [20]. As recent evidence supports that ATF3 engages in a complex protein-protein interaction network involving many TFs and transcription co-regulators [16, 21, 22], it is likely that the interactions with other nuclear proteins define the genomic sites where ATF3 binds and the transcription programs that ATF3 regulates. Characterization of genome-wide ATF3 binding sites would thus lead to further elucidation of the ATF3 interaction network and a better understanding of how ATF3 regulates expression of disease-associated genes.

In this study, we present the first comprehensive analysis of ATF3 binding profiles in the human genome. We show that ATF3 bound a large portion of active enhancers

characterized by p300 binding and enriched with K27 acetylated histone H3 (H3K27ac) under the basal condition where ATF3 was expressed at a very low level. While the expression of genes proximal to these enhancers tended to be regulated by ATF3, ATF3 was co-localized with p53 and regulated p53-target gene expression in response to DNA damage. Our results thus suggest that ATF3 likely bookmarks genes for transcriptional regulation under basal and stressed conditions.

Results

Genome-wide mapping of ATF3 binding sites using isogenic cell lines

To profile global ATF3-binding sites, we first employed a genome-editing approach based on recombinant adeno-associated viruses (rAAV) to generate a cell line in which *ATF3* expression was knocked out. Towards this end, we constructed an AAV targeting vector containing left (LA) and right homology arms (RA) flanking the exon 3 of the *ATF3* gene, and introduced the vector into HCT116 human colon cancer cells via rAAV infections [23]. Homologous recombination between the homology arms and the *ATF3* fragments resulted in the insertion of a selection gene (TK-neo) into an *ATF3* allele. A small deletion (22 bp) in the exon 3 was subsequently generated by Cre-mediated excision of the selection gene (Fig. 1a). The same strategy was employed to target the second *ATF3* allele, generating a cell line (ATF3-KO) in which *ATF3* expression was disrupted. We confirmed that ATF3 was not expressed and ATF3 expression was not induced by camptothecin (CPT) - a DNA-damaging agent - in the knockout cells (Fig. 1b).

We thus subjected the wild-type (ATF3-WT) cells and the knockout cells to chromatin immunoprecipitation using an ATF3 antibody. Precipitated DNAs were then labeled and subjected to next-generation sequencing and sequencing reads were mapped to human genome and analyzed for enrichment. Although ATF3 was expressed at a low level (Fig. 1b, lane 1), we identified 33,681 high-confident ATF3-binding peaks in the sample derived from ATF3-WT cells (Fig. 1c). Out of them, a majority of peaks (32,058) were ATF3 specific, as they were not found in the ATF3-KO cells (Fig. 1c and d). A few examples of ATF3 peaks were shown in Fig. 1e. Of note, like a majority of identified sites, these ATF3 peaks were found only in the ATF3-WT sample but not in the ATF3-KO sample (Fig. 1e). Consistent with an early result that ATF3 represses its own expression [24], we found that ATF3 strongly bound its own promoter (Fig. 1e). Using quantitative PCR (qPCR) to examine samples from an independent ChIP experiment, we confirmed that ATF3 bound to all of the tested genomic sites identified by ChIP-seq (Fig. 1f). Again, ATF3 bound to its own promoter in the ATF3-WT cells but not in the knockout cells (Fig. 1g).

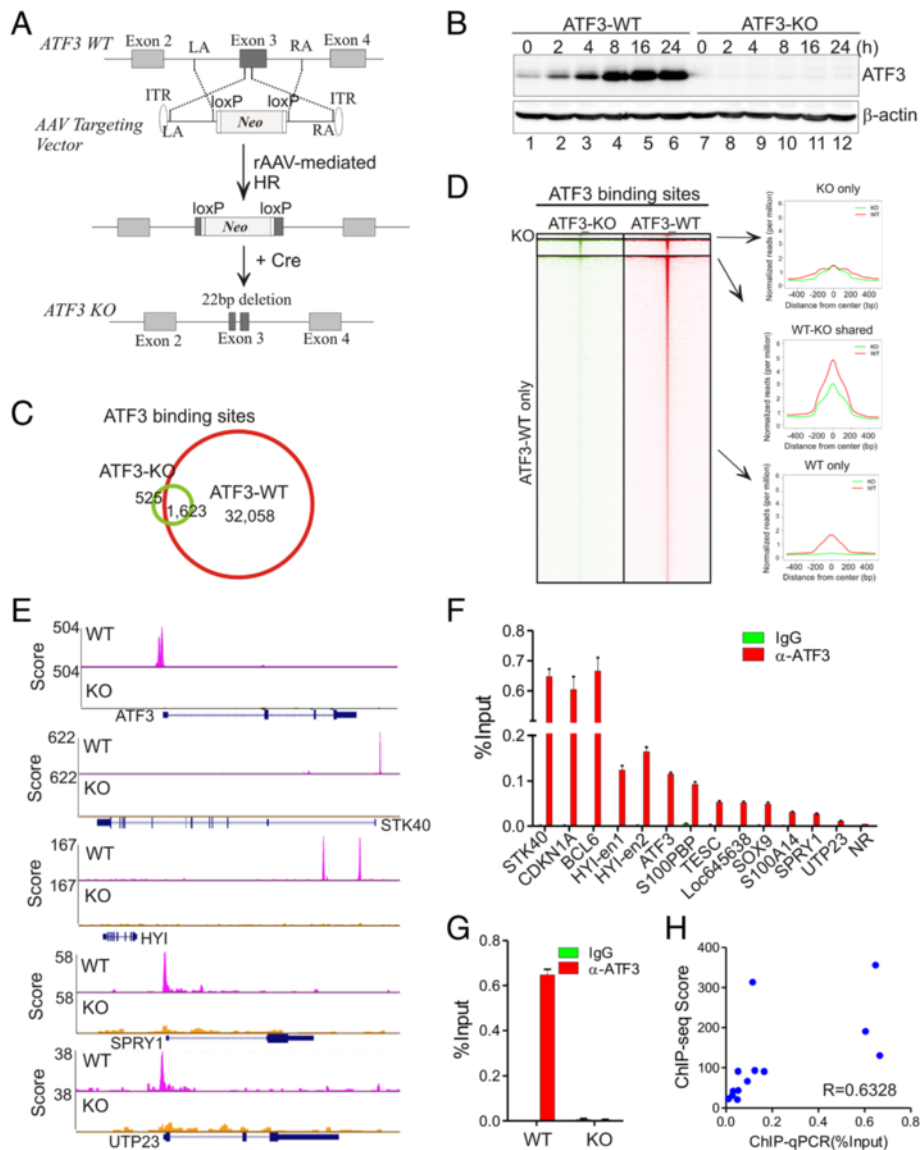


Fig. 1 ATF3 binding profiling using isogenic HCT116 cells. **a** rAAV-mediated genome editing was applied to generate ATF3-knocked out HCT116 cells. rAAV-mediated homologous recombination led to insertion of the AAV targeting vector into *ATF3* exon 3. A deletion of 22 bp was generated in one *ATF3* allele after Cre-mediated excision of the *Neo* selection gene. LA and RA, left and right homology arms; ITR, inverted terminal repeat; KO, knockout. **b** ATF3 expression was completely abolished in ATF3-KO cells. Indicated cells were treated with 1.5 μ M of CPT and subjected to Western blotting. **c** Venn diagram showing ATF3-binding peaks in ATF3 wild-type (ATF3-WT) and knockout (ATF3-KO) cells. **d** Heatmap and intensity plots showing ATF3 peaks in ATF3 WT and KO cells. **e** Representative genome browser views of ATF3 peaks. ATF3 peaks near *ATF3*, *STK40*, *HYL1*, *SPRY1*, and *UTP23* were shown for both ATF3-WT and KO cells. **f, g** ChIP-qPCR was used to validate ATF3 binding to representative genome sites that were referred to as the names of their annotated genes. NR, no-binding control region. Error bars represent SD for three replicate measurements. **h** The binding intensity determined by independent ChIP-qPCR assays was correlated with ChIP-seq scores of peaks tested in (**f**) and (**g**)

The strengths of ATF3 binding to these sites measured by ChIP-qPCR were well correlated with the ChIP-seq scores ($R = 0.6328$), demonstrating high reproducibility and reliability of our ChIP-seq data.

Global ATF3-binding profile and motif analysis

The 32,058 ATF3-specific peaks were annotated to 10,262 unique genes. We analyzed the distribution of

these binding sites relative to TSS in the human genome. Consistent with the ATF3’s role as a transcription factor, about one fifth (19.4 %) of the ATF3 peaks were localized in promoters, which was defined as regions that were ± 2 kb surrounding TSS (Fig. 2a). Given that only a small portion of DNA in the whole genome can be defined as promoters, these results indicate that ATF3 were enriched in promoters. However, ATF3 also bound

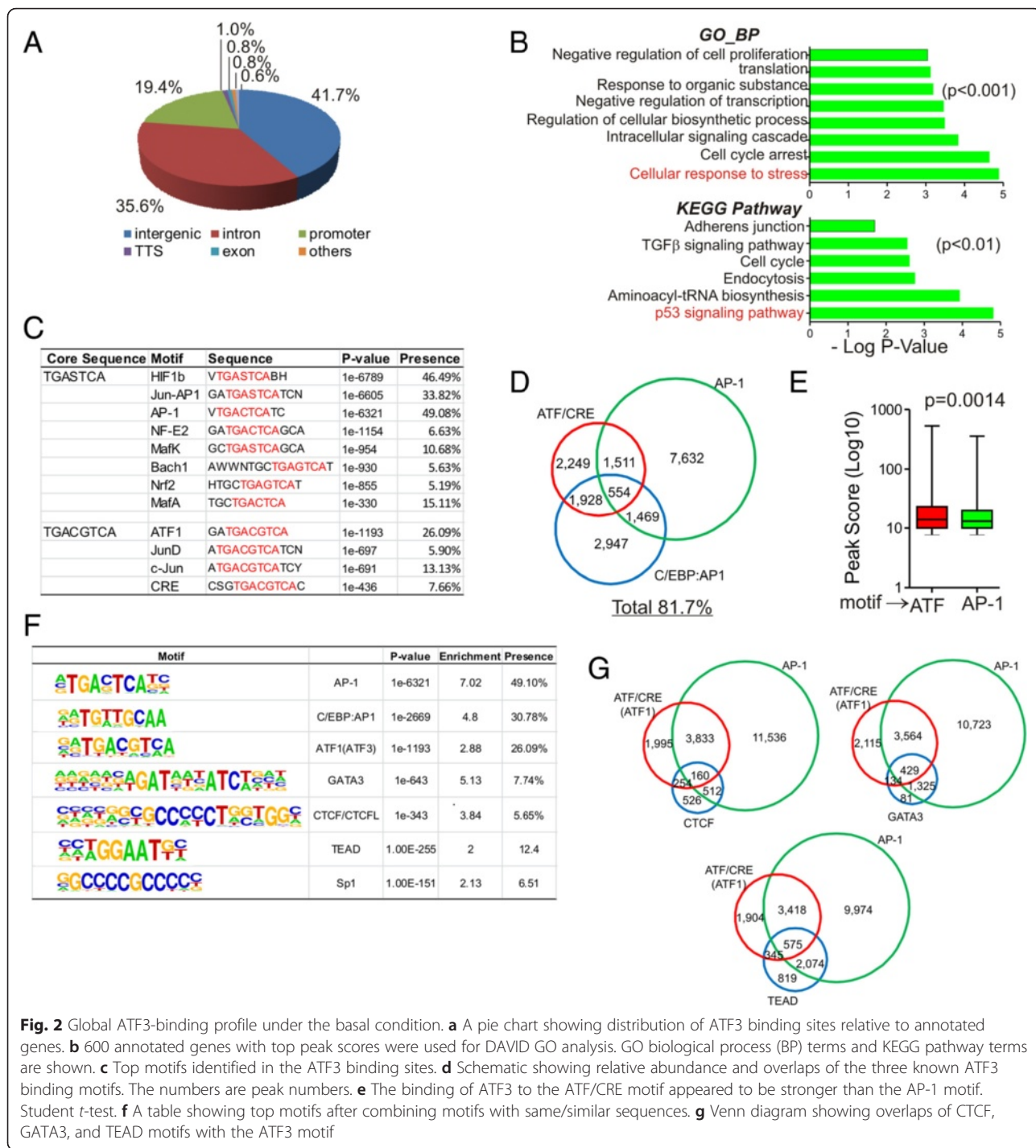


Fig. 2 Global ATF3-binding profile under the basal condition. **a** A pie chart showing distribution of ATF3 binding sites relative to annotated genes. **b** 600 annotated genes with top peak scores were used for DAVID GO analysis. GO biological process (BP) terms and KEGG pathway terms are shown. **c** Top motifs identified in the ATF3 binding sites. **d** Schematic showing relative abundance and overlaps of the three known ATF3 binding motifs. The numbers are peak numbers. **e** The binding of ATF3 to the ATF/CRE motif appeared to be stronger than the AP-1 motif. Student *t*-test. **f** A table showing top motifs after combining motifs with same/similar sequences. **g** Venn diagram showing overlaps of CTCF, GATA3, and TEAD motifs with the ATF3 motif

genomic regions far removed from TSS (Fig. 2a), suggesting that ATF3 also likely regulates transcription via long-range interactions. Gene Ontology (GO) analysis of the top 600 annotated genes with high binding scores revealed that ATF3 preferably bound to regulatory elements for genes involving in biological processes such as cellular response to stress, cell cycle arrest and intracellular

signaling cascade, as well as pathways such as p53 signaling pathway (Fig. 2b). Interestingly, “cellular response to stress” and “p53 signaling pathway” turned out to be the top GO terms for the ATF3-bound genes, consistent with the well-established roles that ATF3 plays in regulating cellular stress responses and the p53 pathway [16, 18].

We also searched the ATF3 binding sites for known TF binding motifs using the Homer *de novo* motif discovery software. A total of 140 motifs were identified with a p value smaller than 0.01. With only one exception (CEBP:AP1 motif), the top 12 identified motifs contained either the canonical ATF/CRE sequence (i.e., 5'-TGACGTCA-3') or the AP-1 sequence (i.e., 5'-TGASTCA-3'; S = C/G) (Fig. 2c). As C/EBP harbors a bZip domain that can mediate dimerization with other bZip proteins including ATF3 [25], it might be that ATF3 bound the CEBP:AP1 motif through dimerization with C/EBP. Overall, 81.7 % of ATF3 binding sites contain an element predicted to be bound by ATF3 - collectively referred to as the ATF3 motif hereafter (Fig. 2d) - suggesting that ATF3 directly binds genomic DNA in most cases. Interestingly, although more ATF3 peaks contained the AP-1 motif (Fig. 2e), the binding affinity of ATF3 to the canonical ATF/CRE element appeared to be higher than that for ATF3 binding to the AP-1 element (Fig. 2e). In addition to these known ATF3 binding motifs, other top ATF3 binding motifs (i.e., Enrichment > 2) include GATA3, CTCF, TEAD, and Sp1, which was presented in 7.7 %, 5.6 %, 14.8 %, and 6.5 % of ATF3 peaks, respectively (Fig. 2f). Although these ATF3-binding peaks often contain a known ATF3 motif (Fig. 2g), ATF3 might also bind these motifs through interacting with corresponding TFs. Indeed, ATF3 has been shown to interact with Sp1 [26].

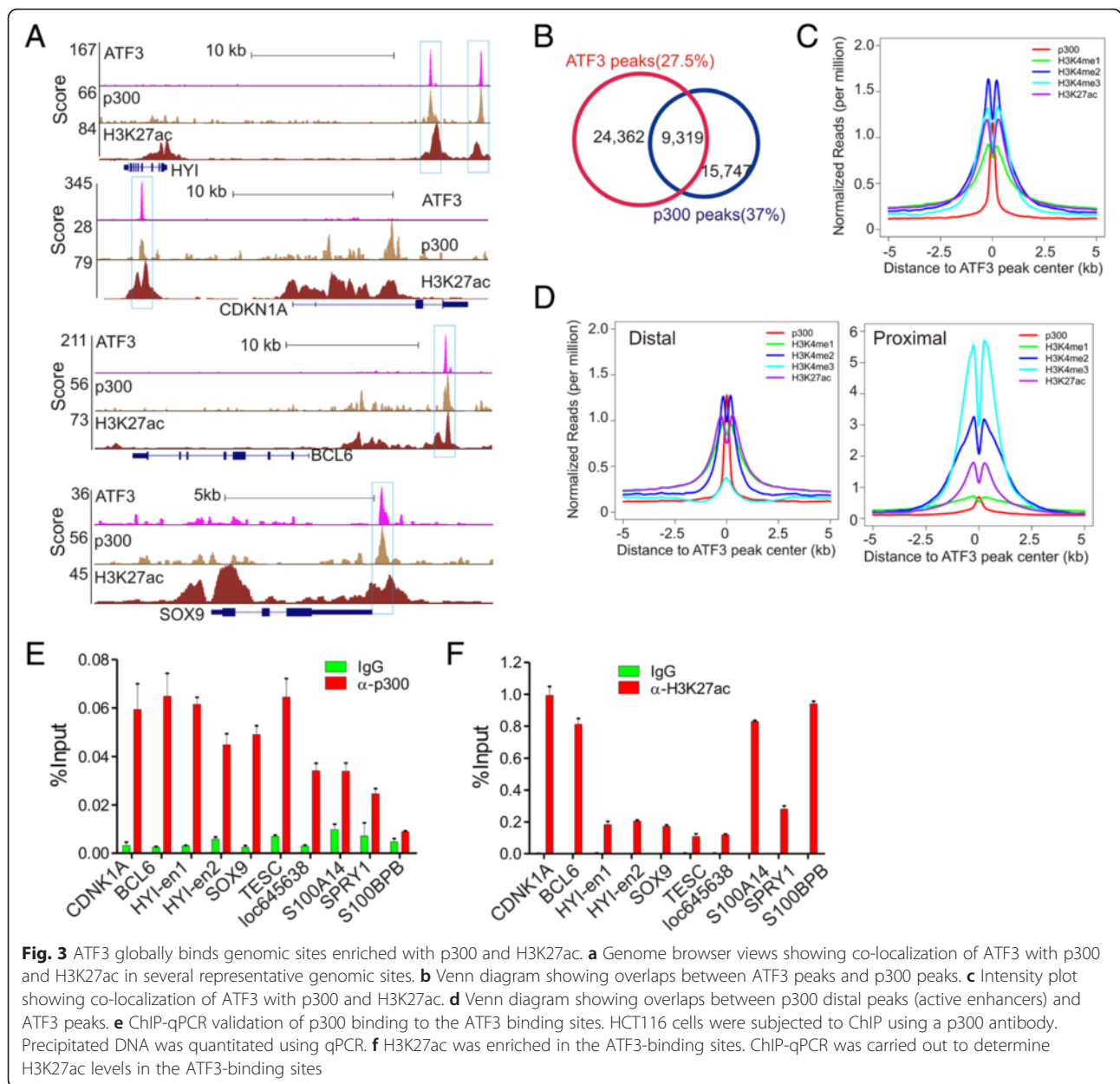
ATF3 globally binds active enhancers enriched with p300 and H3K27ac

As ATF3 bound genomic sites far removed from TSS, we sought to determine whether these sites are coincided with active enhancers that are often marked by p300 binding and flanked with high levels of H3K27ac [3–5]. Towards this end, we acquired p300, H3K27ac, H3K4me1, and H3K4me3a ChIP-seq data (HCT116 cells) from the Gene Expression Omnibus (GEO) database GSE51176 and GSE38447 [27, 28]. We first examined the ATF3 peaks in the Genome Browser, and found that ATF3 bound to many sites that were also bound by p300 and flanked by regions with high levels of H3K27ac (Fig. 3a), suggesting that ATF3 bound to active enhancers. Indeed, unbiased statistics analysis revealed that up to 27.5 % of ATF3 peaks were overlapped with p300 peaks, and 37 % of p300 peaks were bound by ATF3 (Fig. 3b). Intensity plots also show that p300 was globally co-localized with ATF3 and that the H3K27ac histone marker surrounded the ATF3/p300 peaks as expected (Fig. 3c). We segregated the ATF3 peaks into proximal sites (within 2 kb) and distal sites (>2 kb) based on their distances to TSS, representing H3K4me3-enriched promoters and H3K4me1-enriched enhancers, respectively (Fig. 3d). The intensity plots revealed that it was the distal sites, but not the proximal sites, that were coincided with p300 binding events (Fig. 3d). Using qPCR, we validated

that p300 bound to all of the tested ATF3 binding sites in an independent ChIP experiment (Fig. 3e). Similarly, the enrichment of H3K27ac in these ATF3 sites was also validated (Fig. 3f). Of note, as p300 is not the only enzyme that can acetylate H3 at the K27 site, the H3K27ac level was not strictly correlated with the p300 level in some genome sites. Taken together, our results have revealed that a large portion of ATF3 bound active enhancers.

ATF3-regulated gene expression correlates with ATF3 enhancer binding

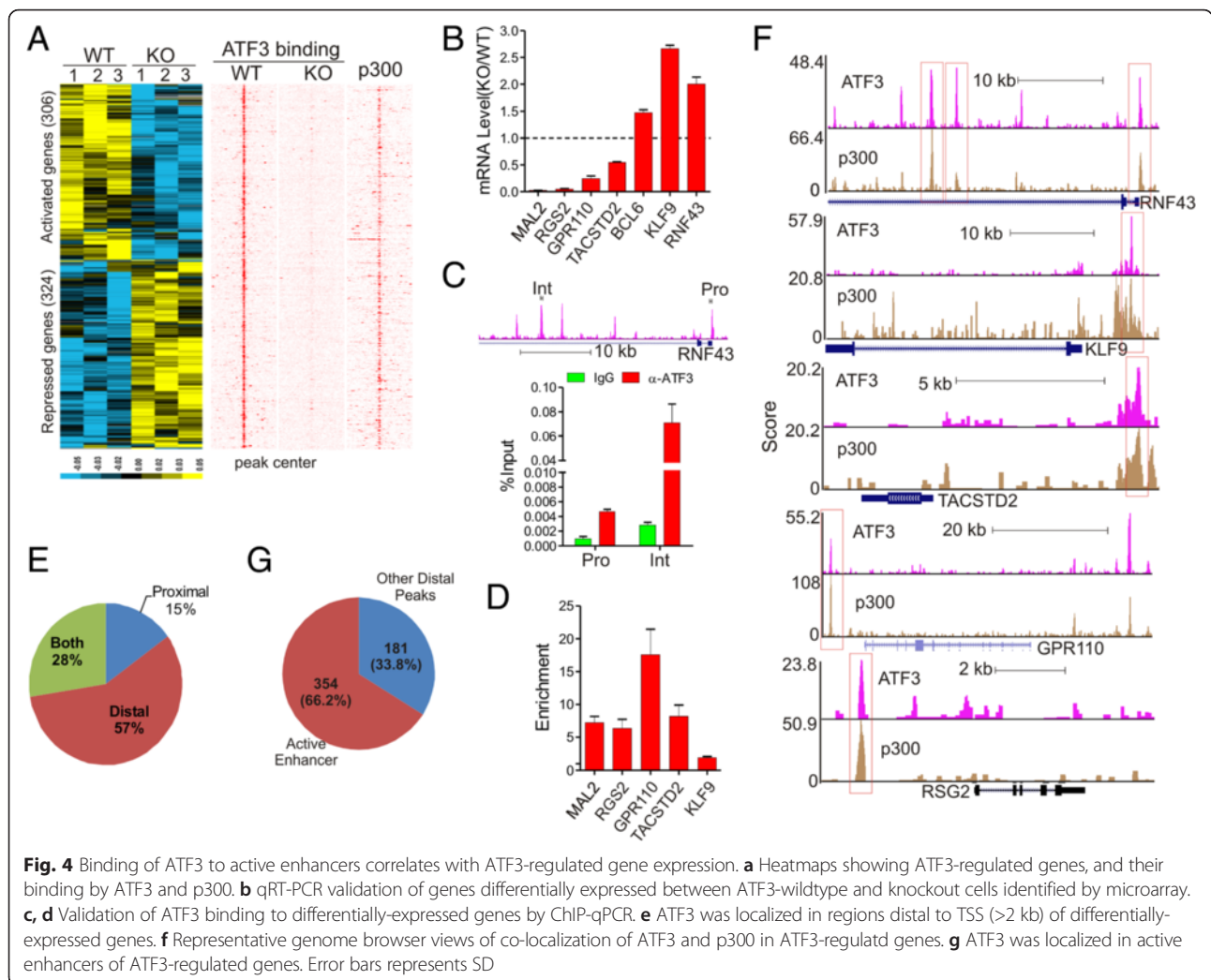
An interesting question surfaced as to how ATF3 binding to genomic sites regulates gene expression. To address this question, we subjected the ATF3-wildtype and knockout cells to cDNA microarray assays. Although ATF3 bound to 10,262 genes, only 1,087 unique genes, including several known ATF3 targets (i.e., *ASNS*) [29], were differentially expressed between the WT and KO cells (FDR < 0.05, Additional file 1: Figure S1A and S1B). Among these genes, 630 (60 %) were bound by ATF3 and thus more likely to be directly regulated by ATF3 (Fig. 4a). Roughly equal numbers of genes was either activated or repressed by ATF3 (Fig. 4a), suggesting that ATF3 can function as both a transcription repressor and a transcription activator. In line with the reported tumor suppressor role in colon cancer [30, 31], ATF3 appeared to induce expression of genes involving in mitosis and stress responses while repressing genes regulating vasculature development, migration, and apoptosis (Additional file 1: Figure S1C). We validated 7 differentially-expressed genes by quantitative RT-PCR (Fig. 4b) and their binding by ATF3 by independent ChIP-qPCR assays (Fig. 4c and d). Interestingly, although ATF3 were often reported to regulate gene expression by binding to a ATF3 motif localized in promoters, only 15 % (95/630) of the ATF3-regulated genes identified herein were bound by ATF3 exclusively at their promoters (proximal genomic regions) (Fig. 4e). The rest of genes either were bound by ATF3 exclusively at distal regions (57 %, or 361/630), or at both promoters and distal regions (28 %, or 95/630) (Fig. 4e). These results suggest that ATF3 could regulate gene expression by binding to distal *cis*-regulatory elements localized in active enhancers. Indeed, except *MAL2*, all other validated ATF3-target genes were bound by ATF3 at distal regions overlapped with p300 peaks (Fig. 4f). Of the 535 genes containing distal ATF3-binding sites, 354 (66.2 %) were associated with active enhancers enriched with p300 and bound by ATF3 (Fig. 4g). Interestingly, ATF3-repressed genes appeared to be more likely to harbor distal ATF3 regulatory elements than ATF3-activated genes (Additional file 1: Figure S1D), although the TF motifs contained in the ATF3-binding sites in these two groups of genes were similar (Additional file 1: Figure S1E).



DNA damage alters the ATF3-binding landscape for gene regulation

As a common stress sensor, ATF3 may regulate cellular stress responses by altering the gene expression landscape. To understand how cellular stresses alter genome-wide ATF3 binding profile for transcriptional regulation, we subjected HCT116 cells treated with CPT for ChIP-seq assays. As CPT could increase the ATF3 expression level (Fig. 1b) [32], it was not surprising that the DNA-damaging treatment increased the number of ATF3-binding sites to 70,231 (Fig. 5a) – one fold more than that under the basal condition. However, we found that a large number of sites (7,172, 21.3 %) bound by ATF3 under the basal condition were not detected after the CPT treatment

(Fig. 5a and b, “WT-only”). ATF3 bound these sites more weakly than the remained sites (Fig. 5b, “WT-only” vs. “Shared” peaks, $p = 7.46e-05$). Of the “shared” peaks, DNA damage increased ATF3 binding to 13,253 sites but decreased its binding to the rest 13,256 sites (Additional file 1: Figure S2A). Interestingly, while the CPT-increased sites appeared to be bound by ATF3 more strongly than the CPT-decreased sites under the basal condition (Fig. 5c), the increased sites were also often bound by p300, or enriched with H3K4me1, suggesting that DNA damage promoted ATF3 to bind to active enhancers (Fig. 5c). In contrast, CPT tended to decrease ATF3 binding to those sites localized in promoters and thus often flanked by a high level of H3K4me3 [33] (Fig. 5c).



Consistent with these observations, although DNA damage did not significantly change the overall genome distribution and motif composition of the ATF3 binding sites (Additional file 1: Figure S2B and S2C), it promoted ATF3 to bind to the sites distal to TSS (Fig. 5d). Similarly, DNA damage increased the number of sites bound by both ATF3 and p300, and the number of these ATF3-bound active enhancers was increased from 37 % under the basal condition to 57.6 % upon stress (Fig. 5e). Interestingly, the new sites bound by ATF3 after DNA damage (“CPT only” in Fig. 5b) had weaker ATF3-binding affinities than the sites bound by ATF3 under the basal condition ($p = 1.73e-07$, comparing “CPT only” vs “Shared” peaks in Fig. 5b), but had stronger affinities than those lost peaks ($p = 0.000345$, “CPT only” vs “WT only”, Fig. 5b). Our results thus suggest that ATF3 not only increased its level, but also altered its genome binding in response to DNA damage.

We next addressed the question as to what changes in gene expression the altered ATF3-binding would cause under the DNA damage condition. Treating HCT116

cells with CPT for 4 h resulted in an increase in expression of 733 genes and a decrease in expression of 1095 genes (fold > 1.5, $p < 0.05$) (Fig. 5f). 1,300 (71.1 %) of these altered genes were bound by ATF3 after DNA damage (Fig. 5g), and thus were more likely regulated by ATF3. Interestingly, 82.9 % of ATF3-bound, CPT-regulated genes were also bound by ATF3 before the cells were treated with CPT (Fig. 5g), suggesting that ATF3 were pre-loaded on the genomic sites for gene regulation under stressed conditions. However, stressed ATF3 appeared to bind these sites more strongly than the quiescent protein (Fig. 5h). Given that CPT equally increased or decreased ATF3 binding on the “shared” sites (see above), these results indicate that DNA damage selectively promoted ATF3 to bind to genomic sites associated with regulated genes.

To further determine the relationship between ATF3 binding and gene regulation under the stressed condition, we analyzed the gene expression data for ATF3 knockout cells, and generated a curated list of 93 genes

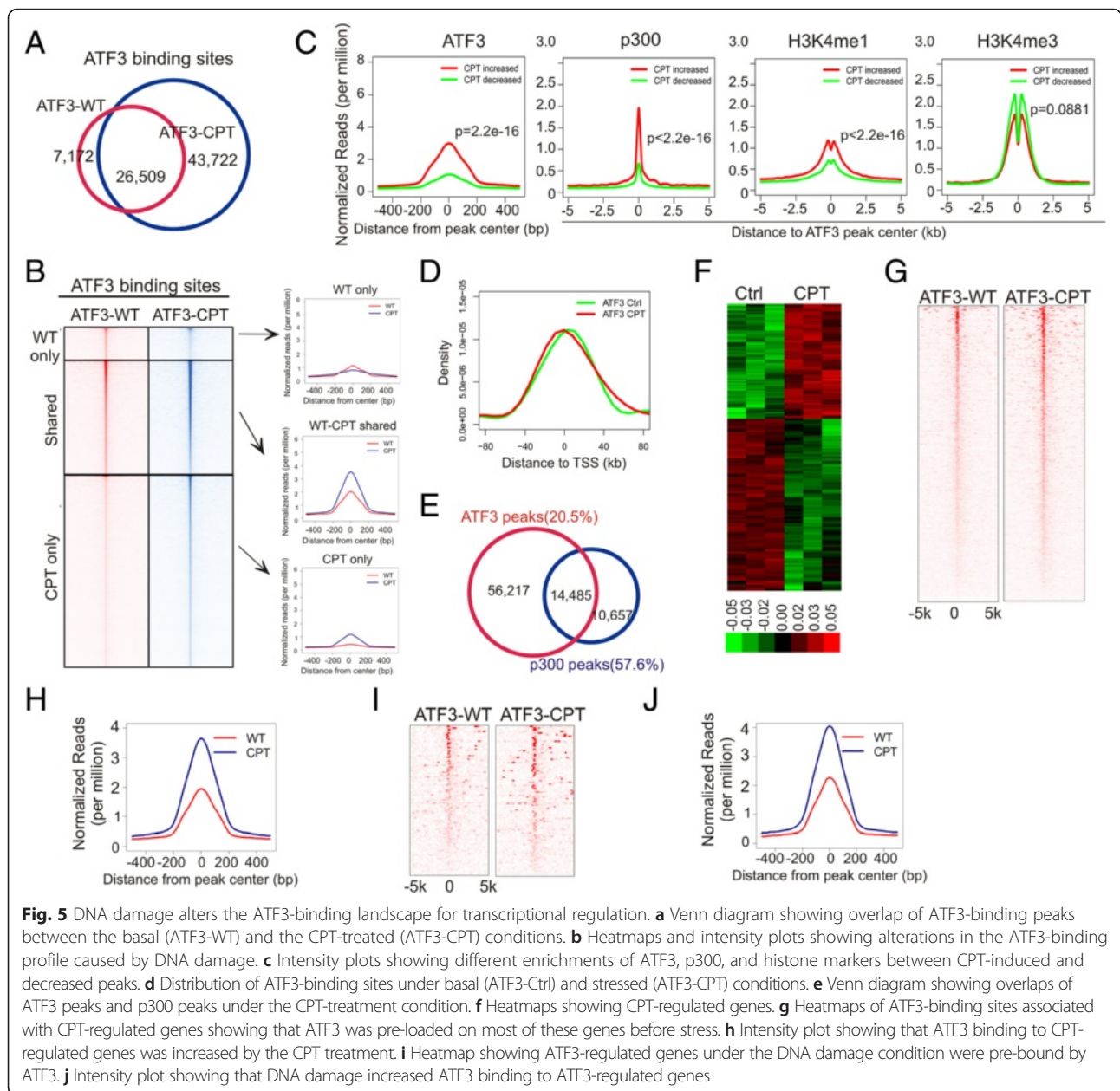


Fig. 5 DNA damage alters the ATF3-binding landscape for transcriptional regulation. **a** Venn diagram showing overlap of ATF3-binding peaks between the basal (ATF3-WT) and the CPT-treated (ATF3-CPT) conditions. **b** Heatmaps and intensity plots showing alterations in the ATF3-binding profile caused by DNA damage. **c** Intensity plots showing different enrichments of ATF3, p300, and histone markers between CPT-induced and decreased peaks. **d** Distribution of ATF3-binding sites under basal (ATF3-Ctrl) and stressed (ATF3-CPT) conditions. **e** Venn diagram showing overlaps of ATF3 peaks and p300 peaks under the CPT-treatment condition. **f** Heatmaps showing CPT-regulated genes. **g** Heatmaps of ATF3-binding sites associated with CPT-regulated genes showing that ATF3 was pre-loaded on most of these genes before stress. **h** Intensity plot showing that ATF3 binding to CPT-regulated genes was increased by the CPT treatment. **i** Heatmap showing ATF3-regulated genes under the DNA damage condition were pre-bound by ATF3. **j** Intensity plot showing that DNA damage increased ATF3 binding to ATF3-regulated genes

that were judged, with high confidence, as ATF3-regulated genes in response to DNA damage (Additional file 1: Figure S2D), based on (1) that fold changes before and after the CPT treatment were significantly different ($p < 0.05$, paired t -test) between ATF3-wildtype and -knockout cells, (2) that the genes bound by ATF3 with a small binding score (< 10) and thus more likely to be derived from experimental errors were excluded. Once again, while 82 (88.2 %) of these genes had already been bound by ATF3 under the basal condition, CPT further increased ATF3 binding to these regulated genes, regardless whether their expression was induced or repressed by CPT (Fig. 5i and j). Interestingly, about a half (43, or 46 %)

of these genes contained one or more active enhancers that were bound by both p300 and ATF3 (Fig. 5i), consistent with our previous conclusion that ATF3 can bind to active enhancers to regulate gene expression.

ATF3 collaborates with p53 in regulating target gene expression

p53 is a master transcription factor that transactivates genes (e.g., *CDKN1A* and *BBC3*, best known as *p21* and *PUMA*, respectively) essential for driving cellular responses (e.g., cell cycle arrest and apoptosis) to DNA damage [34]. As ATF3 can bind p53 [16] and we also found that ATF3-bound genes engage in the p53 signaling pathway (Fig. 2c), we

sought to determine how ATF3 interacts with p53 at genomic sites to regulate gene expression in response to CPT-induced DNA damage. We first profiled global p53 binding by subjecting CPT-treated HCT116 cells to ChIP-seq

analysis. We identified 1,412 p53-binding peaks (Fig. 6a), a number which was low but within the same range (from 743 to 4,785) as other reports [35–37]. These identified binding sites included 3 previously-characterized p53-

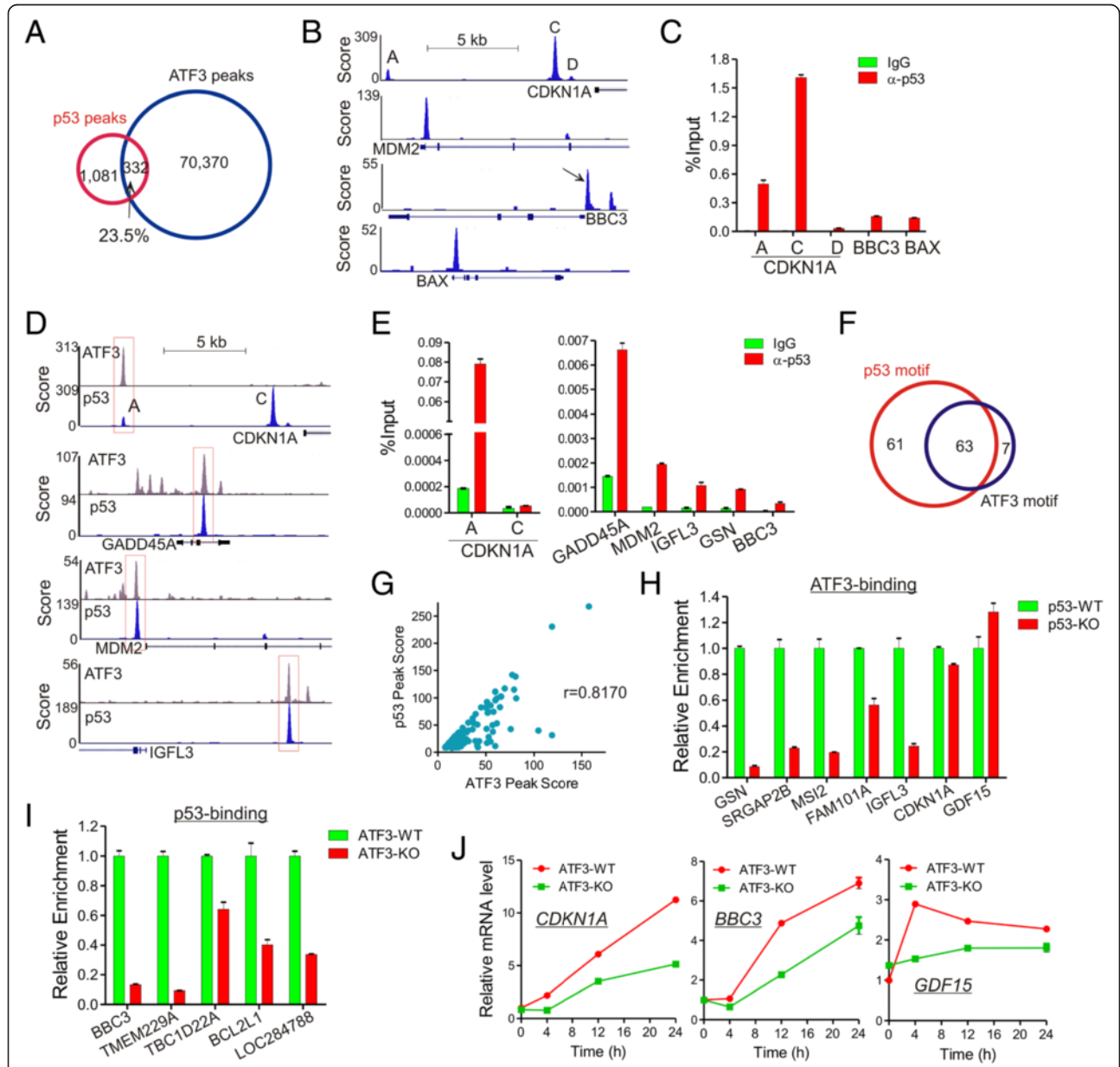


Fig. 6 Co-localization of ATF3 and p53 in genomic sites regulates gene expression in the DNA damage response. **a** Venn diagram showing the overlap between ATF3 peaks and p53 peaks under the DNA damage condition. **b** Genome browser views of p53 binding to several well-characterized p53 target genes. **c** Binding of p53 to indicated sites was validated by independent ChIP-qPCR assays. **d** Genome browser views of co-localization of ATF3 and p53 in representative genomic sites. **e** ATF3 and p53 were co-localized in genomic sites as demonstrated by re-ChIP assays. HCT116 cells treated with 1.5 μ M of CPT for 4 h were first subjected to ChIP using the ATF3 antibody. The chromatin precipitated by the ATF3 antibody was then eluted from agarose beads, and subjected to the second round of ChIP using the p53 antibody. qPCR assays were used to quantitate re-ChIPed DNA. **f** Venn diagram showing the overlap of p53-binding sites containing the p53 motif or the ATF3 motif. **g** The ATF3 peak score correlated with the p53 peak score in the sites co-localized by ATF3 and p53. **h** ATF3 binding was often decreased in p53-knockout cells. p53-wildtype and knockout (p53-KO) HCT116 cells were subjected to ChIP-qPCR to measure binding of ATF3 to the indicated sites. **i** p53 binding was decreased in ATF3-knockout cells. ATF3-wildtype and knockout (ATF3-KO) HCT116 cells were subjected to ChIP-qPCR to measure binding of p53 to the indicated sites. **j** Expression of p53 target genes was repressed in ATF3-KO cells. Indicated cells were treated with 1.5 μ M of CPT for qRT-PCR assays. ATF3 binding to these genes before and after CPT treatments in ATF3-WT cells were shown in Additional file 1: Figure S3

binding sites in the *CDKN1A* enhancer and promoter regions (site A, C and D, respectively) (Fig. 6b) [35], and sites localized in the promoters of well-characterized p53 target genes *MDM2*, *BBC3* and *BAX* (Fig. 6b). These p53-binding sites were validated by independent ChIP-qPCR assays (Fig. 6c). Consistent with the notion that ATF3 is a p53 regulator [16], we found that ATF3 bound to 23.5 % (332) of p53-binding sites (Fig. 6a), including the *CDKN1A* site A (but not site C and D), and the sites associated with *GADD45A*, *MDM2* and *IGFL3* (Fig. 6d). Using re-ChIP assays, we confirmed that ATF3 was co-localized with p53 at Site A, but not Site C, of *CDKN1A*, and other tested genomic sites associated with *GADD45A*, *MDM2*, *IGFL3*, *GSN*, and *BBC3* (Fig. 6e). Of these ATF3/p53 co-localized sites, 61 only carried a p53 motif, 7 only carried an ATF3 motif, and 63 harbored both motifs (Fig. 6e; Additional file 2: Table S1). Given that ATF3 can directly bind p53 [16], co-localization of ATF3 with p53 at genomic sites might be owing to p53-mediated recruitment of ATF3 to sites containing the p53 motif, and/or ATF3-mediated recruitment of p53 to sites harboring the ATF3 motif. Indeed, we found a strong correlation between the ATF3-binding score and the p53 peak score at these genomic sites ($r = 0.8170$, Fig. 6g). Moreover, p53 depletion dramatically impaired ATF3 binding to 5 out of 7 tested p53-motif-only sites (Fig. 6h). Of note, although p53 was previously shown to be required for ATF3 induction by DNA damage caused by γ -irradiation [38], we did not see decreased ATF3 expression in p53-knockout cells under our experimental condition (data not shown). The reason why p53 knockout did not decrease ATF3 binding to the *CDKN1A* Site A and the *GDF15* p53-binding site that lacked the ATF3 motif was unclear, but other TFs might recruit ATF3 to these sites. Interestingly, p53 binding to the sites containing only the ATF3 motif was significantly decreased by ATF3 knockout as well (Fig. 6i), suggesting that ATF3 could also recruit p53 to genomic sites that do not contain a p53 motif. Thus, the ATF3-p53 interaction might expand the list of genes that can be regulated by p53. Interestingly, 19.5 % (58/297) of the ATF3/p53 co-localized sites, including the site associated with *CDKN1A*, *BBC3* and *GDF15*, were also enriched with p300, suggesting that many of these sites were active enhancers and thus the ATF3-p53 interaction on genomic sites were likely functional. Indeed, we demonstrated that knockout of ATF3 expression impaired CPT-induced *CDKN1A*, *BBC3*, and *GDF15* expression (Fig. 6j). Therefore, our results indicate that ATF3 could interact with p53 at genomic sites thereby regulating gene expression in the DNA damage response.

Discussion

It is often shown that ATF3 binds the ATF/CRE *cis*-acting element localized in gene promoters and regulate expression of genes associated with human diseases [12–14]. We

carried out this study in light of the fact that a genome-wide ATF3-binding profile in the human genome was lacking. Employing engineered ATF3-knockout cells as the specificity control, we identified 33,681 specific ATF3-binding sites across the human genome under the basal condition. Although this number was surprisingly large given that the basal ATF3 expression level was low, it was comparable to 22,521 sites identified in mouse dendritic cells [39]. As 81.7 % of the ATF3-binding sites contained a known ATF3 motif (Fig. 2e) [40], ATF3 might directly bind a majority of these sites. It was thus likely that the low level of constitutively-expressed ATF3 was sufficient to bind most of available sites in the genome. Interestingly, ATF4, a family member sharing the same binding motif with ATF3, binds only 1,210 sites in the mouse genome [39]. While this difference might be owing to different DNA-binding affinity, interactions with other transcription regulators could poise ATF3 for a higher level of genome binding. The latter possibility is supported by the fact that ATF3 differs from ATF4 in its ability of interacting with other proteins [25]. It is worth noting that the ATF3 genome-occupancy level is lower than that of pioneer factors, which often bind more than 50,000 genomic sites [39], but significantly higher than that of most of gene-specific TFs (e.g., p53) that generally occupy a few thousands of genomic sites (Fig. 6a). It is thus tempting to hypothesize that ATF3 serves as a molecular beacon, or “primer factor”, that binds genomic sites subsequent to binding of pioneer factors, and directs other TFs or transcription co-regulators to appropriate genomic sites upon stimulation [39]. This hypothesis was partly supported by the findings that ATF3 directly interacts with many TFs (e.g., p53, p63, AR, Sp1) [16, 21, 26, 41] and histone modifying enzymes (e.g., Tip60 and HDAC) [17, 22]. Importantly, while the GO analysis revealed that the ATF3-bound genes were associated with cellular response to stress under the basal condition (Fig. 2c), we found that the genes whose expression was regulated by DNA damage were often pre-bound by ATF3 (Fig. 5g). Thus, like the transcription factor p63 [42], ATF3 might bookmark genes for transcriptional regulation. In this regard, it is likely that ATF3 recruits diverse sets of TFs to genomic sites pre-bound by ATF3 upon varying stimuli, thereby regulating gene expression and mounting rapid, appropriate responses to varying cellular stresses. However, DNA damage-induced changes in ATF3 binding were more dynamic than what the “primer-factor” hypothesis suggests [39]. DNA damage not only increased the number of ATF3 binding sites by 1 fold, but abolished up to one-fifth of the basal binding events (Fig. 5b). In addition, CPT increased ATF3 binding to some genomic sites but decreased its binding to almost equal numbers of other sites. While stress-induced loss of genomic binding has also been reported for other stress-inducible TFs (e.g., JunB) [39], the decrease in ATF3 binding to a substantial number of

genomic sites argues against the notion that the dynamic changes in ATF3 binding was a mere consequence of elevated ATF3 expression induced by DNA. As DNA damage can alter chromatin structure [43–45], it might allow access of some genomic sites to, while shielding other sites from, ATF3. Interestingly, the CPT treatment appeared to promote ATF3 to bind to sites distal to TSS (Fig. 5d). While the exact mechanism remains elusive, it might be that the epigenetic environments where the distal sites reside are favorable for TF binding. Indeed, these distal sites often coincide with p300/H3K27ac-enriched active enhancers (Fig. 3d), which are known to have lower nucleosomal density [5].

Like other TFs [36, 42], binding of ATF3 to the regulatory region of a gene did not always result in a change in gene expression. Indeed, although ATF3 bound more than 10,000 genes, a complete loss of ATF3 expression only altered expression of a small number of genes under both the quiescent and the stressed condition. While RNA-based assays (*e.g.*, microarray and RNA-seq) may not serve as accurate measurements of transcription activity [42], other TFs capable of binding the same motifs (*e.g.*, JunB) [39] might compensate for ATF3 loss. Interestingly, the ATF3-binding sites often contained motifs of other TFs in addition to the ATF3 motif (Fig. 2), suggesting that ATF3 might act in concert with other TFs to regulate gene expression. Our results also indicate that ATF3 can activate or repress gene expression depending on gene context. While the location and motif composition of the ATF3-binding site did not appear to determine whether ATF3 activates or represses gene expression (Additional file 1: Figure S1D and S1E), it is very likely that the epigenetic environment surrounding the ATF3-binding sites determine the availability of transcription co-activators (like Tip60), or transcription co-repressors (*e.g.*, HDAC), which consequently transactivate or repress expression of ATF3-bound genes. Thus, the early notion that ATF3 homodimers and heterodimers respectively repress and activate transcription appears oversimplified and misleading.

An important finding from this study is that ATF3 bound to 37 % of genomic sites that were bound by p300 and characterized by high levels of H3K27ac under the basal condition (Fig. 3b). These genomic sites are defined as active enhancers and have been shown to contain functional regulatory elements that drive proximal gene expression during embryonic development [3, 4]. Interestingly, DNA damage increased the percentage of active enhancers bound by ATF3 to 57.6 %. Moreover, although ATF3 binding alone was not sufficient to regulate transcription, most of genes regulated by ATF3 appeared localized proximal to ATF3-bound active enhancers (Fig. 4). This strong correlation between TF binding to active enhancers and the regulation of gene expression was not without precedent. The

transcription factor p63, for instance, was recently shown to bind H3K27ac-enriched active enhancers, and the binding correlates with dynamic gene expression regulated by p63 during epidermal differentiation [42]. As active enhancers often contain a cluster of motifs allowing for binding by multiple TFs, it is likely that these TFs collaboratively interact with the basal transcription machinery in core promoters to regulate gene expression. Therefore, the observed correlation between enhancer binding and transcriptional regulation is consistent with our notion that ATF3 needs to cooperate with other TFs to regulate gene expression.

The tumor suppressor p53 drives a transcription program for eliciting diverse cellular responses to DNA damage. Previously, we reported that ATF3 can activate p53 by binding and directly blocking its ubiquitination [16]. We also found that ATF3 can induce p53 activation by promoting the activity of a histone acetyltransferase Tip60 and the subsequent activation of ATM [22]. In this study, we revealed an additional mechanism by which ATF3 regulates p53, *i.e.*, co-localization with p53 at genomic sites. Indeed, we found that ATF3 was co-localized with p53 at more than 20 % of p53-binding sites identified by ChIP-seq (Fig. 6a). As ATF3 can interact with p53 [16], such co-localization might be a consequence of p53-mediated ATF3 recruiting (Fig. 6h), or vice versa (Fig. 6i). On the other hand, some co-localized genomic sites contained both the p53 and the ATF3 motif, and thus could be bound by p53 and ATF3 simultaneously. Regardless, close proximity between ATF3 and p53 at genomic sites might directly alter p53 conformation thereby regulating the p53 transcriptional activity (Fig. 6j). Our results are supported by a recent report, which carried out ATF3 ChIP-chip assays and shows binding of ATF3 to promoters of many known p53 target genes [46]. However, Our study indicates that a large number of co-localized sites were far beyond promoter regions [47] and were also often bound by p300. Therefore, the genomic co-localization of ATF3 and p53 serves as an additional mechanism for fine tuning p53 activity in the DNA damage response.

Conclusions

Our results indicate that ATF3 likely preoccupies genomic sites regulatory for genes involved in the cellular stress response, and thus bookmarks these sites for transcriptional regulation under basal and stressed conditions.

Methods

Cell culture and generation of ATF3-knockout cells

HCT116 wild-type and p53-knockout cells (obtained from Bert Vogelstein) were cultured in McCoy's 5A medium supplemented with 10 % fetal bovine serum.

H1299 cells and 293 T cells were cultured in RPMI 1640 and DMEM medium, respectively. We knocked out ATF3 expression in HCT116 cells using a rAAV-based approach [23]. Briefly, left and right homology arms flanking a small region (22 bp) in the exon 3 of *ATF3* were amplified by PCR, and sequentially ligated into pAAV-TK-Acceptor [23] via restriction enzyme digestion. The resulted plasmid was then transfected into AAV-293 cells for rAAV packaging using the AAV Helper-free System (Agilent) following the manufacturer's protocol. For viral infections, HCT116 cells in 60 mm dishes were incubated with 2 ml of viral supernatant overnight, followed by re-suspension in medium containing 500 µg/ml of G418 for selection. Genomic DNAs were then prepared from resistant single clones as describe previously [48], and used for PCR to identify targeted clones. To remove the inserted selection gene, targeted clones in 24-well plates were transfected with a Cre-expression plasmid. Single clones regaining G418 sensitivity were accordingly identified, and subjected to the 2nd round of genome editing to knock out the 2nd *ATF3* allele as describe above. The sequences of primers used in this report are available upon request.

Chromatin immunoprecipitation

Chromatin immunoprecipitation was performed essentially as described previously [49]. Briefly, cells (2×10^7) treated with or without 1.5 µM of CPT for 4 h were cross-linked with 1 mM of di(N-succinimidyl) glutarate (DSG) for 45 min, followed by 1 % formaldehyde for 10 min at room temperature. After treating with 0.125 M of glycine for 5 min, cells were resuspended in 10 ml of Solution I (10 mM Hepes-KOH, pH7.5, 10 mM EDTA, 0.5 mM EGTA, and 0.75 % Triton X-100), and incubated at 4 °C for 10 min. Cells were further incubated with 10 ml of Solution II (10 mM Hepes-KOH, pH7.5, 200 mM NaCl, 1 mM EDTA, and 0.5 mM EGTA) at 4 °C for 10 min before lysed in cold FA lysis buffer (50 mM Hepes-KOH, pH7.5, 140 mM NaCl, 1 mM EDTA, 1 % Triton X-100, 0.1 % sodium deoxycholate, and proteinase inhibitors). Chromatin was sheared by sonication using Bioruptor to an average fragment size of 500 bp, and then incubated with 2 µg of the antibody (ATF3, sc-188; p53, sc-126; p300, sc-585) or normal IgG (rabbit, sc-3888; mouse, sc-2025) purchased from Santa Cruz, at 4 °C overnight. Immuno-complexes were precipitated with 30 µl of ssDNA-protein A/G agarose (Millipore) at 4 °C for 2 h, and sequentially washed with Buffer I (50 mM Tris-HCl, pH8.0, 150 mM NaCl, 1 % SDS, 0.5 % sodium deoxycholate, 1 % NP 40, and 1 mM EDTA), Buffer II (buffer I with 500 mM NaCl), Buffer III (50 mM Tris-HCl, pH8.0, 250 mM LiCl, 0.5 % sodium deoxycholate, 1 % NP 40, and 1 mM EDTA), and TE buffer (50 mM Tris-

HCl, pH8.0, and 1 mM EDTA). Bound chromatin was eluted with 0.3 ml of Elution buffer (50 mM Tris-HCl, pH8.0, 1 % SDS, and 1 mM EDTA). After reversal of crosslinking, RNase A and Proteinase K was added, and DNA was purified by phenol extraction and ethanol precipitation. For re-ChIP assays, chromatin immunoprecipitated with the ATF3 antibody was eluted in 0.15 ml of Elution buffer, and then diluted by 20 times with re-ChIP buffer (20 mM Tris-HCl, pH8.0, 150 mM NaCl, 1 % Triton X-100, and 2 mM EDTA), followed by incubation with the p53 antibody as described above.

ChIP-seq and data analysis

ChIP-seq libraries were prepared according to standard protocols using Bioscientific's DNA Sample Kit (cat#514101) [50]. Libraries were sequenced using Illumina Hi-Seq platforms. Sequence reads were aligned to the Human Reference Genome (assembly hg19) using Burrows-Wheeler Alignment (BWA) Tool Version 0.6.1. Peak identification, overlapping, subtraction and feature annotation of enriched regions were performed using Hypergeometric Optimization of Motif EnRichment suite (HOMER). Heatmaps and intensity plots of peaks were generated by Perl script, R and/or java Treeview. HOMER was used to check motif enrichment.

Microarray data analysis

Total RNA was prepared using Agilent Total RNA Isolation Mini Kit (cat# 5185-6000). Microarray expression profiling was performed using HumanHT-12 v 4.0 Expression BeadChip (Illumina). Data were preprocessed and normalized by GenomeStudio. Differentially expressed genes were identified by Bioconductor limma package and GenePattern. Heatmap view of differentially expressed genes was created by Cluster and Java Treeview. GO term enrichment was determined using DAVID.

Western blotting and quantitative PCR

Western blotting assays were performed as described previously [16]. In brief, cells were lysed in RIPA buffer containing 50 mM Tris-HCl, pH 7.4, 1 % Nonidet P-40, 0.25 % sodium deoxycholate, 150 mM NaCl, 1 mM EDTA, 1 mM PMSE, and 1 mM NaF, 1 mM Na₃VO₄, and protease inhibitor cocktail (Roche), and then resolved in SDS-polyacrylamide electrophoresis for immunoblotting. Quantitative PCR assays were carried out using SYBR Green as described elsewhere [49].

Availability of supporting data

The data sets supporting the results of this article are available in the GEO with the accession number GSE74363 (<http://www.ncbi.nlm.nih.gov/geo/query/acc.cgi?token=yfozycagbfojfkz&acc=GSE74363>).

Additional files

Additional file 1: This pdf file contains Figure S1, S2 and S3. (PDF 531 kb)

Additional file 2: Table S1. A list of unique genes containing overlapped ATF3 and p53 peaks where both ATF3 and p53 motifs are present. (XLSX 32 kb)

Competing interests

The authors declare that they have no competing interests.

Authors' contributions

JZ analyzed most of the ChIP-seq and microarray data. XL validated the ChIP-seq and microarray results. MG prepared ChIP-seq and microarray samples. CY conceived the study, analyzed and organized the data with JY. CY wrote while JY edited the manuscript. All authors read and approved the final manuscript.

Acknowledgements

We thank Dr. Bert Vogelstein and Dr. Todd Waldman for providing cell lines and plasmids.

Funding

This work was supported by National Institutes of Health grants (R01CA139107, and R01CA164006), and a US Department of Defense award (W81XWH-15-1-0049) to CY.

Author details

¹Department of Medicine, Division of Hematology and Oncology, Northwestern University Feinberg School of Medicine, Chicago, IL, USA. ²Georgia Cancer Center, Augusta University, Augusta, GA, USA. ³Department of Biochemistry and Molecular Biology, Medical College of Georgia, Augusta University, Augusta, GA, USA. ⁴Center for Cell Biology and Cancer Research, Albany Medical College, Albany, NY, USA.

Received: 8 December 2015 Accepted: 26 April 2016

Published online: 04 May 2016

References

- Pennacchio LA, Bickmore W, Dean A, Nobrega MA, Bejerano G. Enhancers: five essential questions. *Nat Rev Genet.* 2013;14:288–95.
- Levine M, Cattoglio C, Tjian R. Looping back to leap forward: Transcription enters a new era. *Cell.* 2014;157:13–25.
- Visel A, Blow MJ, Li Z, Zhang T, Akiyama JA, Holt A, Plajzer-Frick I, Shoukry M, Wright C, Chen F, Afzal V, Ren B, Rubin EM, Pennacchio LA. ChIP-seq accurately predicts tissue-specific activity of enhancers. *Nature.* 2009;457:854–8.
- Creyghton MP, Cheng AW, Welstead GG, Kooistra T, Carey BW, Steine EJ, Hanna J, Lodato MA, Frampton GM, Sharp PA, Boyer LA, Young RA, Jaenisch R. Histone H3K27ac separates active form poised enhancers and predicts developmental state. *Proc Natl Acad Sci USA.* 2010;107:21931–6.
- Rada-Iglesias A, Bajpai R, Swigut T, Brugmann SA, Flynn RA, Wysocka J. A unique chromatin signature uncovers early developmental enhancers in humans. *Nature.* 2011;470:279–83.
- Zaret KS, Carroll JS. Pioneer transcription factors: Establishing competence for gene expression. *Genes Dev.* 2011;25:2227–41.
- Weinhold N, Jacobsen A, Schultz N, Sander C, Lee W. Genome-wide analysis of noncoding regulatory mutations in cancer. *Nat Genet.* 2014;46:1160–5.
- Wolford CC, McConoughey SJ, Jalgaonkar SP, Leon M, Merchant AS, Dominick JL, Yin X, Chang Y, Zmuda EJ, O'Toole SA, Millar EKA, Roller SL, Shapiro CL, Ostrowski MC, Sutherland RL, Hai T. Transcription factor ATF3 links host adaptive response to breast cancer metastasis. *J Clin Invest.* 2013;123:2893–906.
- Wu X, Nguyen B, Dziunycz P, Chang S, Brooks Y, Lefort K, Hofbauer G, Dotto G. Opposing roles for calcineurin and ATF3 in squamous skin cancer. *Nature.* 2010;465:368–72.
- Yuan X, Yu L, Li J, Xie G, Rong T, Zhang L, Chen J, Meng Q, Irving AT, Wang D, Williams ED, Liu JP, Sadler AJ, Williams BR, Shen L, Xu D. ATF3 suppresses metastasis of bladder cancer by regulating gelsolin-mediated remodeling of the actin cytoskeleton. *Cancer Res.* 2013;73:3625–37.
- Wang Z, Xu D, Ding H-F, Kim J, Zhang J, Hai T, Yan C. Loss of ATF3 promotes Akt activation and prostate cancer development in a Pten knockout mouse model. *Oncogene.* 2015;34:4975–84.
- Gold ES, Ramsey SA, Sartain MJ, Selinummi J, Podolsky I, Rodriguez DJ, Moritz RL, Aderem A. ATF3 protects against atherosclerosis by suppressing 25-hydroxycholesterol-induced lipid body formation. *J Exp Med.* 2012;209:807–17.
- Hoetzenecker W, Echtenacher B, Guenova E, Hoetzenecker K, Woelbling F, Bruck J, Teske A, Valtcheva N, Fuchs K, Kneilling M, Park J-H, Kim K-H, Kim K-W, Hoffmann P, Krenn C, Hai T, Ghoreschi K, Biedermann T, Rocken M. ROS-induced ATF3 causes susceptibility to secondary infections during sepsis-associated immunosuppression. *Nat Med.* 2012;18:128–34.
- Zhou H, Shen D-F, Bian Z-Y, Zong J, Deng W, Zhang Y, Guo Y-Y, Li H, Tang Q-Z. Activating transcription factor 3 deficiency promotes cardiac hypertrophy, dysfunction, and fibrosis induced by pressure overload. *PLoS One.* 2011;6:e26744.
- Beleza-Meireles A, Tohonon V, Soderhall C, Schwentner C, Radmayr C, Kockum I, Nordenskjold A. Activating transcription 3: A hormone responsive gene in the etiology of hypospadias. *Eur J Endocrinol.* 2008;158:729–39.
- Yan C, Lu D, Hai T, Boyd DD. Activating transcription factor 3, a stress sensor, activates p53 by blocking its ubiquitination. *EMBO J.* 2005;24:2425–35.
- Gilchrist M, Thorsson V, Li B, Rust AG, Korb M, Roach JC, Kennedy K, Hai T, Bolouri H, Aderem A. Systems biology approaches identify ATF3 as a negative regulator of Toll-like receptor 4. *Nature.* 2006;441:173–8.
- Yan C, Boyd DD. ATF3 regulates the stability of p53: A link to cancer. *Cell Cycle.* 2006;5:926–9.
- Hai T, Wolfgang CD, Marsee DK, Allen AE, Sivaprasad U. ATF3 and stress responses. *Gene Expression.* 1999;7:321–5.
- Walter P, Ron D. The unfolded protein response: From stress pathway to homeostatic regulation. *Science.* 2011;334:1081–6.
- Wang H, Jiang M, Cui H, Chen M, Buttyan R, Hayward SW, Hai T, Wang Z, Yan C. The stress response mediator ATF3 represses androgen signaling by binding the androgen receptor. *Mol Cell Biol.* 2012;32:3190–202.
- Cui H, Guo M, Xu D, Ding Z-C, Zhou G, Ding H-F, Zhang J, Tang Y, Yan C. The stress-responsive gene ATF3 regulates the histone acetyltransferase Tip60. *Nat Commun.* 2015;6:6752.
- Kim J-S, Bonifant C, Bunz F, Lane WS, Waldman T. Epitope tagging of endogenous genes in diverse human cell lines. *Nucleic Acid Res.* 2008;36:e127.
- Wolfgang CD, Liang G, Okamoto Y, Allen AE, Hai T. Transcriptional autorepression of the stress-inducible gene ATF3. *J Biol Chem.* 2000;275:16865–70.
- Newman JRS, Keating AE. Comprehensive identification of human bZIP interactions with coiled-coil arrays. *Science.* 2003;300:2097–101.
- Kiryu-Seo S, Kato R, Ogawa T, Nakagomi S, Nagata K, Kiyama H. Neuronal injury-inducible gene is synergistically regulated by ATF3, c-Jun, and STAT3 through the interaction with Sp1 in damaged neurons. *J Biol Chem.* 2008;283:6988–96.
- Hu D, Gao X, Morgan MA, Herz H-M, Smith ER, Shilatifard A. The MLL3/MLL4 branches of the COMPASS family function as major histone H3K4 monomethylases at enhancers. *Mol Cell Biol.* 2013;33:4745–54.
- Frietze S, Wang R, Yao L, Tak YG, Ye Z, Gaddis M, Witt H, Farnham PJ, Jin VX. Cell type-specific binding patterns reveal that TCF7L2 can be tethered to the genome by association with GATA3. *Genome Biol.* 2012;13:R52.
- Pan Y, Chen H, Siu F, Kilberg MS. Amino acid deprivation and endoplasmic reticulum stress induce expression of multiple activating transcription factor-3 mRNA species that, when overexpressed in HepG2 cells, modulate transcription by the human asparagine synthetase promoter. *J Biol Chem.* 2003;278:38402–12.
- Bottone FG, Moon Y, Kim JS, Alston-Mills B, Ishibashi M, Eling TE. The anti-invasive activity of cyclooxygenase inhibitors is regulated by the transcription factor ATF3 (activating transcription factor 3). *Mol Cancer Ther.* 2005;4:693–703.
- Hackl C, Lang SA, Moser C, Mori A, Fichtner-Feigl S, Hellerbrand C, Dietmeier W, Schlitt HJ, Geissler EK, Stoeltzing O. Activating transcription factor-3 (ATF3) functions as a tumor suppressor in colon cancer and is up-regulated upon heat-shock protein 90 (Hsp90) inhibition. *BMC Cancer.* 2010;10:668.
- Mo P, Wang H, Lu H, Boyd DD, Yan C. MDM2 mediates ubiquitination and degradation of activating transcription factor 3. *J Biol Chem.* 2010;285:26908–15.
- Calo E, Wysocka J. Modification of enhancer chromatin: What, how, and why? *Mol Cell.* 2013;49:825–37.
- Vousden KH, Prives C. Blinded by the light: The growing complexity of p53. *Cell.* 2009;137:413–31.
- Botcheva K, McCorkle SR, McCombie WR, Dunn JJ, Anderson CW. Distinct p53 genomic binding patterns in normal and cancer-derived cancer cells. *Cell Cycle.* 2011;10:4237–49.

36. Menendez D, Nguyen T-A, Freudenberg JM, Mathew VJ, Anderson CW, Jothi R, Resnick MA. Diverse stresses dramatically alter genome-wide p53 binding and transactivation landscape in human cancer cells. *Nucleic Acid Res.* 2013;41:7286–301.
37. Broz DK, Mello SS, Bieging KT, Jian D, Dusek RL, Brady CA, Sidow A, Attardi LD. Global genomic profiling reveals an extensive p53-regulated autophagy program contributing to key p53 responses. *Genes Dev.* 2013;27:1016–31.
38. Fan F, Jin S, Amundson SA, Tong T, Fan W, Zhao H, Zhu X, Mazzacurati L, Li X, Petrik KL, Fornace AJ, Rajasekaran B, Zhan Q. ATF3 induction following DNA damage is regulated by distinct signaling pathways and over-expression of ATF3 protein suppresses cells growth. *Oncogene.* 2002;21:7488–96.
39. Garber M, Yosef N, Goren A, Raychowdhury R, Thielke A, Guttman M, Robinson J, Minie B, Chevrier N, Itzhaki Z, Blecher-Gonen R, Bornstein C, Amann-Zalcenstein D, Weiner A, Friedrich D, Meldrim J, Ram O, Cheng C, Gnirke A, Fisher S, Friedman N, Wong B, Bernstein BE, Nusbaum C, Hacohen N, Regev A, Amit I. A high-throughput chromatin immunoprecipitation approach reveals principles of dynamic gene regulation in mammals. *Mol Cell.* 2012;47:810–22.
40. Chen B, Wolfgang C, Hai T. Analysis of ATF3, a transcription factor induced by physiological stresses and modulated by gadd153/Chop10. *Mol Cell Biol.* 1996;16:1157–68.
41. Wei S, Wang H, Lu C, Malmut S, Zhang J, Ren S, Yu G, Wang W, Tang DD, Yan C. The activating transcription factor 3 protein suppresses the oncogenic function of mutant p53 proteins. *J Biol Chem.* 2014;289:8947–59.
42. Kouwenhoven EN, Oti M, Niehues H, van Heeringen SJ, Schalkwijk J, Stunnenberg HG, van Bokhoven H, Zhou H. Transcription factor p63 bookmarks and regulates dynamic enhancers during epidermal differentiation. *EMBO Rep.* 2015;16:863–78.
43. Ikura T, Tashiro S, Kakino A, Shima H, Jacob N, Amunugama R, Yoder K, Izumi S, Kuraoka I, Tanaka K, Kimura H, Ikura M, Nishijubbo S, Ito T, Muto A, Miyagawa K, Takeda S, Fishel R, Igarashi K, Kamiya K. DNA damage-dependent acetylation and ubiquitination of H2AX enhances chromatin dynamics. *Mol Cell Biol.* 2011;27:70287040.
44. Lukas J, Lukas C, Bartek J. More than just a focus: The chromatin response to DNA damage and its role in genome integrity maintenance. *Nat Cell Biol.* 2011;13:1161–9.
45. Ayrapetov MK, Gursoy-Yuzugullu O, Xu C, Xu Y, Price BD. DNA double-strand breaks promote methylation of histone H3 on lysine 9 and transient formation of repressive chromatin. *Proc Natl Acad Sci USA.* 2014;111:9169–74.
46. Tanaka Y, Nakamura A, Morioka MS, Inoue S, Tamamori-Adachi M, Yamada K, Taketani K, Kawachi J, Tanaka-Okamoto M, Miyoshi J, Tanaka H, Kitajima S. System analysis of ATF3 in stress response and cancer reveals opposing effects on pro-apoptotic genes in p53 pathway. *PLoS One.* 2011;6:e26848.
47. Yonger ST, Kenzelmann-Broz D, Jung H, Attardi LD, Rinn JL. Integrative genomic analysis reveals widespread enhancer regulation by p53 in response to DNA damage. *Nucleic Acid Res.* 2015;43:4447–62.
48. Lang L, Ding H-F, Chen X, Sun S-Y, Liu G, Yan C. Internal ribosome entry site-based bicistronic in situ reporter assays for discovery of transcription-targeted lead compound. *Chem Biol.* 2015;22:957–64.
49. Yan C, Boyd DD. Histone H3 acetylation and H3 K4 methylation define distinct chromatin regions permissive for transgene expression. *Mol Cell Biol.* 2006;26:6357–71.
50. Yu J, Yu J, Mani R, Cao Q, Brenner CJ, Cao X, Wang X, Wu L, Li J, Hu M, Gong Y, Cheng H, Laxman B, Vellaichamy A, Shankar S, Li Y, Dhanasekaran SM, Morey R, Barrette T, Lonigro RJ, Tomlins SA, Varambally S, Qin ZS, Chinnaiyan AM. An integrated network of androgen receptor, polycomb, and TMPRSS2-ERG gene fusions in prostate cancer progression. *Cancer Cell.* 2010;17:443–54.

Submit your next manuscript to BioMed Central and we will help you at every step:

- We accept pre-submission inquiries
- Our selector tool helps you to find the most relevant journal
- We provide round the clock customer support
- Convenient online submission
- Thorough peer review
- Inclusion in PubMed and all major indexing services
- Maximum visibility for your research

Submit your manuscript at
www.biomedcentral.com/submit

